STUTTGARTER BEITRÄGE ZUR PRODUKTIONSFORSCHUNG

MATTHIAS REUSS

Modeling Method for Simulation of Assembly Variances

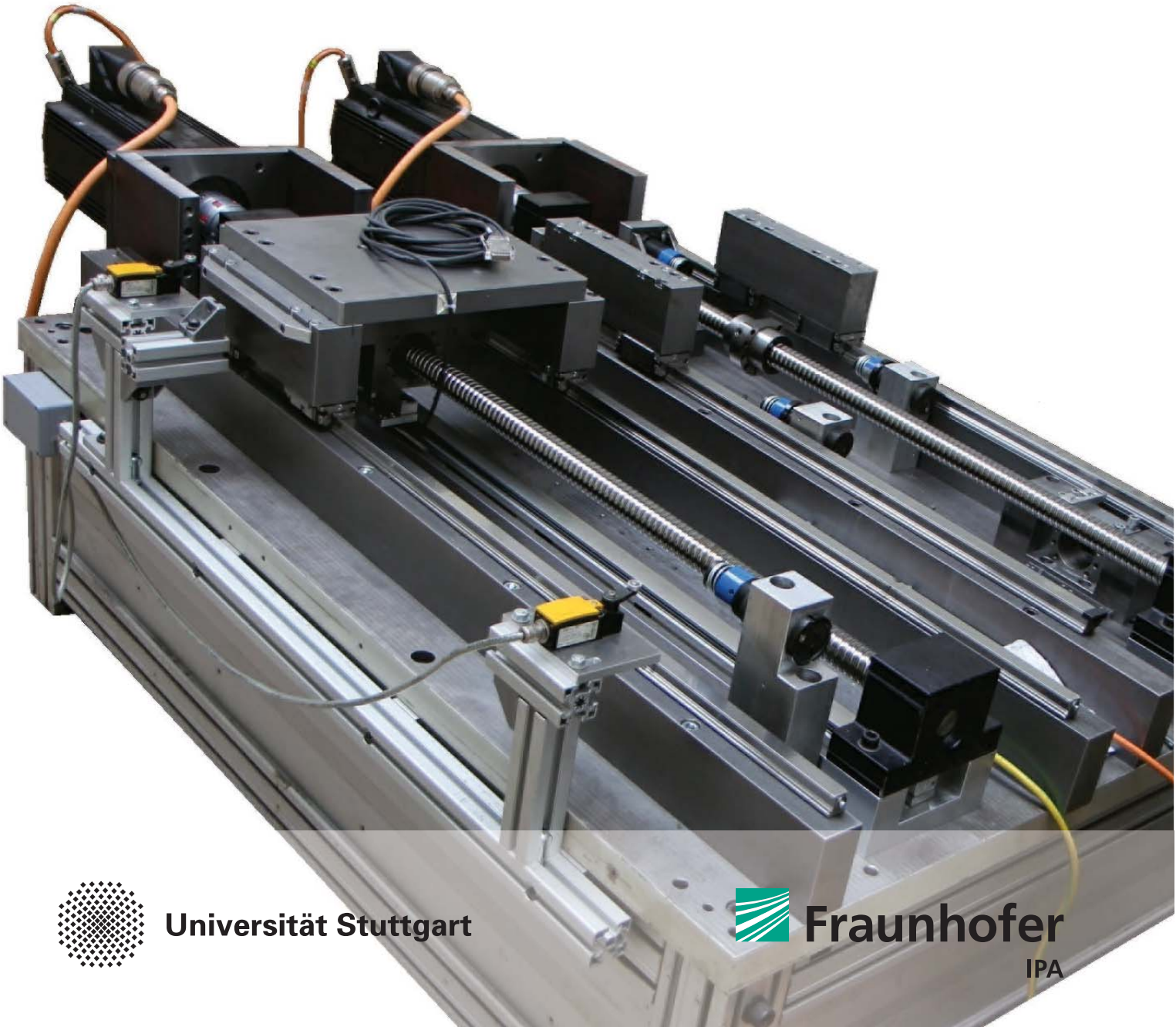

Universität Stuttgart

Fraunhofer IPA

STUTTGARTER BEITRÄGE ZUR PRODUKTIONSFORSCHUNG BAND 72

Herausgeber:
Univ.-Prof. Dr.-Ing. Thomas Bauernhansl
Univ.-Prof. Dr.-Ing. Dr. h.c. mult. Alexander Verl
Univ.-Prof. a. D. Dr.-Ing. Prof. E.h. Dr.-Ing. E.h. Dr. h.c. mult. Engelbert Westkämper

Matthias Reuß

Modeling Method for Simulation of Assembly Variances

FRAUNHOFER VERLAG

Kontaktadresse:
Fraunhofer-Institut für Produktionstechnik und Automatisierung IPA, Stuttgart
Nobelstraße 12, 70569 Stuttgart
Telefon 0711 970-00, Telefax 0711 970-1399
info@ipa.fraunhofer.de, www.ipa.fraunhofer.de

STUTTGARTER BEITRÄGE ZUR PRODUKTIONSFORSCHUNG

Herausgeber:
Univ.-Prof. Dr.-Ing. Thomas Bauernhansl
Univ.-Prof. Dr.-Ing. Dr. h.c. mult. Alexander Verl
Univ.-Prof. a. D. Dr.-Ing. Prof. E.h. Dr.-Ing. E.h. Dr. h.c. mult. Engelbert Westkämper

Fraunhofer-Institut für Produktionstechnik und Automatisierung IPA, Stuttgart
Institut für Industrielle Fertigung und Fabrikbetrieb (IFF) der Universität Stuttgart
Institut für Steuerungstechnik der Werkzeugmaschinen und Fertigungseinrichtungen (ISW)
der Universität Stuttgart

Titelbild: @ Matthias Reuß

Bibliografische Information der Deutschen Nationalbibliothek
Die Deutsche Nationalbibliothek verzeichnet diese Publikation in der Deutschen Nationalbibliografie; detaillierte bibliografische Daten sind im Internet über www.dnb.de abrufbar.
ISSN: 2195-2892
ISBN (Print): 978-3-8396-1256-9

D 93

Zugl.: Stuttgart, Univ., Diss., 2016

Druck: Mediendienstleistungen des Fraunhofer-Informationszentrum Raum und Bau IRB, Stuttgart
Für den Druck des Buches wurde chlor- und säurefreies Papier verwendet.

Fraunhofer-Informationszentrum Raum und Bau IRB
Postfach 80 04 69, 70504 Stuttgart
Nobelstraße 12, 70569 Stuttgart
Telefon 0711 970-2500
Telefax 0711 970-2508
E-Mail verlag@fraunhofer.de
URL http://verlag.fraunhofer.de

GELEITWORT DER HERAUSGEBER

Produktionswissenschaftliche Forschungsfragen entstehen in der Regel im Anwendungszusammenhang, die Produktionsforschung ist also weitgehend erfahrungsbasiert. Der wissenschaftliche Anspruch der „Stuttgarter Beiträge zur Produktionsforschung" liegt unter anderem darin, Dissertation für Dissertation ein übergreifendes ganzheitliches Theoriegebäude der Produktion zu erstellen.

Die Herausgeber dieser Dissertations-Reihe leiten gemeinsam das Fraunhofer-Institut für Produktionstechnik und Automatisierung IPA und jeweils ein Institut der Fakultät für Konstruktions-, Produktions- und Fahrzeugtechnik an der Universität Stuttgart.

Die von ihnen betreuten Dissertationen sind der marktorientierten Nachhaltigkeit verpflichtet, ihr Ansatz ist systemisch und interdisziplinär. Die Autoren bearbeiten anspruchsvolle Forschungsfragen im Spannungsfeld zwischen theoretischen Grundlagen und industrieller Anwendung.

Die „Stuttgarter Beiträge zur Produktionsforschung" ersetzt die Reihen „IPA-IAO Forschung und Praxis" (Hrsg. H.J. Warnecke / H.-J. Bullinger / E. Westkämper / D. Spath) bzw. ISW Forschung und Praxis (Hrsg. G. Stute / G. Pritschow / A. Verl). In den vergangenen Jahrzehnten sind darin über 800 Dissertationen erschienen.

Der Strukturwandel in den Industrien unseres Landes muss auch in der Forschung in einen globalen Zusammenhang gestellt werden. Der reine Fokus auf Erkenntnisgewinn ist zu eindimensional. Die „Stuttgarter Beiträge zur Produktionsforschung" zielen also darauf ab, mittelfristig Lösungen für den Markt anzubieten. Daher konzentrieren sich die Stuttgarter produktionstechnischen Institute auf das Thema ganzheitliche Produktion in den Kernindustrien Deutschlands. Die leitende Forschungsfrage der Arbeiten ist: Wie können wir nachhaltig mit einem hohen Wertschöpfungsanteil in Deutschland für einen globalen Markt produzieren?

Wir wünschen den Autoren, dass ihre „Stuttgarter Beiträge zur Produktionsforschung" in der breiten Fachwelt als substanziell wahrgenommen werden und so die Produktionsforschung weltweit voranbringen.

Alexander Verl Thomas Bauernhansl Engelbert Westkämper

Modeling Method for Simulation of Assembly Variances

Von der Graduate School of Excellence Advanced Manufacturing Engineering
der Universität Stuttgart
zur Erlangung der Würde eines Doktor-Ingenieurs (Dr.-Ing.)
genehmigte Abhandlung

Vorgelegt von
Dipl.-Ing. Matthias Reuß
aus Pforzheim

Hauptberichter:	Univ.-Prof. Dr.-Ing. Dr. h.c. mult. Alexander Verl
Mitberichter:	Univ.-Prof. Dr. rer. nat. Dr. h.c. mult. Rainer Gadow
	Univ.-Prof. Dr.-Ing. Konrad Wegener

Tag der mündlichen Prüfung: 12. Oktober 2016

Institut für Steuerungstechnik der Werkzeugmaschinen und
Fertigungseinrichtungen der Universität Stuttgart

2017

Danksagung

Die vorliegende Arbeit entstand während meiner Zeit als Stipendiat der Graduate School advanced Manufacturing Engineering (GSaME), die ich am Institut für Steuerungstechnik der Werkzeugmaschinen und Fertigungseinrichtungen (ISW) der Universität Stuttgart verbracht habe.

Besonders danke ich Herrn Professor Dr.-Ing Dr. h.c. mult. Alexander Verl für die Unterstützung dieser Arbeit sowie die Übernahme des Hauptberichts. Herrn Professor Dr. rer. nat. Dr. h.c. mult. Rainer Gadow und Herrn Professor Dr.-Ing. Konrad Wegener danke ich für die Übernahme des Mitberichts. Herrn Professor Dr.-Ing. habil. Mitschang für die Übernahme des Prüfungsvorsitzes.

Ein herzlicher Dank geht an alle Kollegen des Instituts und der GSaME, die mich während meiner wissenschaftlichen Tätigkeit begleitet und unterstützt haben. Besonderer Dank geht an Herrn Dr. rer. nat. Konrad Groh, Herrn Dr.-Ing. Friedemann Groh und Herrn Dr.-Ing. Sigfried Frey für die fachliche Durchsicht. Weiterhin möchte ich den Mitarbeitern der technischen Werkstatt danken, welche mich beim Aufbau des Versuchsstands tatkräftig unterstützt haben, und der Verwaltung der GSaME, die mir bei allen Fragen zum Promotionsverfahren jederzeit weitergeholfen haben.

Schließlich danke ich Herrn Professor Dr.-Eng. Atsushi Matsubara für die interessanten Diskussionen und Herrn Dr.-Ing. Alexander Broos der mich für die wissenschaftliche Arbeit begeistert hat.

Zuletzt gilt ein besonderer Dank meiner Familie für das aufgebrachte Verständnis und die Geduld ohne die diese Arbeit nicht gelungen wäre.

Stuttgart, im Juni 2017 Matthias Reuß

Short Summary

High quality machine tools are necessary for industrial production of precise workpieces. In this work a method is displayed, which allows to monitor and ensure the production of these machine tools with a constant precision and quality. This method is based on measuring of the complete friction of the linear axes by current of the servo motors, which is available in the NC controller. Thereby, a deviation between identical machine tool axes becomes obvious. This deviation allows drawing conclusions on the assembly conditions of components. At the machine tool maker's production this measurement can be conducted and be used as reference during its life expectancy in order to supervise changes of behavior. The discussed measurements have been conducted at machine tools during start-up and at a test rig with distinct assembly failures. Furthermore, a modeling method for simulation of assembly variations is introduced. By this simulation method effects on friction can be estimated at an early stage of the product development. Hence, critical assembly steps can be determined and assessed during the design phase. This allows an improvement of assembly planning by increase of effort in critical steps, whereas it becomes possible to reduce the effort for noncritical steps.

Kurzinhalt

Qualitativ hochwertige Werkzeugmaschinen sind eine notwendige Bedingung zur präzisen industriellen Fertigung von Bauteilen. In der vorliegenden Arbeit wird eine Methode vorgestellt, mit der die gleichbleibende Genauigkeit und Qualität bei der industriellen Herstellung baugleicher Werkzeugmaschinen überprüft und erreicht werden kann. Diese basiert auf einer Messung der gesamten Reibung der Linearachsen über die Motorströme als in der Steuerung verfügbare Messgröße. Dabei zeigt sich eine deutliche Streuung zwischen einzelnen baugleichen Achsen, die auch Rückschlüsse auf den Einbauzustand einzelner Komponenten erlaubt. Eine solche Messung kann bereits als Referenzmessung beim Maschinenhersteller geschehen und nachfolgend beim Maschinennutzer wiederholt werden, um Veränderungen zu beobachten. Zur Verifizierung wurden sowohl an Werkzeugmaschinen beim Maschinenhersteller als auch an einem Versuchsstand, in den definierte Montagefehler eingebracht wurden, Messungen durchgeführt. Weiterhin wird eine Methode, die die Modellierung von Montagestreuungen in Simulationsmodellen ermöglicht, vorgestellt. Es wird gezeigt, dass sich mit dieser Methode frühzeitig Aussagen über die Auswirkungen von Motagestreuungen auf die Reibung treffen lassen und sich die Simulation somit für eine erste Beurteilung kritischer Montagevorgänge bereits in der Konstruktionsphase eignet. Dies ermöglicht eine verbesserte Planung der Montage, indem auf die als kritisch identifizierten Schritte mehr Aufwand verwendet werden kann, wohingegen der Aufwand für unkritische Schritte gegebenenfalls reduziert werden kann.

Extended abstract

Introduction and motivation

In modern factories, workpieces are produced in high quality and reliability by machine tools. In machine tools feed drives are used to generate the relative movement between workpiece and tool according to the machining task. Hence, highest demands on the accuracy of machine tools and consequently feed drives are required. If several machine tools constructed and assembled in a similar manner are used to conduct machining operations, identical results are expected without any adaption of NC programs beside tool length and radius compensation. Also, life expectancy and maintenance costs of these machine tools are assumed to be equal. However, there are variations between these identical machine tools mainly caused by assembly variances of feed drives.

As every assembly process is subject to assembly deviations, for example bolt fastening variations or variation of adjustment, the assembly result of such complex systems like feed drives is influenced by a multitude of variances. There is a lack of knowledge of the particular effects of these variations on machine tools. Furthermore, no procedure is developed to measure or estimate by simulation in advance.

Scientific approach and objective

In order to meet the demands of an increasing number of variants and decreasing time for designing machine tools, simulation is a proper way to predict their behavior. Therefore, the variances of identical machine tools are examined and traced back to the assembly situation of components. Thereby, the relevance of the assembly variances for machine tool behavior and thus their effect on components are observed.

Friction is identified as a parameter, which can be measured in serial production of machine tools without extraordinary effort but having high sensitivity to assembly

variances. For further examination of impact of assembly variances, multibody simulation, which is a proper and widespread method for simulating machine tools, is conducted.

The objective of this scientific work is to improve the modeling of assembly variances of machine tools and to increase the understanding of assembly processes and failures. The practical implementation in simulation models is developed and the simulation results are compared with measurements.

Solution process

The scientific course of this thesis ranges from a survey of assembly variances of machine tools to practical implementation on machine tools and a test rig including verification by simulation. In figure 1 the solution process is illustrated.

In chapter 5, first the relevance to praxis is clarified by measurements at identical machine tools at equal conditions. Hence, new machine tools at machine tool makers' production plants are measured after start-up and right before shipping. Furthermore, friction is identified to be a sensitive and measurable parameter and a measuring approach is developed together with the involved machine tool makers. The measuring results show significant variations. Since the assembly of industrial machines cannot be varied, it is impossible to identify the reason for the observed variations. Thus, secondly a test rig is constructed and measurements under varying assembly conditions are conducted. Thereby, the influence of variation of components on friction and its position dependency are estimated.

Since this testing approach requires a huge effort, thirdly in chapter 6 a simulation model is developed to be able to vary the multitude of parameters, which is impossible at a test rig. Several modeling approaches have been compared and multibody simulation fulfills the requirements of modeling machine tools behavior best. Furthermore, it becomes possible to diagnose the influences of variations on components, which are not measurable in reality. The central components are modeled in detail. Especially their position-depending stiffness and their friction behavior are identified and used for parametrization.

In chapter 7 the measuring results of chapter 5 and chapter 6 are compared and the results show that the developed simulation method allows estimating the influence of assembly tolerances on machine tools characteristics and components life expectancy by simulation is developed. Furthermore, the relevance for machine tool assembly is clarified.

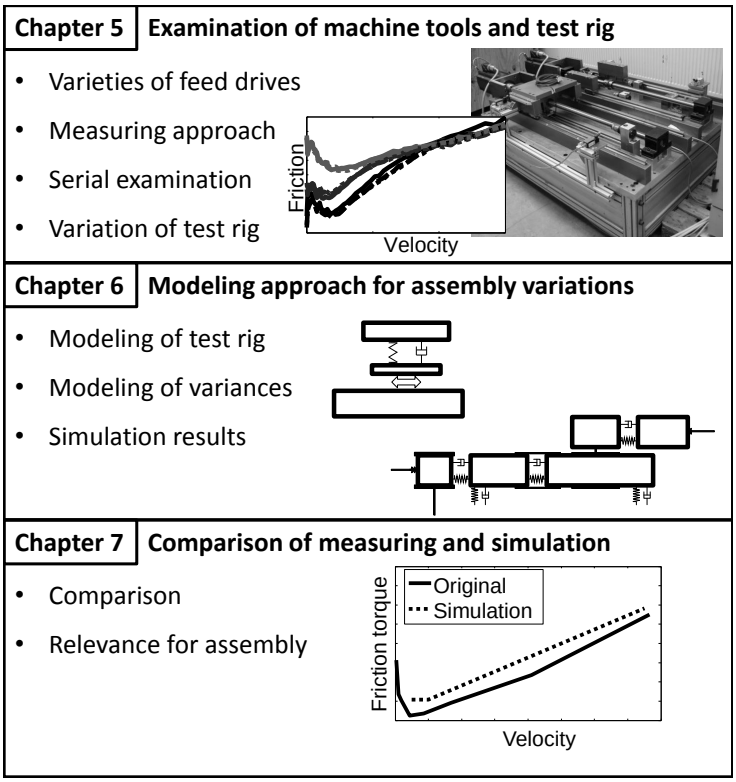

Figure 1: Methodology of the solution process

Summary

Within this thesis, the understanding of variances of identical machine tools is improved and a new method for modeling assembly variances of machine tools is developed and verified by experiments. Thereby, critical assembly steps of feed drives are identified and a general method for the simulation of variances is developed. Proper concepts for measuring identical machine tools reliably and interpreting the measuring results are detailed. Simulation under a variation of assembly conditions is validated by these measurements. Furthermore, a proper concept for the practical implementation of the developed modeling approach is displayed. This modeling method shows high potential for improving the design process of machine tools.

Contents

Abbreviations and Symbols

Abbreviations

CACE	Computer aided control engineering
`*.csv`	Comma separated variable data
DFG	German Research Foundation
DOF	Degree of freedom
FEM	Finite element method
FMEA	Failure mode and effect analysis
FRF	Frequency response function
FWF	Research Association for Machine Tools and Manufacturing Technology
GMS	Generalized Maxwell slip
GUI	Graphical User Interface
MBS	Multibody simulation
`*.mat`	Matlab data format
RPN	Risk priority number
TCP	Tool Center Point
VDI	Association of German engineers
VDW	German machine tool builders' association
`*.xml`	xml data format

Symbols

A	Area
a	Minor radius of ellipse
b	Major radius of ellipse
C	Damping matrix
C_v	Slip exaggeration factor
c	Stiffness
d	Diameter
E	Young's modulus
e	Error
F	Force
F_C	Coulomb friction force
F_N	Normal force
F_R	Friction force
F_S	Static force
F_r	Radial load
f_s	Proportionality constant of mixed friction
f_v	Proportionality constant of viscous friction
G	Shear modulus
$G(j\omega)$	Transfer function
H	Observation matrix
$\mathbf{I}$	Identity matrix
J	Squared residua
j	Imaginary unit
K	Stiffness matrix
k	Stiffness
k_q	Bristle stiffness
M	Mass matrix
m	Mass
l	Length
P_1	Load
p	Pressure
$p_{\max}$	Maximum pressure

Q_s	Generalized force
T	Torque
v	Velocity
v_s	Differential velocity in contact
v_S	Stribeck velocity
u	Displacement
$X(j\omega)$	Input signal
x	Displacement
$Y(j\omega)$	Output signal
α	Parameter of Dahl model
μ	Friction coefficient
ν	Poisson's ratio
$\boldsymbol{\nu}$	Viscosity of lubrication
ε	Strain
$\boldsymbol{\sigma}$	Stress
σ	Standard deviation
$\varphi(j\omega)$	Phase
ω	Frequency
ω_0	Eigenfrequency
ω_d	Damped eigenfrequency
$\hat{.}$	Estimation of .
$\vec{.}$	Vector of .

List of Figures

List of Tables

1 Introduction

1.1 Initial situation

A customer buying several machine tools constructed and assembled in a similar manner expects identical machining results from each of these machine tools. Hence, machining workpieces with identical NC programs, tools and without any adaption should lead to identical results. Furthermore, the life expectancy, namely mean time between failure and maintenance costs, of these machine tools should be equal.

Since machine tools are highly integrated mechatronic systems, a constant and high quality of the purchased components, production and assembly process is necessary.

Thus, the detection of failures at an early stage of production results in a tremendous reduction of costs and production stops. Furthermore, since customers want products with characteristics that satisfy their needs and expectations, an improvement of the product by reduction of deviation becomes possible, which are important sales arguments (DIN EN ISO 9000 2005).

Since tolerances of components, production and assembly process are ineluctable, the desired behavior cannot be fulfilled. Thus, the machine tool consumers with many identical machine tools must adapt their maintenance processes as well as their NC programs on each machine tool, respectively to keep exchangeability geared to the worst. This results in both higher costs and reduced productivity.

1.2 Problem

Since identical machine tools have a different mechanical characteristics caused by production and assembly tolerances (Reuss, Dadalau et al. 2012), both the result of machining and the internal constraining forces of the machine tool components are not equal. It is nearly impossible to estimate assembly failures or alignment errors, which are a major source of constraining forces in components. These constraining forces have no significant effect on the geometrical accuracy but are an additional load on machine components. Thus, even if all assembly tolerances given by the manufacturer of components are ensured, there is a negative influence on the life expectancy (Bosch Rexroth 2006). The change of parameters during the machine's lifetime often has a negative influence on precision. In order to keep high precision, often the feed velocity is reduced (Heidenhain 2013). Furthermore, a variation of the preload of bearings or ball screws leads to variations of stiffness and damping, which directly affect the dynamic performance.

In order to determine reason and impact of such failures, both measurements must be conducted and models must be developed for simulating the estimated behavior. Since most machine tool producers have a multitude of variants, the measuring results from test beds are limited and simulation is an appropriate way to handle this variety (Kipfmüller 2010). However, a survey of the German machine tool builders' association (VDW), which is displayed in table 1.1, shows the German machine tool building companies are mostly small and medium sized enterprises (VDW 2012, 2014). Therefore, it is often impossible to employ simulation experts and to pay expensive software license fees. Hence, they need a competitive and easily realizable solution.

Furthermore, the lot size of machine tools produced in small companies is small, which means the number of tests and prototypes is rather limited, and sometimes problems are detected at the customer's production plant. However, the later a failure is detected the more expensive it becomes, (Rinne and Mittag 1995, Reinhart 1996). Thus, a method for early detection of failures is requested.

Number of employees	Companies [%]				
	2009	2010	2011	2012	2013
1-50	17,9	15,9	16,2	12,6	10,9
51-100	14,6	18,6	14,3	13,6	13,9
101-250	29,3	23,9	26,7	29,1	28,7
251-500	21,1	23,9	23,8	23,3	24,8
501-1000	13,0	13,3	13,3	15,5	14,9
>1000	4,1	4,4	5,7	5,8	6,9

Table 1.1: Company size of German machine tool industry from an annual survey of VDW (2012, 2014).

1.3 Objective and approach

In this work, a method to simulate a multitude of variances of machine tools is developed and validated by comparison with experiments at test stands. These variances are describing effects of assembly failures but also effects of production tolerances, which cause constraining forces and reduce the life expectation of components and machine tools. Thereby, the main advantage of simulation is to allow estimation of both not measurable impacts of assembly variances on components and on complete machine's behavior. However, the extensive costs for prototypes and experimental setup can be reduced.

However, first the relevance for machine tools must be clarified. Thus, the possible assembly variations of machine tools and their effect have to be determined. Therefore, failure mode and effect analysis is chosen as commonly used quality management method.

Secondly, the impact of assembly variations onto machine tool behavior must be estimated. Hence, serial examinations of machine tools must be conducted and the results interpreted with regard to variations of behavior. Therefore, measurements at identical machine tools at equal environmental conditions are conducted. Thus, new machine tools at machine tool makers' production plant after start-up

and right before shipping are measured. Furthermore, friction is identified as a sensitive and measurable parameter and a measuring approach is developed together with the involved machine tool makers. The results of these measurements must be ascribed to assembly uncertainty. This serial examination has several advantages:

- Detection of failures at an early stage
- Recording of the delivery state for each machine tool
- Reliable parameters for construction and simulation

In order to receive parameters for evaluating the developed simulation approach, in a third step, measurements under defined variations must be conducted. Since the assembly of industrial machines cannot be varied, it is impossible to clarify the reason for variations of the machine tool behavior by the serial examination of machine tools. Thus, a test rig is constructed and measurements under varying assembly conditions are conducted. This allows estimating the influence of variation of components on friction and its position dependency.

Since this testing approach requires a huge effort and is impossible to be conducted for every type of machine tool, lastly a simulation model is developed. Thereby it becomes possible to vary a multitude of parameters in a wider range than at a test rig. Several modeling approaches have been compared and multibody simulation meets the requirements of modeling machine tool behavior best. Furthermore, it becomes possible to diagnose the influences of variations on components, which are not measurable in reality. In the simulation the central components are modeled in detail. Especially their position-depending stiffness and friction behavior, which are identified by measurements, are used for parametrization. Thus, a method to estimate the influence of assembly tolerances on machine tool characteristics and life expectancy of components by simulation is developed.

2 Fundamentals

In this chapter, a survey of fundamentals of feed drives, machine tools, friction and simulation methods for machine tool simulation are discussed in detail. Firstly, the construction of a typical machine tool axis including its main components is described. Secondly, frequently used friction models and the sources of friction in machine tool axes are examined and assessed with respect to measure machine tools. Lastly, different simulation methods used in the machine tool design process are explained and assessed with focus on usability for machine tool simulation, especially relating to assembly variances and their parametrization.

2.1 Linear feed axis of machine tools

A typical machine tool axis is a complex mechatronic system consisting of CNC control unit, power electronics, servo drives, potentially mechanical transmission and measurement devices. In general, machine tools for milling, turning or grinding consist of several linear and rotational axes, a spindle-carrying tool or workpiece and peripheral devices for example automatic tool changer or automatic pallet changer. Since accuracy of the feed axes accuracy determines the exactness of the machining result and linear axes are commonly used, these are observed. Nowadays, mainly ball screw driven axes are used. If high demands on axis dynamics are required, linear motors are applied. Furthermore, in huge machine tool gear racks, for high stiffness threaded spindle drives and for good damping hydrodynamic spindles are installed, (Weck and Brecher 2006a). In figure 2.1 ball screw and linear motor driven axes and their components are shown in detail.

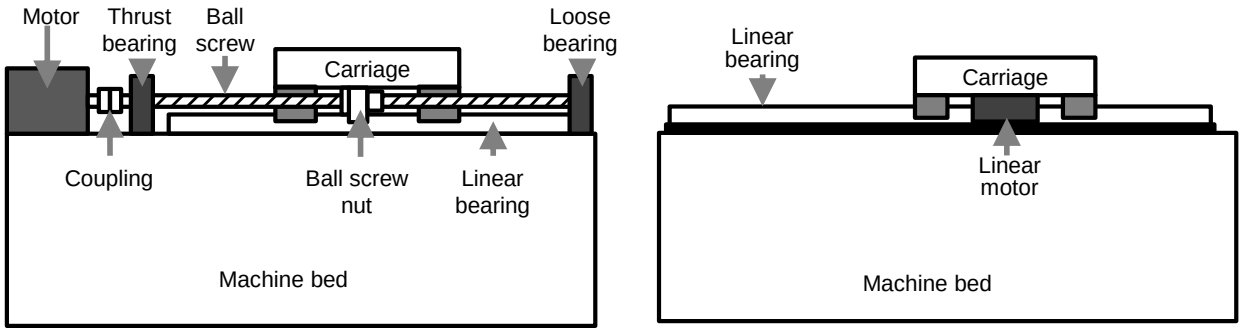

(a) Ball screw driven axis

(b) Linear motor driven axis

Figure 2.1: Structure of typical machine tool axis and their components, (Reuss, Dadalau et al. 2012).

In the following, the focal point is ball screw driven axes because these are commonly used as feed drive systems of machine tools. The servo motor drives through a coupling, if applied, a gear train and the ball screw. Its spindle is supported by a thrust bearing and, if necessary, by an additional loose bearing. The fixed type of support bearings, which consists of two fixed bearings, is also often used. Since temperature-driven elongation leads to restraint and therewith further temperature induction, additional cooling devices are needed, which increase the costs. By the ball screw nut the rotation of the spindle is transformed into translation of the carriage. The carriage bears further axes, the workpiece or tools. To avoid loose and backlash there is a pretension of the nut. This can be induced either by oversized balls or by tensing two nuts against each other. The position of the carriage is detected either by direct measuring devices like linear encoders or indirectly by a rotary encoder at the motor's or the spindle's end. In high precision machine tools usually both types of encoders are used coinstantaneous. The linear bearings define the carriage's moving direction and respectively its degree of freedom. There are several guiding carriages driving on a rail. All lateral forces and torques are deflected by them, thus the ball screw suffers only from axial load. Since the mentioned components are important in order to achieve high accuracy in positioning, they must be protected against dirt, chips and coolant using telescopic covers or bellows. The energy supply of further axes and the data

transmission of measurement devices are ensured by a cable drag chain moving with the carriage.

Bearings and ball screw are the main components of ball screw driven feed drives. They determine the feed drive's mechanical behavior and are discussed in detail in the following sections. In this work, both ball screw and linear motor driven axes are measured. However, the focused feed system is the ball screw because of its common use. It is observed by serial examinations of machine tools at machine tool makers' plants, at a test rig and in a simulation.

2.1.1 Bearings to support ball screws

The ball screw is supported either by fixed loose types of rolling bearings or fixed types of support bearings. For rather short or hanging axes only a fixed bearing can be sufficient. Since friction is the relevant parameter for wear and heat induction, its sources and influencing factors are discussed in detail below. By these bearing concepts both a high rigidity and a low friction can be achieved.

For reasons of accuracy, applicability for high rotation speed and low friction spindle bearings are used as fixed bearing. Often cylindrical roller bearings are used as loose bearings because they already imply the characteristics of a loose bearing. Since friction is one of the interesting parameters, the calculation of macroscopic friction torque is shown in the following sections.

These days, the carriage is usually borne by linear roller bearings. The calculation of their friction force is similar as that for rotational bearings. For special applications like hard turning or planning sometimes sliding bearings, which have a higher friction and damping to reduce vibrations, are used.

Ispaylar (1996) compared the friction behavior of ball roller and sliding bearings. His results show an obvious higher friction and a nonlinear behavior of sliding bearings, especially at low speed because of stick slip transition. By a logarithmic plotting this nonlinearity becomes clearly visible as shown in figure 2.2. On the

other hand, the roller bearings have an approximately constant behavior and facilitate friction compensation.

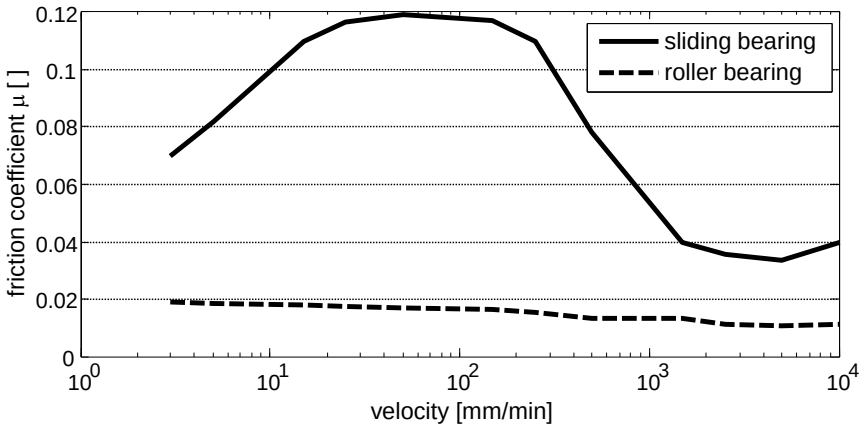

Figure 2.2: Comparison of friction coefficient of sliding and roller bearing, (Ispaylar 1996).

Plotting this figure with linear velocity axes the friction of the sliding bearing results in a Stribeck curve. This means a distinct sticktion superelevation for small velocities, a minimum at the so called Stribeck velocity, here around 5000 [mm/min] and an increase of friction force at high velocities.

Rotational bearings

There are two types of rotational bearings, axial and radial bearings. Furthermore, it can be distinguished between one and two degree of freedom types of bearings, all other directions are inhibited by a high stiffness. In ball screw driven axes usually the axial load can be supported by radial bearings, thus the fixed bearing often is a radial bearing allowing carrying an axial load.

The entire friction of rolling bearings is small compared to sliding bearings and strongly depends on the configuration of the bearing, (FAG 1999). The complete friction torque T can be calculated roughly using the friction coefficient μ, which is given in empirically determined tables, depending on the resulting load F and the diameter of bore of the bearing d.

$$T = \mu F \frac{d}{2} \tag{2.1}$$

However, several boundary conditions have to be fulfilled. These are a preponderating radial load in radial bearings and a medium rotational speed range. Otherwise, the calculation of friction must be separated in a load-independent torque M_0 and a load-dependent torque T_1.

$$T = T_0 + T_1 \tag{2.2}$$

The load-independent torque T_0 depends on the viscosity of lubricant $\boldsymbol{\nu}$ and the rotational speed. However, viscosity is temperature-sensitive, which means there are severe changes by the quantity of heat induced by the bearing's friction. Furthermore, there are influences by the bearing's size d_m and the shape of the contact area f_0.

$$T_0 = f_0 10^{-7} \left(\boldsymbol{\nu} n\right)^{\frac{3}{2}} d_m^3 \tag{2.3}$$

The dependence of friction on viscosity $\boldsymbol{\nu}$, ratio of radial load F_r and static load rating C is shown in figure 2.3.

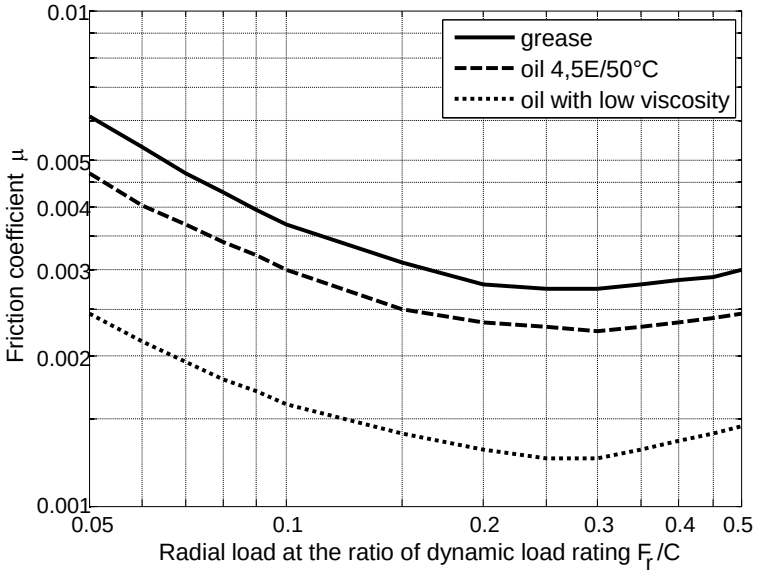

Figure 2.3: Friction coefficient of several lubricants with different viscosity. The friction coefficient is depending on the used lubricant and its viscosity, (INA 1968).

The load-dependent torque T_1 consists of a factor equivalent to load f_1, the load P_1, which is composed of preload, external load and the bearing's size d_m. Alignment failures cause reactive forces, which are to be included in external forces.

$$T_1 = f_1 P_1 d_m \tag{2.4}$$

The sticktion, which means the initial breakaway torque, can explicitly exceed especially at low temperatures and touching seals. The friction caused by seals is highest for new bearings and declines during running-in, (FAG 1999). The velocity dependence of friction leads to a typical Stribeck curve.

During start-up and after greasing the friction torque temporarily increases. However, after a few rotations it drops to the basic value. This is caused by grease entering the raceway, which is pressed out by the moving roller bodies, as shown in figure 2.4, (Baly 2005). Hence the run-in must be finished before conducting measurements; otherwise the results are not reliable.

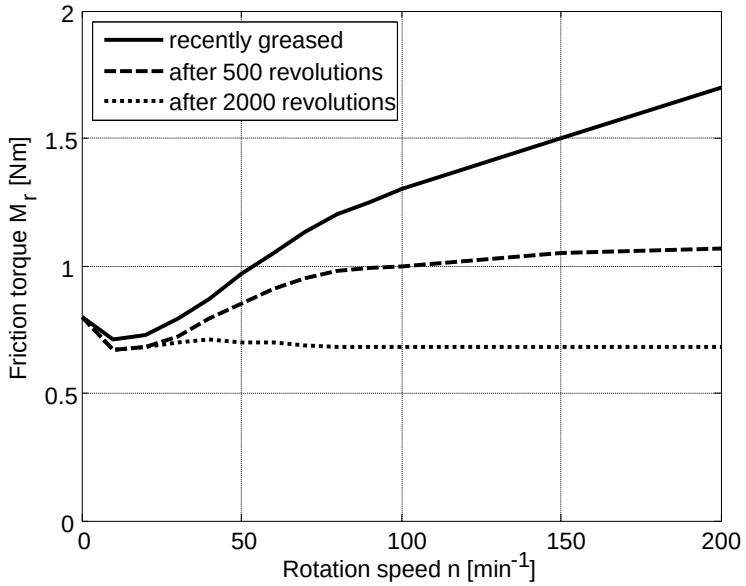

Figure 2.4: Change of friction characteristic during running-in after greasing, (Baly 2005).

Concepts of bearing arrangements The preferred bearing system of two bearings, which is equal a statically determined system of fixed and loose bearing,

can be realized in different bearing arrangements. These are fixed loose bearing, fixed and floating type support bearing. In machine tool axes fixed loose and fixed type of support bearing are commonly used, fixed type of support bearing is often used for the spindle bearing, (Muhs, Wittel et al. 2003, Beitz and Grote 2001).

Fixed loose bearing In a fixed loose bearing the so called fixed bearing supports radial forces and axial loads in both directions. Thus only bearings, which have no axial degree of freedom, can be used. Their inner and outer ring must be fixed again axial movement on the shaft and in the housing. This fixed bearing determines the axial position of the shaft. Thus, it has to transfer both axial and radial forces onto the support. In general, this functionality can be fulfilled by a single bearing, but due to a combination of high axial and radial load often two bearings are used to separate this load in axial and radial portions. The loose bearing can only support radial forces. For adjusting of thermal elongation respectively compensation of tolerances axial movement is possible. This can be realized by a cylinder roller bearing or needle bearing, which already contain an axial degree of freedom. Another possibility for realization of axial movement is a loose fit of the bearing's ring, which is under punctual load. A schema of fixed loose bearing is displayed in figure 2.5.

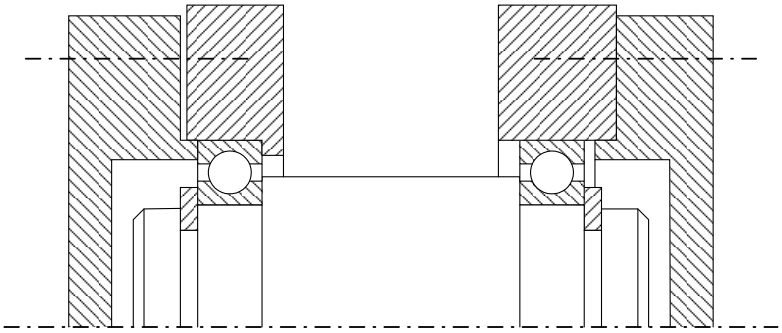

Figure 2.5: Fixed loose type of bearing arrangement.

Support bearings In support bearing the radial force is apportioned on both bearings like the fixed loose bearing. However, each of the two bearings absorbs one direction of the axial force. The support bearing can be either constructed as

floating type, which allows a determined axial movement of the shaft, or as fixed type, which does not allow any movement.

Floating type of support bearings The floating type support bearing is low priced solution, which is preferred in case of great tolerance of axial position of the shaft or if the axial position is determined by other devices for example herringbone gearing.

If the used bearings are self-retaining, they must be mounted that one bearing has an axial clearance S in one direction and the other bearing in the opposite direction. Due to clearance fit of the ring with punctual load of both bearings, axial load moves the shaft 2.6. If the bearings are not self-retaining both rings must be fixed because the movement occurs in the bearing. The bearings support axial load only in one direction. The axial clearance must be defined by construction.

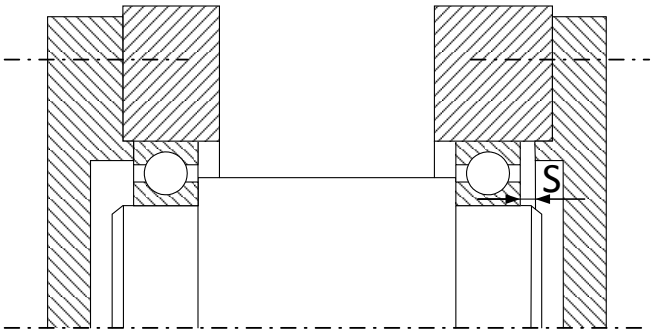

Figure 2.6: Floating type of support bearing.

Fixed type of support bearings In this bearing system two angular contact ball bearings or respectively tapered roller bearings are assembled inversely as displayed in figure 2.7. The clearance and respectively the pretension of the bearings are adjusted by a nut or threaded ring, which fixes the rings of the bearings. After adjustment it must be fixed. For example the fixed type is used in spindle bearings of machine tools.

The adjustment can either be an X- or O-arrangement as shown in figure 2.7. In the O-arrangement the direction of lines of pressure are pointing outside the

bearing system and in the X-arrangement inside. Due to this the span D of the support reaction forces is different. The tilting clearance of the O-arrangement is smaller than the X-arrangement. During construction the thermal elongation must be considered.

This kind of support bearings has a high construction effort and needs a precise assembly process to avoid high preloads, which can damage the bearings. Furthermore, temperature caused elongation of the shaft will increase the preload and consequently the friction in the bearing, which can cause damages, too. This can be avoided by an additional cooling system.

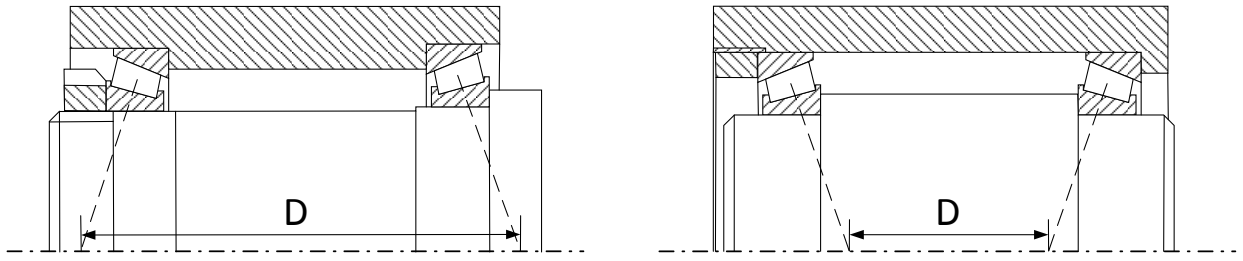

(a) O-type support bearing. (b) X-type support bearing.

Figure 2.7: Fixed type of support bearing with the support span D.

These displayed characteristics of bearing concepts illustrate the common use of fixed type support bearings in spindles and fixed loose bearings for support of ball screws.

Assembly of rotational bearings During the assembly of bearings the pressing force must not cross the rolling bodies. Otherwise the bearing will be damaged. Thus special tooling must be used to avoid damages.

Defect bearings can be detected by sluggishness, backlash, noise, temperature and vibration occurring during rotation.

Whether a bearing reaches its design life time, strongly depends on operating conditions. High load, impact loading, high temperature and intrusion of dirt or water should be avoided. Especially when dealing with dirt and wet conditions encapsulated bearings are available. Depending whether the bearing is used as

fixed or loose bearing, the outer, the inner or both rings must be axially or radially fixed with housing or shaft. Therefore, both shaft and housing must keep tolerances.

In general, the rotating ring - the outer or inner ring - is exposed to circumferential load and the standstill ring to a concentrated load. In order to avoid microslip causing wear, the tolerance of the circumferential loaded ring must keep an interference fit, while the other ring is tolerated in a medium or clearance fit. If there are impact loadings, both rings must keep tight fit, (FAG 1999).

On a shaft the inner ring is pressed against a shaft shoulder by a clamp screw, nut or clamping sleeve.

The outer ring is usually pressed into the housing against a stop bar and fixed with a cover plate or a retaining ring. Loose bearings often have axial backlash. However, there must be enough pressure to avoid the ring rotating.

Linear bearings

Linear bearings allow moving into a designated direction and disable all other linear and rotational directions by a high stiffness, (Ispaylar 1996, Bosch Rexroth 2006). Roller bearings are characterized by a low and uniform displacement resistance. The influences on friction are identical as with rotational bearings:

- load
- pretension
- velocity
- lubricant (viscosity and amount)
- temperature (influence on viscosity of lubricant)
- alignment errors (reactive forces)
- seals (slip force of touching seals)

Thus the resulting friction force is a Stribeck curve similar as with rotational bearings.

Assembly of linear bearings For assembly of linear bearings onto the machine base there are detailed guidelines given by the supplier, for example from Bosch Rexroth (2006). Especially amount and direction of load are determining the number and configuration of collateral shoulders or side fixations. Furthermore, these shoulders or fixations increase the lateral stiffness of the linear guiding system. In order to transmit lateral loads, the shoulders must be placed in direction of the flux of force.

Often there is no need of shoulders for reasons of force transmission, but these have advantages for the accuracy as well. Thus, to achieve of a desired high precision it is indicated to use shoulders for assembly. However, it is recommended to use a shoulder only at one of the parallel rails, otherwise a very precise manufacturing of the shoulders becomes necessary in order to adjust both parallel.

There are three different assembly types displayed in order of the achievable accurateness, (Bosch Rexroth 2006):

1. Without shoulder: The achievable accuracy is strongly depending on the straightness of the assembly process of the guide rail.

2. One shoulder: The accuracy results from precise pressing of the guide rail against the shoulder during assembly and straightness of the shoulder. Furthermore, the accurate attachment of the parallel rail has a severe influence.

3. Two shoulders: The accuracy results from accuracy, especially straightness and parallelism of the two shoulders.

The procedure of adjusting the guide rail is the basis for the accuracy achievable during the assembly process. There are different approaches of assembling linear guides in order to obtain a desired accuracy by limited effort. By precise adjustment of the guide rail before tightening the attachment screws, shoulders can be omitted. In order to determine whether and where shoulders are necessary, the

assembly process must be planned. For a good planning of the assembly process, product-specific assembly instructions must be respected. The achievable accuracy strongly depends on the adjustment process. This is illustrated in table 2.1.

Description	Achievable accuracy
depends on assembly process	no accuracy
adjustment by hand	limited accuracy
adjusting with auxiliary material (indicating caliper, assembly carriage) at a stop face	moderate to high accuracy
adjusting by pressing at a shoulder	high accuracy
adjusting at a shoulder	very high accuracy

Table 2.1: Adjustment process and reachable accuracy of linear bearings, (Bosch Rexroth 2006).

For the usage of shoulders and especially fixation of the rails, additional installation space becomes necessary. This must be conforming to the machine concept.

The shoulders also increase the stiffness of the guiding system, which is beside the higher achievable accuracy a desired behavior.

The load forces and torques affecting the linear guides are used to calculate their life time. However, these are only partly known. It is especially difficult to estimate the forces caused by assembly errors so that they can be used for calculation.

2.1.2 Ball screw

Most feed drives in machine tools and other manufacturing units are driven by ball screws, (Frey, Walther et al. 2010, Frey, Dadalau et al. 2012), which are used to convert rotation into translation. A reduced reaction by the transmission of the lead screw, high achievable axial load and a good price/performance ratio are motives for using ball screws. In machine tools only preloaded ball screws are applied because of dynamic reasons.

Backlash and preload In order to eliminate the backlash between ball screw spindle and nut, several methods for adjusting the preload can be used.

Depending on the spindle diameter and pitch it is possible to transmit dynamic loads of several hundred kN by ball screw drives. The increase of roller friction by preload induces at high velocities, for example at rapid speed, heat. This influences the precision of the involved machine axis by elongation. High axial forces and high velocities put a severe strain onto the screw thread.

It is possible to reduce the load on roller bodies and thread by adaption of the construction and production process. Between two normal bearing roller bodies a distance keeping roller body can be placed, which has a few micron smaller diameter. These bodies do not induce any pressure into the screw threads and thus are not forced to roll. However, they have contact with the bearing roller bodies and their spin is in the opposite direction. This procedure reduces the wear caused by contact of carrying roller bodies, but at the same time also the axial carrying capacity. Another method to reduce the friction between the roller bodies are polymer bearing cages. However, these are very expensive and thus mainly used in special applications like ball screws for high speed axes.

As mentioned above, usually a ball screw is used in machine tools to convert the rotation of the servo motor into a translational movement of the carriage. The ball screw must be stiff and without backlash to avoid additional backlash. The stiffness is depending on the tolerance class of the ball screw. Furthermore, the stiffness is obviously connected with the bearing conditions. In the standard DIN 69051-6 (1989), this difference of axial stiffness of fixed loose bearings and adjusted bearings is described in detail.

Although the ball screw's rotational stiffness is constant, its axial stiffness c_{ax} depends on the carriage position, which is also described by the standard mentioned above. Furthermore, it depends on material and geometry constants like Young's modulus E, diameter d and length l of the spindle. The position dependence and bearing conditions are described by the following equations of the stiffness, (DIN 69051-6 1989):

$$c_{\mathrm{ax}}(x) = \frac{\pi E}{4}\frac{d^2}{x} \qquad \text{fixed/loose bearing} \tag{2.5}$$

$$c_{\mathrm{ax}}(x) = \frac{\pi E}{4}\frac{d^2 l}{x(l-x)} \qquad \text{adjusted bearing} \tag{2.6}$$

Both the position dependency and the bearing conditions are displayed in figure 2.8.

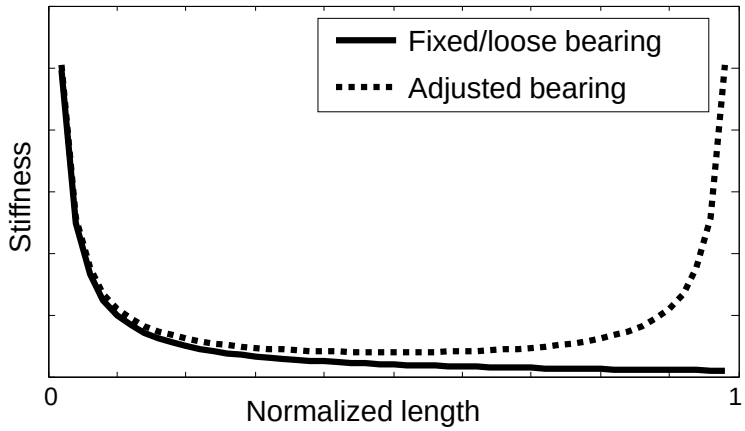

Figure 2.8: Axial stiffness of a ball screw depending on bearing conditions and carriage position over normalized length of spindle, (DIN 69051-6 1989).

Fixed loose bearings are less precise but cheaper than adjusted bearings. Furthermore, usually with adjusted bearings pretension is induced, which increases the stiffness of the ball screw. However, normally additional cooling systems are necessary to avoid forces induced by thermal induced expansion, which increases costs.

2.2 Sources and modeling of friction

In this section, a general review about friction, common models, its sources and parameter estimation from measurements are given. Both static and dynamic models are displayed and assessed with regard to the desired evaluation of assembly deviations.

2.2.1 Important friction models

In general, friction is a resistance against movement, which occurs between the contact surfaces of bodies. In physical models friction is often neglected, especially when it is not measurable or small. The kinetic energy is dissipated as thermal energy. Usually there are stick and slip friction, which are not clearly separable and can occur either simultaneous or alternating. The stick-slip transition is a source of vibration, (Canudas de Wit, Olsson et al. 1995).

There is a multitude of models describing several different aspects of friction. There are several surface forces responsible for friction, these are mainly van der Waals and electrostatic forces, (Ruths and Israelachvili 2011). However, since there are a large number of influences on friction behavior, for example surface texture, material and lubrication conditions, a complete description does not exist yet, and the calculating capacity is still too small to simulate the behavior of these forces in atomic range. Furthermore, these impacts often are subjected to manufacturing and assembly tolerances. In the following sections several important models are depicted. An extensive survey of models developed until the middle of 1990's is given by Armstrong-Hélouvry, DuPont et al. (1994).

In general, friction models can be distinguished between classical static friction models, for example Coulomb, viscous and Stribeck friction model, and dynamic models, which are dealing with jerk and acceleration dependencies or time-depending relaxations. Some typical static friction models are shown in figure 2.9.

Stribeck friction model

The Stribeck friction model is a static friction model and contains dry or Coulomb, viscous and mixed friction. The Coulomb friction F_C is a constant value with velocity direction depending sign. Which means, there is a discontinuity by a change of sign of velocity observable in figure 2.9(a).

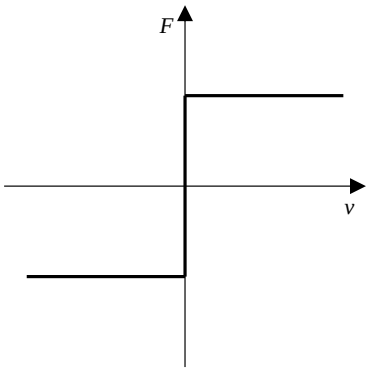

(a) Coulomb or dry friction.

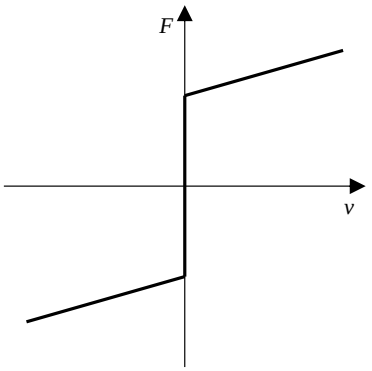

(b) Coulomb with additional viscous friction.

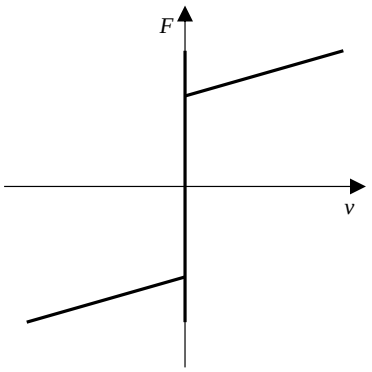

(c) Sticktion with viscous and Coulomb friction, which shows a discontinuity from sticktion to relative movement.

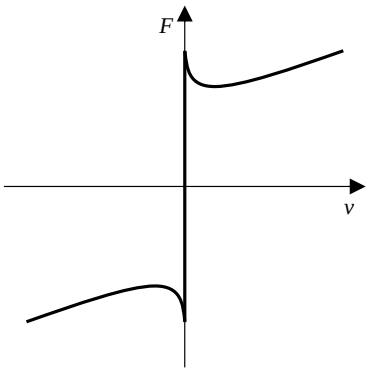

(d) Stribeck model with continuous force decrease from static friction level.

Figure 2.9: Typical static friction models with friction force determined by a static function except for zero velocity, (Olsson, Åström et al. 1998).

$$F_C = \begin{cases} -F_C & v < 0 \\ 0 & v = 0 \\ F_C & v > 0 \end{cases} \tag{2.7}$$

The viscous friction is proportional to velocity with the proportionality factor f_v. The mixed friction term is described by an exponential slope, which depends on velocity v and Stribeck velocity v_S, which is the velocity at which the steady-state friction force begins to decrease when the velocity is positive and increasing, (Drinčić 2012). A typical Stribeck curve is displayed in figure 2.9(d).

$$F_R = F_C + f_v\, v + f_S\, e^{\frac{|v|}{v_S}} \tag{2.8}$$

As visible in equation (2.8), there is a point of discontinuity at $v = 0$, which can cause some problems, for example oscillation in simulation models.

The velocity dependence of friction becomes comprehensible by a microscopic view of the contact shown in figure 2.10. At standstill, there is a direct contact of both surfaces touching on wide areas. At low velocities, there is a mixture of surface contacts and liquid friction and, at high velocities, a liquid film is establishing between the surfaces causing viscous friction. The sticking force is depending on the standstill period, which can be explained, since the lubricant is draining off slowly and the adhesion of the contact surfaces increases, (Teutsch 2005). It is not possible to describe this time-depending effect by a Stribeck model, which is a static friction model, but by using dynamic models with a time-depending velocity.

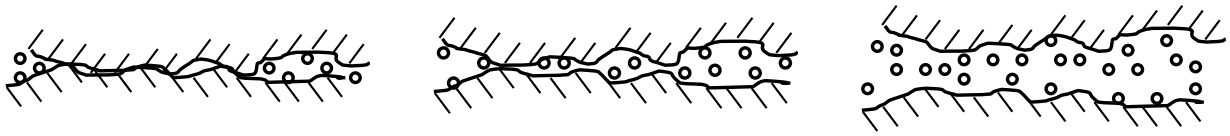

(a) Sticktion $v = 0$ (b) Mixed friction (c) Slipping

Figure 2.10: Microscopic view of lubricated contact surfaces at different velocities causing friction phenomena, (Teutsch 2005).

Extended Stribeck friction model Measurements of machine tool axes, which include many rolling contacts, particularly ball screws with high diameter, small pitch and a high number of carrying threads, show a declining friction behavior at high speed. This can be described by rolling friction and can be included digressive in the Stribeck model by an additional term, (Reuss, Dadalau et al. 2012, Albrecht 2009). This term consists of a proportional factor f_w and a velocity-depending slope.

$$F_R = F_C + f_v\, v + f_S\, e^{\frac{|v|}{v_S}} + f_w |v|^k \tag{2.9}$$

In figure 2.11 the described static friction models and the friction types they consist of are illustrated.

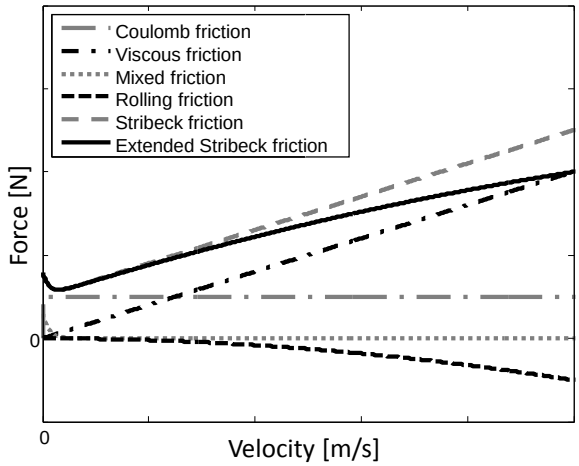

Figure 2.11: Comparison of Stribeck friction and extended Stribeck friction and the contained friction types, (Reuss, Dadalau et al. 2012).

It is obvious that at low speed the model behaves like the Stribeck model, but at higher relative velocity the additional rolling friction term, which effects the friction depending on the value of k. The main disadvantage of using the Stribeck or extended Stribeck model for simulation is the discontinuity at $v = 0$.

Karnopp model

To avoid the problems of sign change occurring in a classical static friction model at velocity zero, an alternative approach has been developed by Karnopp (1985). It eliminates the issue of detecting zero velocity and avoids the discontinuity, which means switching between different states, at change of sign by a steady characteristic of friction, which is also more plausible and improves the simulation results. The Karnopp model differs between stick and slip, where slip is a composition of Coulomb and viscous friction. Within a small velocity band around zero $\pm D_v$, the system is sticking and the sticktion force absorbs the complete driving force, which means the velocity to be zero and the friction to become force-dependent. Hence the friction force F_R is constant and equal to the Coulomb friction F_C at velocities higher than the velocity band and linear around $v = 0$ with the static friction F_S as maximum.

$$F_R = \begin{cases} -\text{sign}\,(v)\,F_C & v > |D_v| \\ vF_S/D_v & v \leq |D_v| \end{cases} \tag{2.10}$$

However, the main disadvantage of this model is its complexity increasing with the systems complexity.

Dahl model

The model introduced by Dahl (1968) is developed for simulation of control systems including friction. The model bases on the stress-strain curve known from classic solid mechanics. This means, while there is displacement the friction force increases until rupture occurs with the Coulomb friction force F_C as maximum of the friction force F_R. The stress-strain curve is modeled as differential equation with the displacement x.

$$\frac{\mathrm{d}F_R}{\mathrm{d}x} = c\left(1 - \frac{F_R}{F_C}\text{sign}\,(v)\right)^{\alpha} \tag{2.11}$$

Consequently, c is the stiffness coefficient, which determines the slope, v the velocity and α a parameter, which determines the curve's form. Usually $\alpha = 1$ is used. In time domain, the model is a generalization of the Coulomb friction. However, neither sticktion nor the Stribeck effects are included.

Bristle model

Haessig and Friedland (1990) described the bristle model first. It consists of two surfaces, which can be moved against each other. In between and connecting them, there are multitude bendable bristles, which are one approach to describe the behavior of the microscopic contact points. Thus, the bristles represent the manifold physical bonds between the two surfaces as shown in figure 2.10. However, due to irregularities of the surfaces it is impossible to represent each microcontact or interaction in reality by these bonds. Therefore, the reality can only

be approximated by a limited number of bristles. These bristles are massless and consist of a flexural resistant and a flexible part. In figure 2.12 on the left, the contact between two bodies represented by multitude bristles is displayed and, on the right, a single bristle is enlarged to illustrate the connection between flexible and rigid part. Rigid and flexible parts become connected when they occupy the same position. The load transmitted by each bristle is limited and proportional to its deformation. If the limit is exceeded, the bristle will break and a new bristle having smaller strain is generated at a random location relative to the previous location.

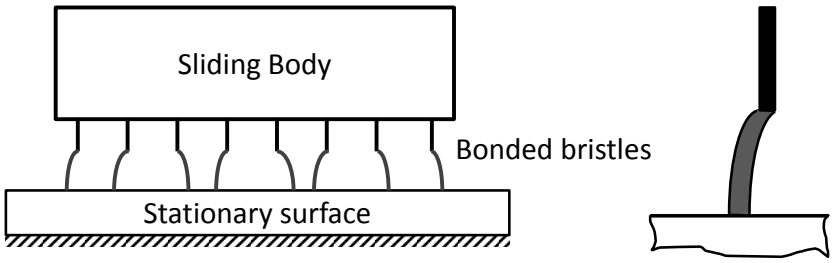

Figure 2.12: Bristle model, on the left side, the contact between two bodies represented by multitude bristles is shown and, on the right, one bristle is enlarged, (Haessig and Friedland 1990)

The friction force is calculated as sum of forces transmitted by each bristle. These are caused by elastic deformation of the N bristles with the stiffness c and the displacement of the position x_i from the position b_i, at which the i-th bristle has been created.

$$F_R = \sum_{i=1}^{N} c\,(x_i - b_i) \tag{2.12}$$

Since the model complexity increases with the number of bristles, only a small number should be used. Reasonable results are found with 20-25 bristles, but even one bristle gives a reasonable quantitative behavior, (Olsson, Åström et al. 1998). The model captures the random nature of friction, but the randomness is depending on the number of bristles. Furthermore, there is no damping, which can result in oscillating motion in a sticktion case.

LuGre model

The LuGre model presented by Canudas de Wit, Olsson et al. (1995) is closely related to the bristle model, which is also an extension of the Dahl model. The average deformation of elastic springs models the friction. By tangential force the bristles will be bent and behave like deformed springs. If the deformation is large enough, the bristles will start slipping. This means, there is a stick-slip transition in the model. For a steady state motion, the velocity determines the average deformation of the bristles, which is low at low velocities. Thus, the deformation decreases with increasing velocity, which represents the separation of surfaces by an intermediate lubricant film. Hence, the LuGre model allows modeling the Stribeck effect very well.

Generalized Maxwell Slip model - GMS

The generalized Maxwell slip model is suitable for describing the friction behavior within a contact. It is a friction model, which is based upon a Maxwell model and can describe several states at the same moment. Thus, it is especially suitable for rolling contacts, in which contact with different velocities occur simultaneously, (Al-Bender, Lampaert et al. 2005). It consists of a discretized contact area, in which there are a finite number of parallel elastoplastic Maxwell or Jenkin elements. They have a common displacement input and are sticking until the stick-slip boundary is reached and, thereafter, they start to slip. This can be imagined to be a set of bristles, which are characterized by spring constant, slip respectively saturation force and their state, (Armstrong-Hélouvry, DuPont et al. 1994, Canudas de Wit, Olsson et al. 1995). During sticking, elastic deformation takes place and thus a deformation force computable with Young's modulus of the contact. During slipping, a friction force is acting against the direction of moving, (Jamaludin, Brussel et al. 2008, Fujita, Matsubara et al. 2011). This causes the typical hysteresis, which describes the energy dissipation by friction, shown in figure 2.13.

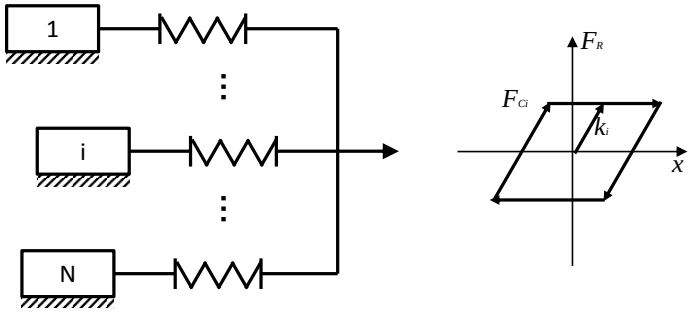

Figure 2.13: Generalized Maxwell slip model with N elementary friction models. On the left the elementary models consisting of mass, spring and friction force are illustrated and on the right the hysteresis of the i-th elementary model, (Jamaludin, Brussel et al. 2008).

Ruderman and Bertram (2011) developed a modified Maxwell slip model. Here the multitude parallel Maxwell elements are replaced by one mass with a spring with variable stiffness. Thus, the presliding behavior, which can already be described satisfyingly with the standard distributed Maxwell slip model, can be modeled with only two parameters.

Assessment of friction models

The described friction models are assessed with regard to their usability for a model to estimate the impact of assembly variances. The assessment is summarized in table 2.2. Thus, the Stribeck model is the only static friction model with low modeling as well as computation effort. However, the correctness of the results is limited but usually sufficient.

Since low modeling and computation effort are important for complex models and the correctness of the Stribeck model is still satisfactory, it is used for simulation in this work. Even though the Karnopp model is satisfying the specifications for modeling friction better, it can be neglected because there is no reversal movement during one simulation run.

In order to illustrate the complexity of friction caused by bearings, in the following section a general method for calculating the contact behavior of two bodies is

	Type	Modeling effort	Computation effort	Correctness
Stribeck	static	-	-	0
Karnopp	static	+	0	0
Dahl	dynamic	+	+	0
Bristle model	dynamic	+	++	+
LuGre model	dynamic	++	++	+
GMS	dynamic	++	++	++

Table 2.2: Assessment of discussed friction models, - means low and ++ very high.

explained. A GMS model is used to describe the friction distribution over the contact area.

2.2.2 Friction induced by bearings

A major source of friction in feed axes is bearings because they are joints between components moving against each other. Here, bearings mean linear bearings and rotational bearings as well as ball screws, which usually use rolling elements to provide the desired degree of freedom. Recently, most linear bearings in machine tools are ball and roller bearings. Still, there are sliding bearings used in some machine tools, but usually for special processes like hard turning or grinding, in which micro vibration has to be damped reliably. In bearings, friction occurs at components moving relative against each other like seals and contacts between ball and cage respectively ball and rail. In this section, a theoretical and general approach to determine friction in rolling contacts between ball and rail is described. The advantage of this approach is the possibility of determining stick and slip separately, (Reuss, Sakai et al. 2016).

Contact between ball and rail

Due to the contact surfaces' curvature there are sliding movements between rolling element and rail in rolling contacts. Hertz (1881) calculated the pressure distribution in the contact zone of a punctiform contact between two elastic and isotropic bodies, for example sphere and rail.

$$p(x,y) = \frac{3}{2}\frac{F_N}{\pi ab}\sqrt{1-\left(\frac{x}{a}\right)^2-\left(\frac{y}{b}\right)^2} \tag{2.13}$$

Teutsch (2005) shows modeling and simulation methods for other shapes of rolling elements, for example barrel-shaped bearings. Since the contact of a ball is easily understandable, it is discussed in detail here. The contact zone of a polydirectional curved punctiform contact is elliptic and there is a maximum of compression in its center $x = y = 0$, which is related to the normal force F_N, (Popov 2009).

$$p_{\max} = \frac{3}{2}\frac{F_N}{\pi ab} \tag{2.14}$$

Using the friction coefficient μ it becomes possible to determine the differential friction force over the contact area caused by the normal force acting on the ball.

$$\mathrm{d}F_R = \frac{3}{2}\frac{\mu F_N}{\pi ab}\sqrt{1-\left(\frac{x}{a}\right)^2-\left(\frac{y}{b}\right)^2}\mathrm{d}A \tag{2.15}$$

The infinitesimal area is described by $\mathrm{d}A = \mathrm{d}x\mathrm{d}y$. In order to calculate the complete friction force in the contact, an integral equation has to be solved. In figure 2.14 the contact between ball and rail is shown in front and side view in detail. Furthermore, top views of the elliptic contact area with differential velocity and friction force are illustrated.

Since the normal force is continuously distributed over the contact ellipse and the velocity has a change of sign at the lines of pure rolling, there is a significant discontinuity of the friction force, as displayed in figure 2.14.

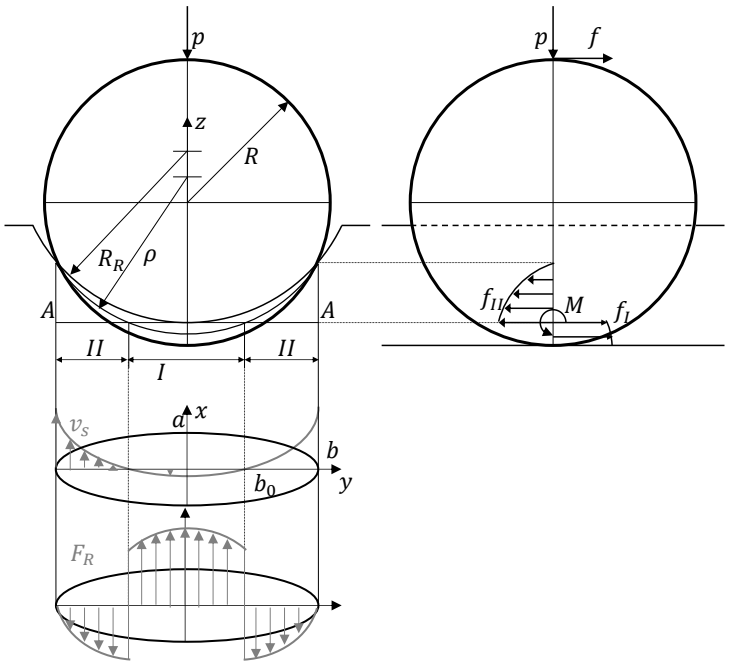

Figure 2.14: Contact of ball and rail in front and side view according to Ito (1957). Furthermore, top view of differential velocity v_s and friction force F_R distribution. The normal force is proportional the friction but remarkable is the discontinuity caused by the change of sign at the lines of pure rolling.

In many reflections, for example made by Ito (1957) or Ispaylar (1996), the tangential or friction force is assumed to be proportional to the pressure pattern. However, this assumption is only valid if there is no stick slip transition. Measurements show a discontinuity at this transition, as visible in figure 2.16. Stick and slip portions are depending on relative velocity and lubricant. To reproduce this behavior, Soda, Kimura et al. (1970) and Kimura, Sekizawa et al. (2002) assume the stick portion to be a linear increasing friction force, which is proportional to bristle stiffness, and the slip portion to be a constant friction force. To get a consistent solution of the integration over the elliptic contact area, the additive slip portion is replaced by a multiplicative one, (Reuss, Sakai et al. 2016).

$$F_R = \begin{cases} k_q u\,(x,y) & F_R \leq f_{\max} \\ C_v f_{\max} & \text{otherwise} \end{cases} \tag{2.16}$$

The positions of the pure rolling lines calculated with this model are nearly the

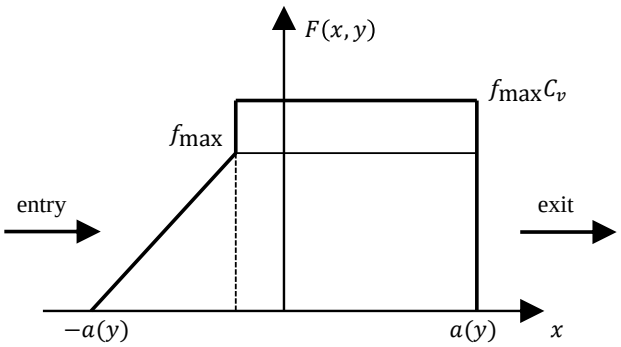

Figure 2.15: Friction model of Soda, Kimura et al. (1970) and Kimura, Sekizawa et al. (2002) distinguishing sticktion and slipping. The friction force at a stripe parallel to the moving direction of the contact ellipse is displayed. The sticktion part is shown by a linear increase of friction until the maximum friction force $f_{\max}$ is reached. Thereafter slipping occurs with the constant slipping friction force $f_{\max} C_v$.

same as given by Ito (1957) and Steinert (1996), although both are using different friction models, and Steinert makes several simplifications. However, in opposition to those approaches, the shown method allows to separate stick and slip portions. In figure 2.16 measurement, filtered measurement and simulation with an algorithm developed by Fujita, Matsubara et al. (2011) are compared. Further measurements comparing different lubrication conditions - dry, with grease and oil - are shown by Matsubara, Sayama et al. (2014). There the contact area is split into differential elements, which allow a numerical integration.

2.2.3 Estimation of friction

To estimate parameters for simulative or theoretical analysis from measurements often the least square estimation developed by Gauss (1825) is used.The model functions can be linear combinations of any in general non-linear functions. For this kind of model functions it is possible to solve the minimization problem analytically using the extremum. However, the friction consists of several nonlinear functions, which are impossible to be separated, thus the least square estimation is a rough approximation but at least sufficient for estimating the slipping friction.

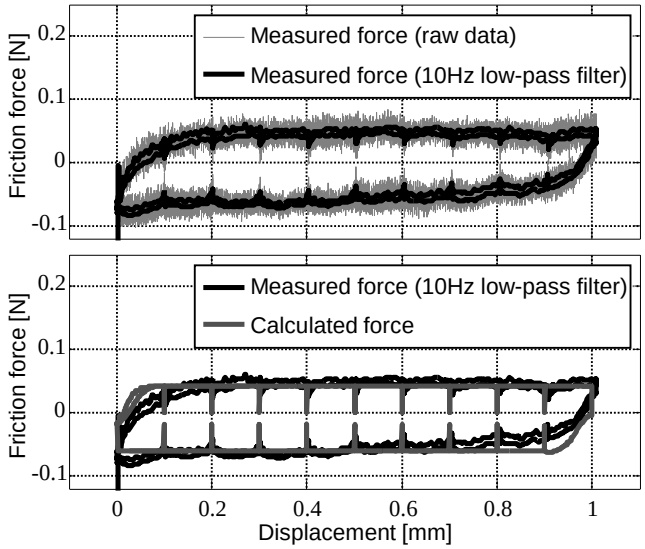

Figure 2.16: Comparison of measurement and simulation result of sticktion and slipping of ball and rail. The noisy raw data are filtered and compared with simulation results. Both the sticktion and slipping friction are estimated well, (Reuss, Sakai et al. 2016, Reuss 2016).

The least square method uses the parameter vector y, its estimation $\hat{y}$, the uncertain observations $\hat{x}$, the ideal observations x and its combination by a linear observation model with the observation matrix H.

$$x = Hy \tag{2.17}$$

The real disturbed observation contains both the ideal observation and an ideal stochastic error e.

$$\hat{x} = x + e \tag{2.18}$$

Thus the ideal observation error e is

$$e = \hat{x} - Hy \tag{2.19}$$

The parameter vector is estimated, because in general its true value is impossible to be observed, and the measurement failures must be approximated.

$$\hat{e} = \hat{x} - H\hat{y} \tag{2.20}$$

This approximation of the error is called residuum. A small residuum is equivalent to a model fitting the observations. By a good estimator the residuum between measurement results and model must be minimized, which can be done by the method of least squares.

$$J(\hat{y}) = \hat{e}^T\hat{e} = (\hat{x} - H\hat{y})^T(\hat{x} - H\hat{y}) \rightarrow \min \tag{2.21}$$

This quadratic function becomes minimal for a certain value of $\hat{y}$. It can be determined by the derivative, which has to be zero.

$$\frac{\delta J(\hat{y})}{\delta \hat{y}} = 2\left(-H^T\hat{x} + H^TH\hat{y}\right) \stackrel{!}{=} 0 \tag{2.22}$$

Thus the least square estimator results to:

$$\hat{y} = \left(H^TH\right)^{-1}H^T\hat{x} \tag{2.23}$$

$\left(H^TH\right)^{-1}H^T$ is the so called pseudo or Moore-Penrose inverse. It is unique and exists always, (Petersen and Pedersen 2008).

Uncertainty

The uncertainty can be estimated with a random experiment. n uncorrelated observation errors $e = (e_1, e_2, \ldots, e_n)^T$ are generated and their mean square value is the standard deviation σ times the identity matrix $\mathbf{I}$.

$$E\left\{ee^T\right\} = \sigma^2\mathbf{I} \tag{2.24}$$

This results in a covariance matrix without correlation. The deviation of the measurements $\Delta x = e$ propagate towards an error of the parameter vector.

If unbiasedness of the estimations is postulated $E\{\Delta x\} = 0$, the estimator will also be unbiased.

$$E\{\Delta y\} = E\left\{\left(H^T H\right)^{-1} H^T \Delta x\right\} = \left(H^T H\right)^{-1} H^T E\{\Delta x\} \tag{2.25}$$

For estimation of the deviation around the true value, the expected value of the squares of the error is observed.

$$E\left\{\Delta y \Delta y^T\right\} = \left(H^T H\right)^{-1} H^T E\left\{\Delta x \Delta x^T\right\} H \left(H^T H\right)^{-1} = \sigma^2 \left(H^T H\right)^{-1} \tag{2.26}$$

This result is called a covariance matrix.

Model quality

One advantage of least square estimation is the possibility to get a direct predication about the model quality. Thus the model assumptions can be evaluated to fit the reality. Therefore, the residua are compared with the measuring deviation.

$$J(\hat{y}) = \sum_{i=1}^{n} \hat{e}_i^2 \leq \sum_{i=1}^{n} e_i^2 \tag{2.27}$$

This inequation is valid because the least square estimator is determining the parameters with the minimum J. The expectancy value of the residua is

$$E\left\{\sum_{i=1}^{n} \hat{e}_i^2\right\} = (n - m)\,\sigma^2 \tag{2.28}$$

Thus, the more parameters m are estimated, the smaller become the residua. If the number of observed parameters is equal the measuring $m = n$, the set of linear

equations can be solved exactly and the residuum disappears. To estimate the model quality, the reduced χ-square test can be used. Therefore, the residuum $\hat{e}$ is determined and its square is compared with $(n-m)\,\sigma^2$.

$$\sum_{i=1}^{n} \hat{e}_i^2 \leq k\,(n-m)\,\sigma^2 \tag{2.29}$$

Often a measurement is accepted if k is smaller than 10, (Stiller 2006).

2.3 Simulation of machine tools as mechatronic system

The development process of machine tools can be supported by simulation. Thus examinations and manipulations become possible, whereas the realization with prototypes of the machine tool is expensive, dangerous or impossible. Simulation permits modeling and comparing a multitude of variants with limited effort and allows estimating the impact of various characteristics of components and variations within the assembly process. Thus, cost-intensive experiments with prototypes can be avoided.

Simulation models can be physical-technical as well as mathematical-abstract. Here, mathematical-abstract means a theoretical model to explain the behavior in reality, while physical-technical is a physical model, for example a prototype or a test rig. Obviously, mathematical-abstract models are easier to modify. Usually, mathematical-abstract models calculated by digital computers are used to understand observations in reality and to verify model concepts. In this work, measurements of machine tools are validated by examination with physical-technical models, which means prototypes or test rigs. From the results of these examinations mathematical models are derived, modeled in a mathematical-abstract model and verified by simulation.

In contrast to prototypes, the mathematical- abstract models allow to examine numerous variants with limited effort. This advantage is only available if

it succeeds to fit reality respectively in the field of machine tools the designer's approaches into computable algorithms. Therefore, the association of German engineers proposes in its guideline VDI 2206 (2004) the procedure shown in figure 2.17. Since machine tools are highly integrated mechatronic systems, this approach can also be used, (Broos 2012, Kipfmüller 2010). In a first step, elements and their couplings with a significant influence on the systems behavior have to be determined. These must be described by adequate physical parameters. In the next step, the designated parameters have to be converted into a mathematical model using physical equations. Finally, this model has to be preprocessed to allow computation.

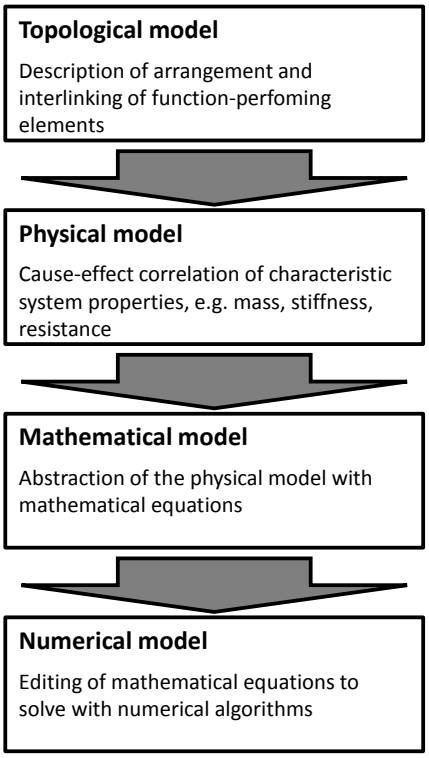

Figure 2.17: Modeling of mechatronic systems, (VDI 2206 2004).

The core of a machine tool is a mechanic system, which is driven by electrical components and controlled by electronically processed devices. Therefore, in the following sections simulation methods, which are applicable to represent mechanic systems, are discussed. Furthermore, methods for modeling mechatronic systems and especially machine tools are displayed and assessed.

2.3.1 Simulation of mechanical systems

The challenge of each simulation is to reproduce reality with a mathematical model, in which certain states or activities can be examined using numerical procedures. In mechanical simulation and consequently in machine tool simulation, mainly two methods are used depending on the application. These are multibody simulation (MBS) and the finite element method (FEM). FEM is focusing on structural deformation at a distinguished working point. MBS observes the machine tool's behavior during movements. Of these simulation methods FEM is more widespread in industry because often it is available as a plug-in in CAD systems and thereby available for constructing engineers. In the following sections, FEM and MBS are discussed but other common used simulation methods are introduced and finally assessed by referring to estimate variances caused by assembly failures.

Finite element simulation - FEM

The finite element method (FEM) is especially used to investigate strain and stress of structures under static or dynamical load. A real flexible structure has an infinite number of degrees of freedom (DOF) and can be calculated only in a few exceptions. Thus, there is the challenge to reduce these DOFs to a limited number. FEM splits the body into a finite number of elements, whose mechanical behavior is well known, and connects them at nodes using springs, dampers and constraints. In this manner there is a system with a finite number of DOFs, which can be described by a set of coupled differential equations or a matrix differential equation.

Static deformation can be calculated with Hooke's law, which is a direct correlation between the force acting on an element and its displacement. The resulting equations must be coupled appropriately with the element's bonds, thus a matrix equation system results:

$$F = kx \tag{2.30}$$

In this equation, the connection between the force F acting on a node and its displacement x in direction of its DOFs is described by a constant stiffness k, which is related to Young's modulus of the structure's material.

At first, the geometry and the DOFs of the mechanical structure must be modeled using a pre-processor. This model is meshed with appropriate algorithms, which means generating nodes and elements. With the material laws provided by the database of FE-software, a system of equations is determined and parametrized. The calculation is made by a solver and thereafter the results are visualized in a post-processor. Thus, it becomes possible for the user to interpret and analyze these.

The determination of eigenfrequencies and eigenmodes is analogous but a set of differential equations has to be solved. Usually this set is written

$$M\ddot{x} + C\dot{x} + Kx = F \tag{2.31}$$

Thereby the force vector F is calculated by mass matrix M, damping matrix C, stiffness matrix K and the displacement x and its derivations.

It is possible to reduce this matrix equation to an eigenvalue problem by several approaches for example with an exponential approach:

$$x = \hat{x}e^{\lambda t} \tag{2.32}$$

If there is no attenuation and for free oscillation, the following eigenvalue problem results:

$$\left(K - \lambda^2 M\right) x = 0 \tag{2.33}$$

Then the eigenfrequencies and eigenmodes of a mechanic system can be calculated. Often this approach is called “dynamical analysis in frequency domain”.

Multibody simulation - MBS

In order to calculate the dynamic behavior of a mechanic system, not in a single working point but during movement, multibody dynamics of rigid bodies is used as a first step of discretization, (Wittenburg 1977, Croon and Pruschek 2005, Shabana 2005). In general, MBS describes a mechanical system using rigid bodies respectively lumped masses, which are connected to each other. These bodies are connected by constraints, which restrict the DOFs in joints, springs, dampers and forces. The constraints lead to consistent motion of the bodies, which can be described by absolute or relative position of the bodies during time. The constraints can be modeled either by joints or directly with algebraic equations. In simulation software, usually the joints displayed in table 2.3 are available.

Type of joint	Revolute joint	Translational joint	Screw joint	Cylindrical joint	Cardan joint	Spherical joint
Degree of freedom	1	1	1	2	2	3
Example	rotational bearing	linear bearing	ball screw	quill, cylinder roller bearing	parallel kinematic	parallel kinematic

Table 2.3: Typical joints in multibody models

Besides the joints there are forces caused by spring-damper elements, contacts or directly as force vectors. These are mathematically specified by the equations of motion. Together with algebraic equations describing the constraints, this results in differential algebraic equations, which characterize the system’s behavior.

Contrary to FEM, MBS can calculate displacements and rotations, which are geometric nonlinearities generally not computable with FEM software. MBS software usually offers the following analysis tools:

- **Assembly analysis**: During assembly analysis the nonlinear equation derived from the modeled mechanism is solved. Thus, failures in modeling like

overdeterminations are detected. Therefore this analysis should be performed before MBS.

- **Kinematic analysis**: The kinematic analysis simulates position and orientation of all bodies in time domain with pretended motion. The DOFs constrained by the actuators must equal the DOF of the system.

- **Dynamic analysis**: Dynamic analysis calculates position and orientation of all bodies respectively with dynamical forces. Usually, the kinematic constraints in joints are substituted by flexible elements like springs and dampers. If the position of all bodies is only affected by external forces, the system will be a set of ordinary differential equations. If kinematic constraints exist simultaneously, this will result in a set of algebraic differential equations.

- **Inverse-dynamic analysis**: A movement pattern of one or several bodies is given to perform an inverse-dynamic simulation. This results in actor forces and loads in joints of the mechanical system. Especially this type of analysis is used to configure drives of machine tools.

- **Static analysis**: The static analysis is due to dynamic analysis and results in the system's state of equilibrium.

MBS is especially suitable to calculate the forces acting in joints and other coupling points. Furthermore, it permits to calculate displacement of the bodies against each other. The structural dynamics are neglected respectively concentrated in coupling points. This limits the exactness of the results, (Queins 2005).

The movements of a body in space are, for example, described by Newton-Euler equations. Here, the Newton equation represents the behavior of translational moving masses by the relation between force F and acceleration $\ddot{x}$ with the mass m as proportionality factor:

$$m\ddot{x} = F \tag{2.34}$$

For rotating masses the Euler equation describes the relation of torque M, inertia I and angular velocity ω and its derivation:

$$I\dot{\omega} + \omega \times I\omega = M \tag{2.35}$$

The challenge of MBS is to calculate position, orientation and interactions of bodies in space. Therefore, different algorithms can be used, for example the orientation can be calculated using Euler angles, which can be computed using quaternions. Quaternions are an expansion of real numbers and consist of a scalar and a vectorial part with the following characteristics:

$$Q = (u, \overrightarrow{v}) \tag{2.36}$$

$$Q_1 + Q_2 = (u_1, \overrightarrow{v_1}) + (u_2, \overrightarrow{v_2}) = (u_1 + u_2, \overrightarrow{v_1} + \overrightarrow{v_2}) \tag{2.37}$$

$$Q_1 Q_2 = (u_1, \overrightarrow{v_1})\,(u_2, \overrightarrow{v_2}) = (u_1 u_2 - \overrightarrow{v_1}\,\overrightarrow{v_2}, u_1\overrightarrow{v_2} + u_2\overrightarrow{v_1} + \overrightarrow{v_1} \times \overrightarrow{v_2}) \tag{2.38}$$

If two successive rotations are described by Euler angles, the complete rotation can be described using the product of the quaternions. Furthermore, reversal rotation is describable by change of sign in the quaternion:

$$\begin{aligned} A &= \quad Q = \quad (q_0, \vec{q}) \\ A^T &= \tilde{Q} = \quad (q_0, -\vec{q}) \end{aligned} \tag{2.39}$$

In simulation, mostly iterative computation algorithms are used to solve the Newton-Euler equations. This means, in each step the forces and torques in the model's joints are calculated and used to calculate the differential equations of motion.

Another method used for calculating multibody models is the Lagrange equations. For this a system of r generalized coordinates is used. Thus the Cartesian coordinates of each of the N mass points of the system can be determined by the following equation:

$$\begin{aligned} x_r &= x_r\left(q_1, q_2, \ldots, q_n, t\right) \\ y_r &= y_r\left(q_1, q_2, \ldots, q_n, t\right) \\ z_r &= z_r\left(q_1, q_2, \ldots, q_n, t\right) \\ r &= 1, \ldots, N \end{aligned} \tag{2.40}$$

Using the principle of d'Alembert forces of inertia and thereafter constraints are induced. The generalized forces can be calculated that describe the system's behavior. They also contain the torques.

$$Q_s = \sum_{r=1}^{N} F_r + M_r \tag{2.41}$$

The calculation can be easily expanded for rigid bodies. The Lagrange equations are suitable for computation algorithms, (Seemann 2006).

The computation of MBS is completely different compared to FEM. Whereas FEM calculation is solved using previously defined boundary conditions to solve the mechanism in a distinguished pose, is in MBS the differential equation solved by stepwise integration in time domain. Thus, the orientation and load of the mechanism can change during simulation. In machine tool engineering this can be used to drive along curves, while the load acting on the tool center point (TCP) is changing. Hence the strain of a machining operation in the joints can be calculated.

However, it is impossible to calculate the dynamic behavior of a machine tool using MBS because its components are interacting with drives and controller,

(Baudisch 2003). Therefore, a complete simulation of such a mechanism requires a detailed mechatronic model.

Hybrid multibody simulation

A recent trend in machine tool construction is lightweight design of moving parts. Since the impact of structural stiffness and damping on the static and dynamic behavior of machine tools has the same extent as stiffness and damping of the joints, it is necessary to consider the structural influence. For this purpose, the so called hybrid multibody simulation can be used. It combines the advantages of both simulation methods mentioned above - MBS and FEM - by integrating flexible bodies into a multibody model. Such a model consists of flexible bodies, which are interconnected by spring-damper elements or joints. As a first approximation, bars can be modeled by beam elements, (Botz 1992). Here bending modes of slim parts can be observed. Nowadays, the simulation software can import geometries calculated with FEM software. In order to get an efficient calculation method for hybrid multibody simulation, it is necessary to reduce the describing matrices to a minimal form without changing its dynamical behavior. Therefore, mostly the modal reduction is used together with the substructuring method developed by Craig and Bampton (1968), which allows to integrate the structural dynamics computed with FEM software with minimal effort, (Croon and Pruschek 2005, Kipfmüller 2010, Queins 2005). With hybrid multibody simulation the interaction of deformation of complex bodies with huge displacement can be observed. Furthermore, it is possible to combine MBS with topology optimization methods, which means, the forces acting on components in workspace are used to optimize their structures, (Neithardt 2004).

Computer aided control engineering - CACE

As the name suggests, CACE is mainly used in control engineering. Since it is a kind of modeling differential and algebraic equations as a block diagram, it allows modeling mechatronic systems in a very abstract way. Therefore, it is necessary

to determine the differential algebraic equations, which is difficult for complex systems. Furthermore, the model is complex and debugging is laborious. Since it is a very abstract model, it enables simulation of various physical domains in one simulation environment as demanded for mechatronic simulation.

Kinematic simulation

Kinematic simulation can be considered as simplified multibody simulation, which means only the joints' degrees of freedom, the joint' position and the bodies they connect are defined. It is often already integrated in CAD-systems to support the designers detecting collisions, even with a very rough model of the kinematic chain, during early stages of product development. Due to omitting of dynamics the calculation is very fast and the results can be interpreted easily. However, there are no reaction forces calculated and, therefore, this simulation method is not sufficient for dimensioning of machine tools and sophisticated analysis.

2.3.2 Challenges of simulation of mechatronic systems

The concept of mechatronics was introduced by the Japanese company Yaskawa Electric Corporation, who added electronic to mechanical products. Until today, this definition has been extended and includes the co-action of mechanical systems coupled with electrical or electronic systems and information technology. Here, the mechanical system can contain fluidic, this means hydraulic or pneumatic systems, and is mainly responsible for the function of the mechatronic system. Since there are synergies, mechatronic systems are more than a pure addition of the involved disciplines, (Isermann 2008, VDI 2206 2004). A diagram of a mechatronic system as combination of information technology and mechanics is shown in figure 2.18.

Designing a complex mechatronic system like a machine tool leads to a synthesis problem discussed by Heimann, Gerth et al. (2007): A system consisting of sensors, controllers and actuators, which is able to carry out the desired tool

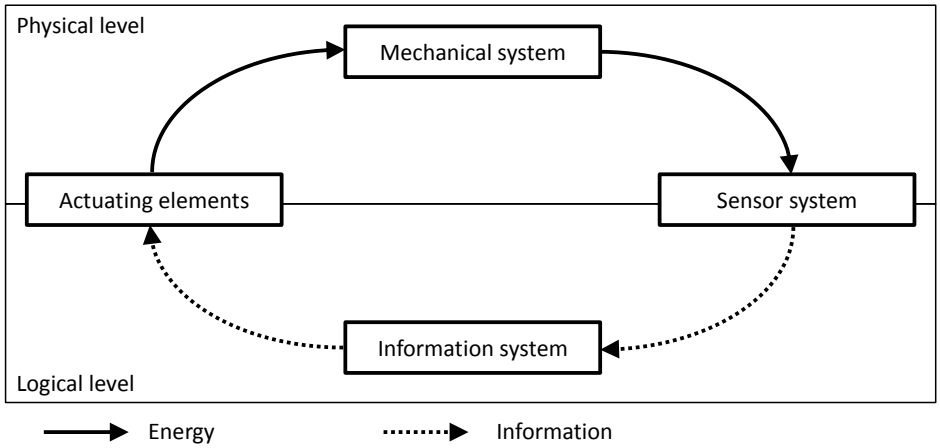

Figure 2.18: Mechatronic system as combination of mechanical and information system connected by sensors and actuators.

motion under disturbances, for example by process force, must be designed. Then the components, which have to be simulated in a mechatronic simulation model, can be determined. The components of a mechatronic model of a machine tool are shown in figure 2.19.

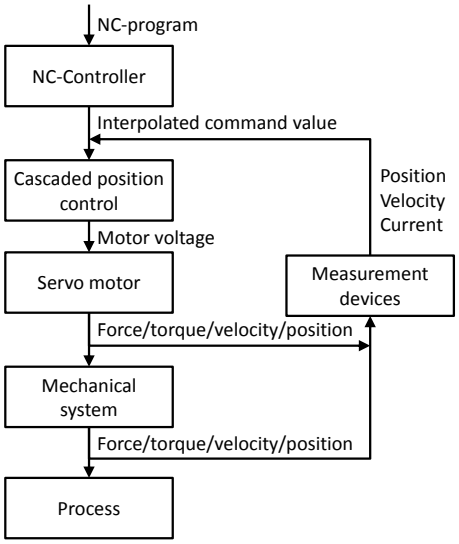

Figure 2.19: Schematic diagram of a machine tool as mechatronical system, (Kipfmüller 2010).

In order to describe the dynamical behavior of a machine tool, the interaction of controller, servo motor, the machine's mechanics and excitation by the process must be simulated. Mechanical and electrical quantities as well as signals must be simulated, which means simulation of a mechatronic system has to be proceeded.

Therefore, either one single simulation tool working in a very high degree of mathematical abstraction to allow combination of these different physical systems (Isermann 2008) or several simulation tools, specialized in the different physical domains, which must be coupled (Croon and Pruschek 2005), can be used.

There are different tools to solve the model either as co-simulation or as abstract mathematical model. However, these tools are not focusing on the demands of machine tool development, which is mainly hallmarked by the small key market and complexity of function. Especially the NC controller and its real-time communication are quite difficult to handle since geometry interpolation algorithms and controller structure are hardly known and not describable in a closed mathematical way without simplifications. Thus, the methods have to be combined to get an efficient support of the development process of machine tools.

2.3.3 Assessment of simulation methods

An extensive comparison of appropriateness of different simulation methods for machine tools during the product development process is made by Kipfmüller (2010). Furthermore, multibody simulation is used in several other works dealing with machine tools' behavior along their traveling distance, (Broos 2012, Kunc 2007). There, a good adequacy of multibody simulation is shown. This is especially based on the possibility of simulating the complete traveling range, which is an inherent characteristic of machine tools. Furthermore, a co-simulation to model a controller in computer aided-control engineering software is possible but leads to a tremendous increase of calculation time. The finite element method gives stationary better results than multibody simulation but the effort for modeling and simulating along the traveling distances is much higher. However, for special problems like structural stiffness and damping or optimization it is an important method. By hybrid multibody simulation, better results are reached than by using multibody simulation but the effort for modeling is much higher. Computer-aided control engineering allows to model mechanical systems, too. However, the models are very abstract and difficult to interpret. Kinematic sim-

ulation is both easy to model and very fast in calculation. However, the dynamic behavior is not modeled and thus the results contain no forces. The assessment is displayed in table 2.4.

	Traveling distance	Computing time	Modeling effort	Expert for modeling	Load calculable	Mechatronic simulation	Result
FEM	-	-	0	-	++	+	0
MBS	+	+	+	+	+	+	++
HMBS	+	- -	-	-	+	+	0
CACE	+	+	+	- -	+	++	+
Kinematic	+	++	++	+	-	-	-

Table 2.4: Assessment of discussed simulation methods. ++ means the requirements are completely fulfilled and - - they are not fulfilled.

Since neither the load can be calculated nor it is possible to model mechatronic systems, the kinematic simulation is not sufficient although it meets the other requirements very well.

The multibody simulation fulfills all requirements sufficiently and, therefore, it will be used in this work.

3 State of the art

In this chapter, the state of the art in quality measures for machine tool manufacturing, reasons and effects of assembly variances and measuring methods are discussed. First, important methods and measures of quality management in production and assembly process are described. Secondly, the reason for assembly variances and their impact on machine tools' general behavior are discussed in detail. Thirdly, measuring methods used for measuring machine tools' behavior are illustrated. These are finally quantified in order to be conducted at machine tool makers' shop floor during serial production.

3.1 Quality assurance in machine tool assembly

The quality of machine function depends on the quality of construction, the quality of manufacturing of components and the quality of the assembly process, (Spur 1996).

- **Function quality**: Is the capability of a machine to fulfill the customer requirements.
- **Construction quality**: Is simplicity and robustness of a machine against variances of components and assembly process. This can be assured for example by easily adaptable assembly interfaces.
- **Manufacturing quality**: Quality and tolerances of the machine's components.

- **Assembly quality**: Likelihood of appearance of errors and variances during the assembly process.

The superior quality is the function quality, which is an attribute of the complete product and contains the other types of quality. Secondary is the assembly of the components. The result of the assembly process strongly depends on the quality of the components and the construction. The construction quality is characterized by avoiding assembly failures. The relationship between these qualities is shown in figure 3.1.

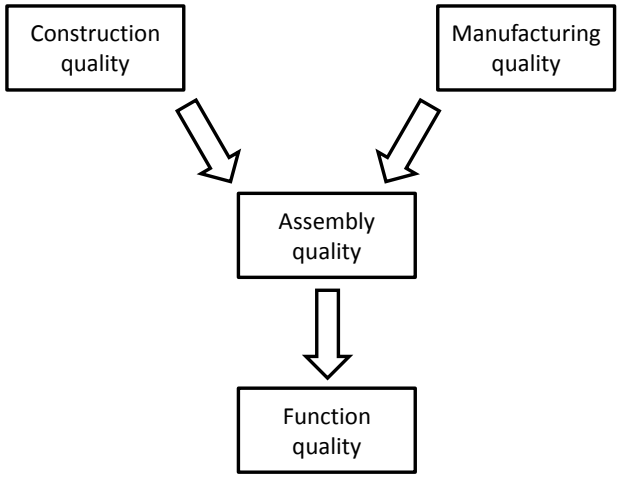

Figure 3.1: Influences on the function quality of machines, (Spur 1996).

Furthermore, there are several standards describing tolerances of components' geometry, assembly accuracy and of test workpieces in detail, (DIN ISO 230-1 1999, DIN ISO 230-2 2011).

The traditional methods of quality management are developed for individual processes, which mean they observe only effects of one quality characteristic. Thus, the possibility of applying these in complex assembly processes is limited, (DIN EN 60812 2006, Hielscher 2008).

3.1.1 Quality management

Quality management is all organizational measures to increase the process quality, the performance and thus the product. It is a key task of the management.

In machine tool engineering, the standardization of processes is not as technically mature as in, for example, aerospace or automotive engineering, because the lots are smaller. However, requirements on safety for the operating personnel is increasing, thus the standardization of development and assembly must also increase to get reliable results. Recently, guidelines for safety of machine tools have become engineer standards (DIN EN ISO 13849-1 2008) replacing former guidelines.

In the following, commonly used quality management methods are discussed.

Failure mode and effect analysis - FMEA

FMEA is a standardized analytical method to evaluate the reliability in quality management, (DIN EN 60812 2006). Hence all possible failures of a construction or process and their effects are evaluated. The FMEA observes the system behavior with regard to a breakdown of one component, but not of several components at the same time. It is used preemptively to increase the reliability of products. Thus, potential failures are analyzed by identification of failure location, determination of failure type and description of the error propagation, (DGQ 2012).

The fundamental idea of FMEA is to prevent failures before they occur. By an early identification and evaluation of reasons for failures, the costs for measurements and error correction during production or even at the customer's plant are avoided. Furthermore, the gain of knowledge allows avoiding the repetition of design faults in new constructions or processes. There are several different types, namely design and process FMEA, which are discussed in the following paragraphs.

Design-FMEA In order to improve the quality of constructions and to avoid problems in later steps of product life-cycle, the construction is analyzed for failures and their effects to be expected, (Tietjen and Müller 2003).

Process-FMEA The process-FMEA enhances the results of the design-FMEA, which has detected the weak points of the construction. Therefore, the production process, the production quality and their failures are focused on. The methods to estimate and interpret the quality and the tolerances are widely standardized and adopted in industry. Process-FMEA allows estimating the consequences of failures during the production or assembly process, but fails in evaluating the interrelation of several failures, (Tietjen and Müller 2003).

Robust design

The construction quality can be enhanced by "robust design" approaches. This method allows reducing the effects of variations of assembly process or components. Robust design uses nonlinearities of the system to minimize the impact of failures, (Taguchi, Chowdhury et al. 2000). This means the parameter of the command variable, which is the desired behavior of the system, are set to a point with minimal effect of failures.

In figure 3.2 a schema of the robust design approach is shown. The parameter and the command variable are related by the nonlinear curve. Even a small variation of the first parameter (I) leads to a huge variance of the command variable, whereas a wide variation of the second parameter (II) has nearly no effect. If such nonlinearity can be detected in a system, it allows increasing tolerances and reducing costs. Thus, in robust design nonlinearities of the system are used to minimize the influence of tolerances onto the system, (Molinari 2007).

Machine and process capability

In production processes the industry has high requirements to comply small tolerances. Machine and process capabilities are two essential criteria for evaluating this, (Schmidt 2005, Roenpage, Staudter et al. 2006). During the production planning of manufacturers the machine tools are benchmarked in order to decide, which machine can be used to produce the required parts. Machine and process

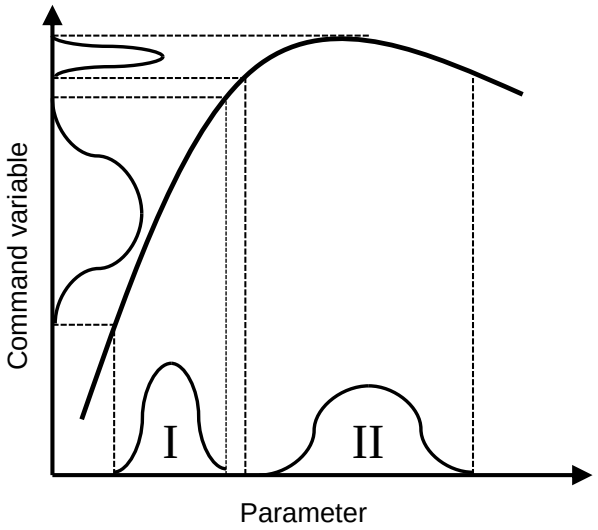

Figure 3.2: In robust design the nonlinearity of a system is used to minimize the effect of variations, (Taguchi and Asian Productivity Organization 1986).

capabilities describe the variances of the machine tool itself and the manufacturing process.

Machine capability distinguishes the stability and reproducibility of a machine tool, whereas process capability determines the production process. Thus, the capabilities give information about the tolerances a machine tool and process can keep and how many defective goods will be produced, (Abler, Felten et al. 2004).

3.2 Assembly errors of machine tool axes

Since the assembly process is stochastic, it is not possible to avoid assembly errors. However, if these are within tolerances defined by construction, the machine's operation capability will not be affected, (Schmidt 2005). Tolerances are profoundly discussed and standardized in several industrial standards. In the following, sources of assembly variances are discussed and results of former research are displayed.

3.2.1 Reasons of failures

The reasons for breakdown of machine tools must be examined, before the different kinds of assembly errors can be analyzed and evaluated. A detailed survey of failure causes of machine tools has been conducted by Fleischer, Schopp et al. (2007), Schopp and Munzinger (2009). Therein it crystallizes that one of the main reasons for breakdown of machine tools are the axes with about 38%. By further examination of the reasons for breakdown of machine tool axes, ball screw and both linear and rotational bearings are identified. In this work, the covers are neglected because of their tremendous variety and a lack of data. The data acquired by Schopp and Munzinger (2009) are displayed in figure 3.3.

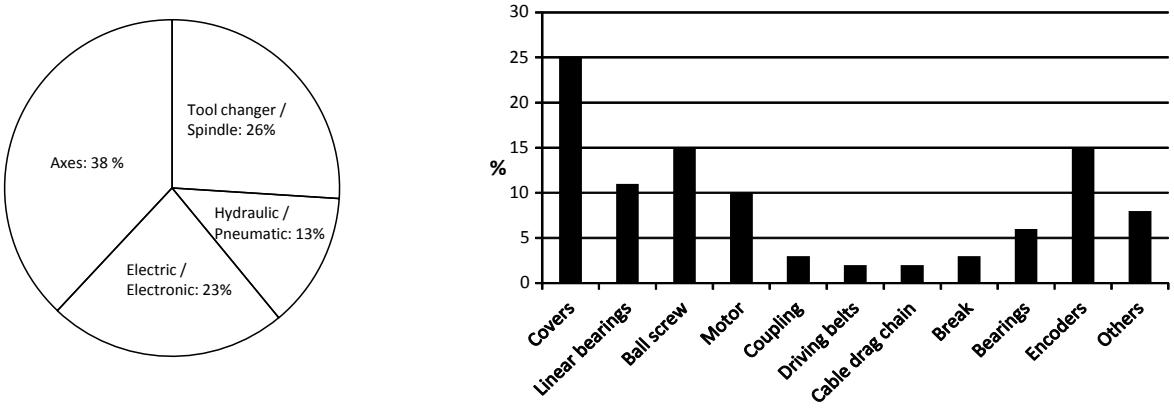

(a) Reasons for breakdown of machine tools.

(b) Reasons for breakdown of axes.

Figure 3.3: Detailed reasons for breakdown of machine tools and axes, (Schopp and Munzinger 2009).

Since obviously more than 10% of all breakdowns are caused by bearings and ball screws and these are standard components, they are focused in the following.

3.2.2 Tolerances

Since tolerances allow the exchange of components from different suppliers without a loss of functionality, tolerances for manufacturing and assembly are an important topic of engineering standards. Thus, the standardization of tolerances is

extensive and a basis for contracts, (Beitz and Grote 2001, Muhs, Wittel et al. 2003).

However, even if the tolerances given by the manufacturer of the components are well kept during the assembly process, there might be an impact on the components' duration by constraining forces and coaction of several variances, which can increase wear (Bosch Rexroth 2006). Thus, the interaction of assembly variances of several components must be considered.

3.2.3 Preload

A guideline given by the association of German engineers (VDI), (VDI 2230-1 2003), defines by means of the tightening process a calculation factor and, beyond this, it presents the variation to be anticipated by the particular tightening process. Even with the most accurate and, for this reason, expensive process, namely elongation-controlled tightening with ultrasound, this variance is ± 10%. However, elongation-controlled tightening is usually not used in machine tool assembly. From this follows that already the adjustment of pretension in bearings or ball screw nut has severe variations. Furthermore, complex assembly processes, especially with small lots, have a significant variation because the procedures change often and there is no routine or learning effect. Thus, it is rather difficult to produce complex machines like machine tools in constant high quality.

These assembly-related variances cause variances of preload and induce significant differences in stiffness and damping of joint patches as shown by Petuelli (1983). By increasing the preload, the contact stiffness also increases, whereas the damping decreases as displayed in figure 3.4. Furthermore, if the machining process of the components is changed, there will be a significant impact on stiffness and damping. This can be explained by the microstructure of the contact, (Teutsch 2005). The peaks of the surfaces are in contact and by increasing the preload the number of peaks in contact increases and simultaneously at the contact area. Thus, the stiffness increases because these contacts can be considered to be parallel springs. Furthermore, the contact points are solid contacts, which

have a smaller damping than fluidic contacts. Since ground surfaces are flatter than milled surfaces there is more contact at smaller preload. Consequently the contact stiffness increases.

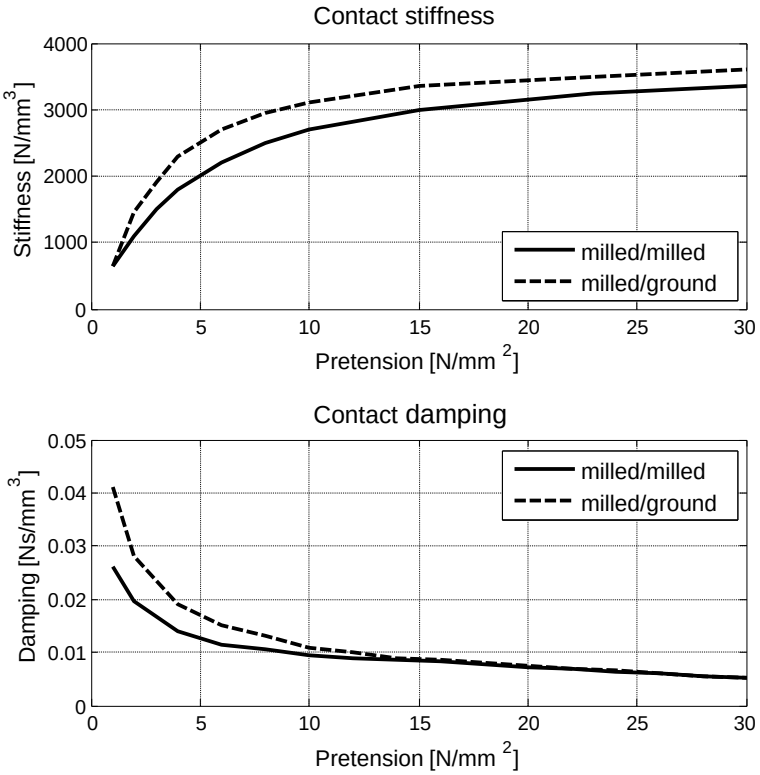

Figure 3.4: Stiffness and damping of joint patches under varying load, (Petuelli 1983).

Effects on damping

As mentioned by Petuelli (1983), the impact of joint damping on machine tools has been researched by Löwenfeld (1955). There has been demonstrated that, compared with the joint damping the structural damping of machine tools is negligible, because it is about one order of magnitude smaller than joint damping as shown in figure 3.5. The research of Löwenfeld has been done during the assembly process. On the left, there is the cast iron bed with a damping ratio of about 0.004, which only has structural damping, and on the right, the complete machine tool including the joint damping with a damping ratio of about 0.04 is shown.

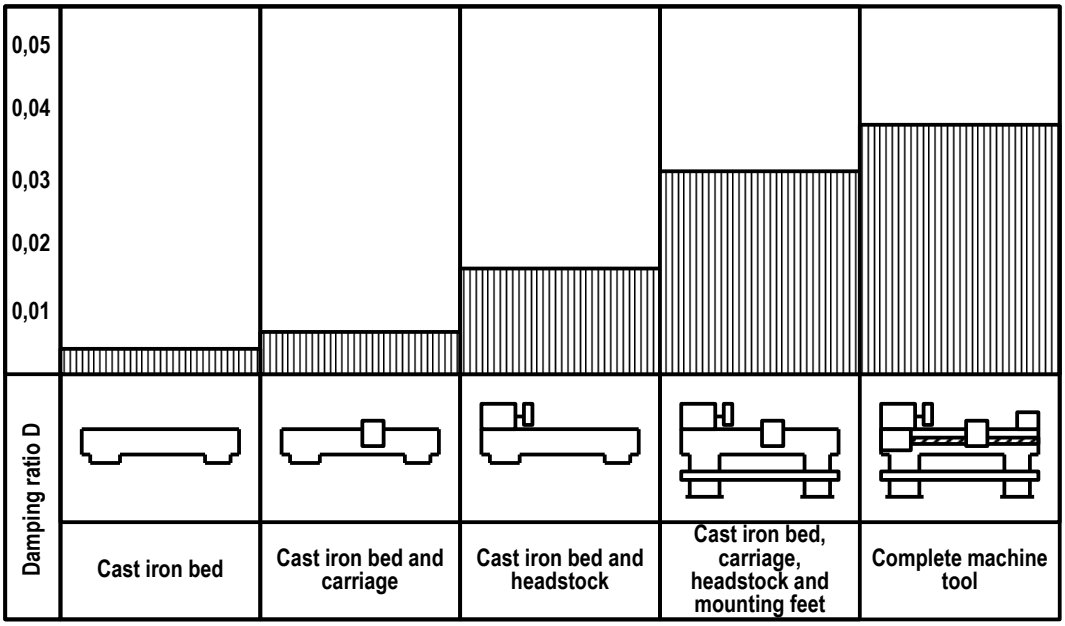

Figure 3.5: Damping of machine structures and joints researched by Löwenfeld (1955), (Petuelli 1983).

In a research project of the research association for machine tools and manufacturing technology (FWF) Kunc (2007) determined relevant damping influences in machine tools using a test rig and multibody simulation. He showed that the main source of mechanical damping and friction are caused by bearings and ball screw in feed direction. Further friction and damping sources like coupling, structural damping and damping perpendicular to feed direction have a minor influence on system attenuation. In his PhD thesis Kunc (2013) researched the examination of identification and modeling of nonlinear damping influences of machine tools.

The research unit FOR-1087 “Damping effects in Machine Tools” supported by the German Research Foundation (DFG) investigates the relationship between damping of single machine components and their assembly in machine tools. Here, damping of single components like bearings, linear guides, ball screws, machine beds and columns is examined as well as mounted feed drives in appropriate test rigs measured by adequate measurement methods. Brecher, Fey et al. (2012) have been focusing on components like linear bearings and developed a test rig and an identification method for damping parameters in standstill. In the near future, there will be catalog data for damping of linear bearings, (Fey 2013). Niehues, Schwarz et al. (2012) and Zäh, Niehues et al. (2011) are researching the

structural damping of machine tool structures and installation conditions. In order to increase the knowledge, a complete machine tool is assembled and measured. Since these are usually massive parts, the influence of placement has been analyzed in detail. Furthermore, the influence of simplifications on results in FEM was examined and model failures reduced.

3.2.4 Geometrical variances

Klein has inter alia inquired the possibility of measuring adjustment failures of monorail guidance and ball screw alignment, (Klein 2011). It has been shown that the accuracy of loose bearing of the ball screw has a strong position-depending influence onto the friction, which can be seen in the motor torque. The reason for this type of failure can be inappropriate assembly, subsidence or collisions during machining. However, irregularities of linear bearings' parallelism cause reaction forces, but because of the gear transmission ratio, which includes the ball screw transmission ratio, these have only a small influence on the motor current. Since the reaction forces are acting on the linear bearings, they will have an effect on their life expectancy.

3.3 Measurement methods in machine tools

In this section, several measurement methods for estimating machine tools accuracy, static and dynamic behavior are discussed and benchmarked with respect to their adequacy to be used in machine tools and during assembly process. It is to be considered, that machine tool makers as well as customers prefer controller-internal measuring, which means to use signals already available within the controller. Thus, there are no costs for additional sensors and evaluation systems and additional malfunction sources can be avoided, (Walther 2011).

3.3.1 Requirements

First the requirements for measuring in industry must be clarified. Together with machine tool makers the following measuring criteria have been identified, (Reuss, Dadalau et al. 2012):

- **Internal sensors**: To avoid additional effort and sources of failures internal sensor devices shall be used. Furthermore, this has the advantage, that in measuring the same machine tool, there is no variation caused by additional sensors and their mounting. However, there is the disadvantage of comparability of measuring results from different machine tools.
- **Internal recording**: The data logging during measuring shall be done controller-internal to avoid communication problems.
- **External analysis**: The analysis of the measured data is done externally and offline because the computing capacity of the NC controller is limited and there are usually no analysis tools available in the controller.
- **No modification**: Since the start-up is just finished, modification of the machine tools is not allowed at all.
- **Expert staff**: The measurement shall be conducted by technicians without special education.
- **Automatable**: To keep the effort small the measuring shall be automated.
- **Costs**: The additional costs shall be kept as small as possible.
- **Duration**: Since the machine tools are measured right before shipping to the customer, the duration must be kept as short as possible.

The requirements show several interdependences, for example, the duration of the measuring is closely correlated with the costs, with the machine hour rate as proportionality constant.

3.3.2 Positioning accuracy and repeatability

Since the geometrical accuracy, positioning accuracy and repeatability are defined as main criteria at the final inspection of machine tools, machine tool producers already measure and document these. Furthermore, the machine's accuracy is already standardized by several international standards, for example the DIN ISO 230 and 10791 series (DIN ISO 230-1 1999, DIN ISO 230-2 2011, DIN ISO 10791-1 2001, DIN ISO 10791-4 2001). The measuring has to be conducted by external devices like caliper and touchstones or a laser interferometer. Due to their flexibility, miscellaneous adaptability and the good operability, recently laser interferometers have been established as standard in industry.

The deterministic portion of positioning accuracy failures caused by spindle pitch errors or backlash can be compensated by NC controllers.

In order to measure the repeat accuracy, the standard DIN ISO 230-2 (2011) postulates repositioning of the carriage to several destined positions in workspace repeatedly from both directions.

The described measurements must be taken with the machine tool completely assembled. Furthermore, it must be in a stationary thermal state, preferentially 20 degrees Celsius. If there is a different temperature, compensation has to be conducted.

3.3.3 Force measurement

Force measurement using external sensors at critical locations, for example at a ball screw nut, gives detailed information about the load case. Thus, it is helpful to estimate the components durability. There are two types of measuring devices typically used. Namely, these are load cell and strain gauges, (MTS 2017). However, the measuring devices are expensive and it is impossible to integrate them in NC controller without severe modifications.

Strain gauges

In order to avoid stiffness reduction caused by measuring force with a load cell, strain gauges can be used. They register a deformation by change of electric resistance and are glued on the surface of the component, which is to be observed. Thereby, the deformation of the surface of the construction element and its Young's modulus are used to deduce the stress and with it and the known cross-section area to conclude the acting force as described by Hooke's law.

$$\boldsymbol{\sigma} = E\varepsilon = E\frac{\Delta l}{l_0} \tag{3.1}$$

$$F = \boldsymbol{\sigma} A \tag{3.2}$$

The disadvantages of this method are the need of additional sensors, which must be mount similarly in different machine tools, otherwise there will be a measuring failure.

Load cell

There are several types of load cells typically used. These are the spring and the piezo electric type. Both are observing the deformation of the cell by the relative displacement of the two connections to the mechanical system. In the spring type, the deformation of the spring is observed using the strain gauges described in section 3.3.3. The piezo electric type is using the piezo electric effect.

The load cell must be integrated into the force flow directly. However, besides the mentioned disadvantages, this series connection with additional stiffness reduces the overall rigidity, which is an undesired effect.

$$c_{\text{complete}} = \frac{1}{\sum \frac{1}{c_i}} \ , \ \ i = 1, \ldots, n \tag{3.3}$$

Both direct and indirect force measurements need external sensors. Furthermore, the recording of the data with the NC controller is not intended and, consequently, its implementation is a challenge.

3.3.4 Frequency response function estimation

Frequency response function (FRF) estimation is made by comparison of input and output signal. As input signal deterministic, stochastic, periodic or non-periodic signals can be used. However, important is that the input signal has to excite the whole bandwidth, which shall be examined. The complex transfer function $G(j\omega)$ is calculated based on the relation of the Fourier transform of output signal $Y(j\omega)$ and input signal $X(j\omega)$.

$$G(j\omega) = \frac{Y(j\omega)}{X(j\omega)} \tag{3.4}$$

In order to improve the interpretability, the transfer function can be separated into gain

$$G\left(\omega\right) = \sqrt{\left(\mathrm{Re}\left(G\left(j\omega\right)\right)\right)^2 + \left(\mathrm{Im}\left(G\left(j\omega\right)\right)\right)^2} \tag{3.5}$$

and phase shift.

$$\varphi\left(j\omega\right) = \arctan\left(\frac{\mathrm{Im}\left(G\left(j\omega\right)\right)}{\mathrm{Re}\left(G\left(j\omega\right)\right)}\right) \tag{3.6}$$

Typically, a machine tool controller contains a function to conduct frequency response measurements. However, usually a start-up engineer has to position the axes in the center of their traveling ranges and start the measurement manually. Furthermore, this procedure is not automatable. Another disadvantage is that the transformation into a frequency domain is a linearization, which means nonlinearities like friction are neglected, (Stiller 2006).

In figure 3.6 both a typical Nyquist and Bode plot are displayed. By these plots the system's behavior and stability can be investigated graphically.

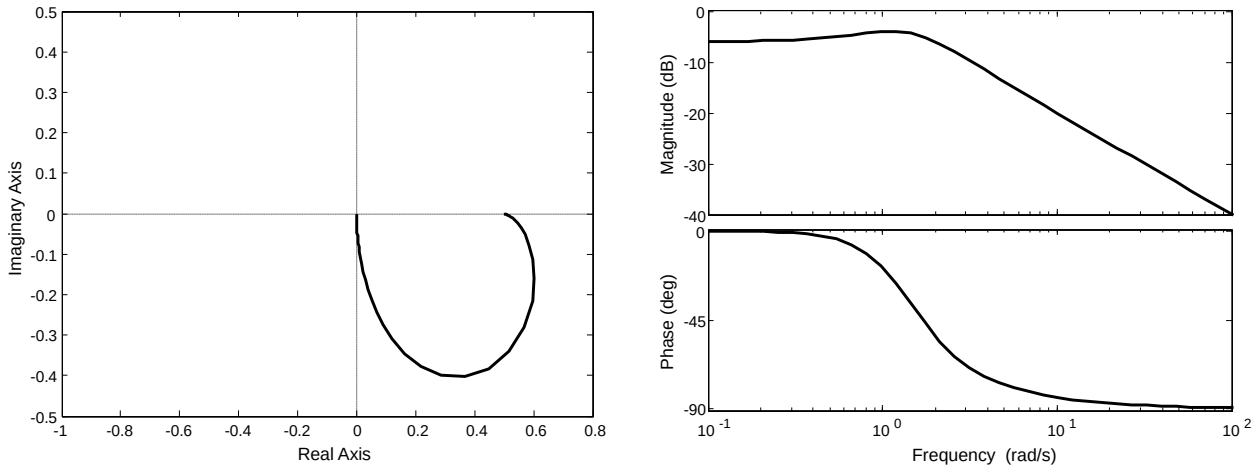

(a) Nyquist plot.

(b) Bode diagram.

Figure 3.6: Nyquist plot and Bode diagram are typical methods to illustrate the frequency response characteristics. The transfer function of the plotted example is $(p+1) \,/\, \left(p^2+2p+2\right)$.

3.3.5 Modal analysis

Modal analysis can be both experimental and numerical calculations of the dynamical characteristics of systems using its modal parameters, eigenfrequency, normal mode of oscillation, modal mass and modal damping. It has a significant advantage over frequency response measurement: Modes of vibration of the components can be observed. It helps to understand the structural characteristics, operating conditions and performance criteria. The main advantage of frequency response measurement is that the modes of vibration are observed giving a more detailed grasp of mechanical behavior, (Montalvão e Silva and Mendes Maia 1997, Ewins 2000).

To estimate the modal parameters of a structure, it must be excited with an adequate source, for example impact hammer or shaker. Here the exciting force is measured, for example, by a piezoelectric force or acceleration sensor. Simultaneously, the response of the structure is measured by accelerometers. The frequency responses can be calculated by Fast Fourier Transform (FFT). The

system's modes can be observed with software. This allows identifying critical modes, which must be avoided by design changes.

3.3.6 Circularity accuracy

Testing the circularity accuracy is used to examine the coupled dynamical behavior of several axes. It is measured either with internal measurement devices, for example rotational or linear encoders, or a grid encoder and ball bar, which has to be clamped in the machine. In modern NC controllers there are functions to provide a circular accuracy test with internal devices. However, external devices provide more accurate results, (DIN ISO 230-4 2001, Weck and Brecher 2006b).

The circular accuracy tests the synchronicity of the involved axes by driving a circle with two axes. Furthermore, the friction- and backlash-depending reversal error can be observed and evaluated. In figure 3.7 the result of a typical measurement of circularity accuracy is shown. At the reversal points, there are obvious reversal errors. The error at 1:30 is caused by a starting movement.

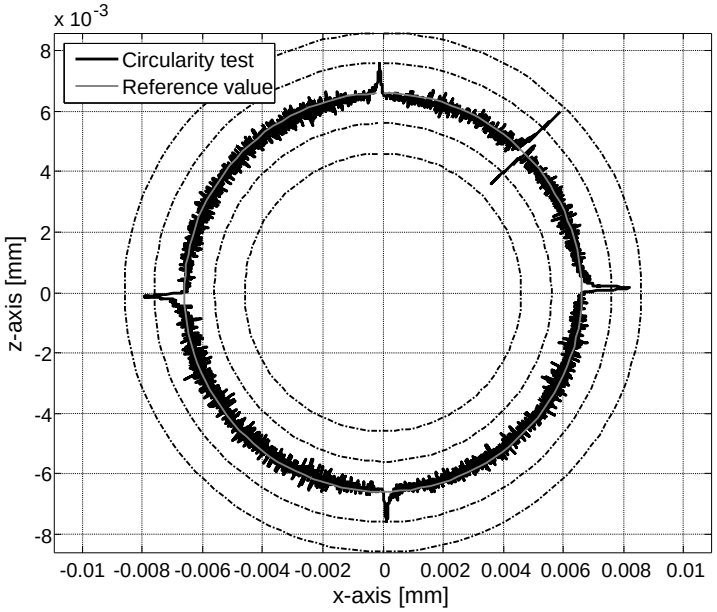

Figure 3.7: Typical result of circularity test with distinct reversal error.

3.3.7 Online friction measurement

A major challenge of taking measurements in industrial used machine tools is their availability. Since these machines are expensive producer durable goods, it is demanded that their productivity is as high as possible. Therefore, the time to conduct measurements is rather limited and usually it is impossible to install additional sensors. Furthermore, changing of the machine configuration is not allowed because the resumption of production must not be endangered. Last but not least, additional costs have to be avoided.

In modern NC cabinets there are measurement and diagnosis tools, which can record several parameters of the feed drives, like motor current, axes' velocities or positions, (Siemens 2008, Beckhoff Automation 2014). Usually, the measured parameters can be exported to analyze with external devices.

A direct measuring of friction force needs additional sensors, which are impossible to mount due to high efforts. Therefore, it is accessed by the motor current, which is proportional to the torque generated by the motor.

$$I \propto M \tag{3.7}$$

This current can be used to determine the friction torque, respectively force in linear motors, of the complete feed drive, but it is rather difficult to identify the influence of single components.

The friction is nonlinear, depending on time and components' wear and temperature but very easy to observe indirectly. These dependencies require carefully prepared and conducted measurements. Otherwise, the results are not comparable.

A further advantage by using an NC program to generate the axis movement is that it is possible to avoid collisions. Therefore, all axes are positioned at distinct positions before the start of repeatable measuring. Since all measurements are conducted by the same program, the results are comparable. Furthermore, every

operator working with machine tools can start an NC program and conduct this measurement without additional education. Hence it is possible to repeat it at the machine tool consumers' plant and observe the friction.

3.3.8 Quantification

The discussed measuring approaches for machine tool accuracy, static and dynamic behavior are quantified with regard to appropriateness for estimation of assembly failures during start-up. Especially the effort generated by external measurement devices and the need of specialized personnel is considered.

	External sensors	Controller internal	Modification	Expert staff	Automatable	Duration	Costs
Force: load cell	-	-	-	+	+	+	-
Force: strain gauge sensor	-	-	-	+	+	+	0
Accuracy	-	-	+	-	+	-	-
Repeatability	+	-	+	-	+	-	-
Frequency response	+	+	+	0	-	++	+
Modal analysis	-	-	+	-	-	- -	- -
Circularity: internal sensors	+	+	+	0	-	+	+
Circularity: grid encoder	-	-	0	-	+	+	-
Friction by NC program	+	+	+	+	+	0	+

Table 3.1: Quantification of discussed measuring approaches for estimation of assembly failures. ++ means the requirements are completely fulfilled and - - they are not fulfilled.

Table 3.1 shows that friction measuring using internal tracing functionality of the NC controller is a convenient method, which allows a reliable detection and evaluation of assembly failures. Its main disadvantage is the duration of measuring, which is compensated by not having to install additional sensors. Furthermore, due to the various influences on friction - for example temperature, lubrication state - comparable conditions during measurement must be provided. Thus, the advantages of internal friction measurements countervail the disadvantages and are used for the measurements conducted in this work.

4 Motivation

Identical machine tools show distinct differences in behavior during measurements as well as during operation. On the one hand, these differences are caused by the variation of component behavior. On the other hand, the larger proportion of differences is caused by variances of the assembly process. Since the used components, for example bearings, are of high stiffness, smallest deviations of a few micrometers induce very high reaction or constraining forces. These forces are caused by shifting the base points of a usually nonlinear spring, which is representing the component, against each other. Usually, it is impossible to measure these deviations directly.

The induced reaction forces result in a shift of preload and, accordingly, the normal forces acting on the joint patches. This leads to a variance of stiffness and damping respectively friction in the contact areas, as shown by Petuelli (1983). The variance of stiffness c directly influences the eigenfrequencies and also the dynamic behavior:

$$\omega_0 = \sqrt{\frac{c}{m}} \tag{4.1}$$

Furthermore, due to a variation of normal force F_N, there is a direct proportional influence on friction F_R as well:

$$F_R = \mu F_N \tag{4.2}$$

Last but not least, the variance of damping also influences the viscous part of friction f_v.

Since some machine tool builders try to avoid the excitation of non-position-depending eigenfrequencies by using notch filters by parametrization of these with standard values without additional measurements (Pruschek 2009, Hofmann 2012), a severe failure in parametrization becomes possible.

On contrary, the damping d has an impact on the amplitude and the eigenfrequency, (Hauger, Schnell et al. 2002).

$$\omega_d = \sqrt{\omega_0^2 - \frac{d}{2m}} \tag{4.3}$$

However, typically for machine tools this damping influence on the eigenfrequency is almost negligible. This means, attention must be paid to the variance of friction. If there is an increase, normally the wear in the moving contact areas will increase and the component's life expectancy will be reduced, (Kato 2000).

Furthermore, an increase of load in the bearings, which can be induced from constraining forces caused by assembly deviations or even failures, leads to a reduction of life expectancy of all involved components and thus the complete axis.

If such a failure in the assembly process occurs, normally retouching work will be conducted. However, for machine tools this usually requires high cost, well educated workforce and time. Hence, if it is possible to detect such an issue early in the assembly process, the effort for correction can be reduced. Due to a lack of knowledge of the impact of assembly deviations and failures of single components on the behavior of machine tool axes, in industry a high effort is made to assemble the components. This results in a high amount of work and cost. However, if the effect of assembly deviations can be estimated in the construction process, it becomes possible to determine both components with great effect and critical steps of the machine tool assembly. This means the tolerances can be adapted and the critical components can be focused. In order to handle this

challenge, in this work a simulation method is developed, which supports machine tool makers in detecting and evaluating critical components and assembly steps. The developed method permits to simulate and estimate the impact of assembly deviations or failures of single components as well as their interaction. Thus, it becomes possible to judge, which particular assembly step can increase the quality and life expectancy by higher effort and respectively for which step higher effort does not lead to a significant improvement of the results. This means in the product development process an early focusing on particular important assembly steps becomes possible. Furthermore, a deeper understanding of the assembly process and the interdependency of assembly deviations of the components is obtained.

4.1 Approach

The friction force has been identified as sensitive and well measurable parameter to observe and identify assembly deviations. In order to detect assembly deviations and failures by friction force and to determine their effect on components, both measurements and simulation are necessary. Furthermore, the allowed variance caused by assembly deviations within distinct tolerances must be determined. Therefore in this thesis the following approach is made:

Firstly, a method for measuring machine tools is developed, which allows deriving variations indirectly from the reaction of the complete system. Then, measurements of identical machine tools are conducted to validate the measuring approach and to show that there is a significant variation caused by assembly deviations and failures.

Secondly, since the reason for the variation is not determinable, measurements at a test rig under variation of installation conditions are performed. Here, only a few components can be varied, and the influences on other components are difficult or impossible to estimate.

Thirdly a multibody simulation of the test rig is modeled and executed under variation. Lastly, the results of measurements and corresponding simulation of varieties are compared. From these results conclusions are drawn and discussed.

Finally, a guideline for machine tool builders for identifying critical components and assembly operations by simulation in early steps of the product development process is evolved.

5 Measurements of machine tools and test rigs

The pertinence of assembly variations for machine tool producers and consumers is obvious. The producers must guarantee machine capability and a customer, who bought several identical machine tools, is interested in having identical characteristics, which means the same productivity and accuracy. Furthermore, NC programs should be exchangeable between identical machine tools without changes besides tool compensation and produce identical results.

Firstly, possible assembly variations and their impact on machine tool behavior are identified by an FMEA. Secondly, in order to clarify the difference between identical machine tools, measurements at machine tool makers' production plants have been conducted. For this purpose, a measuring and evaluation approach basing on a NC program and signal available in the controller has been developed and results from measurements of identical industrial machine tools have been detailed. Since the measuring time at machine tools is limited and it is impossible to vary the assembly of components during start-up of machine tools, thirdly, an analysis of the varieties and their effect has been realized at a test rig. Thus, it is possible to explain the variations observed at machine tools. Furthermore, the component influence resulting from assembly variations can be determined.

5.1 Analysis of varieties

In order to interpret measuring results, the varieties of the assembly process and their effects on friction must be discussed first. For this, an FMEA is conducted and discussed in the following sections.

5.1.1 Failure mode and effect analysis - FMEA

Here only possible failures and their impact on friction behavior are evaluated, but the risk priority number (RPN) is roughly estimated, because there are no data available to calculate probability and especially severity and detectability reliably. Probably, machine tool builders have collected data, but did not publish them. In the following, a rough appraisal and explanation are given.

$$\mathrm{RPN} = \mathrm{detectability} \cdot \mathrm{probability} \cdot \mathrm{severity} \tag{5.1}$$

Since usually assembly failures only lead to an increase of wear and consequently an earlier breakdown, which results in a standstill of the machine tool and some maintenance but not a fatal incident. Thus, the severity of assembly failures can be estimated to be medium. In opposite, assembly failures are very difficult to detect, which results in a high value of detectability. Last but not least, it is not possible to estimate the probability. The measurements conducted at machine tools during this work resulted in an assembly failure probability of about 10%. However, since there are no tolerances, it is impossible to quantify this correctly.

From practical experience of machine tool builders, especially damages of the fixed bearing and the ball screw nut are often reasons for standstill of machine tools and, therefore, they must be examined carefully.

Since they are essential for stiffness and accuracy and, as mentioned in section 3.2.1, are responsible for more than 10% of all breakdowns of machine tools, the bearings and ball screws are focused on. Furthermore, only geometrical variances

are discussed in the following sections. Preload variances and varieties of other components are discussed in the section 5.1.4 “Other varieties”.

Results of FMEA

In order to distinguish the components with severe influence on machine tool axis’ functional capability, a simplified FMEA has been conducted. Here only the components with direct influence on accuracy and force transmission have been examined. These components are:

- rotational bearings
- linear bearings with the subcomponents
  - carriage and
  - rail
- ball screw

Since ball screw and rotational bearings affect each other, they are mentioned twice. In the following paragraphs the results of this examination are given in detail.

Results of FMEA - rotational bearings: There are three possible assembly failures of rotational bearings. These are the adjustment of preload and two kinds of alignment errors, shift and pitch against the central axis of the motor and ball screw.

- Preload
  - If the preload is adjusted too low, the axial stiffness of the system will be reduced and backlash will occur. This results in a decrease of positioning accuracy.
  - If the preload is adjusted too high, friction and consequently wear of the bearing will increase. Thus, the durability of the bearing is reduced.

The effect of preload failures is position-independent.

- Alignment - shift
  - Increase of wear of ball screw and bearing.
- Alignment - pitch
  - Increase of wear of ball screw and bearing.

  Both kinds of adjustment failures of rotational bearings result in position-dependent effects on bearing and ball screw next to the misadjusted bearing.

The fixed bearing is more often affected than the loose bearing, because usually the operating point is located near the fixed bearing for reasons of thermal expansion.

Results of FMEA - linear bearings: The assembly failures of linear bearings are related to the components of the bearing, namely guiding carriage and rail, which both can be misaligned.

- Carriage
  - Alignment

  Since the alignment of the carriage is position-independent, its impact is also position-independent. Thus, an assembly error results in an increased wear of carriage and rail and reduction of durability
- Rail
  - Alignment

  Misalignment of the rail is strongly position-dependent. It also results in an increase of wear of the carriage and a position-dependent wear of the rail, which reduces the life expectancy. Furthermore, there is an impact on the positioning accuracy orthogonal to the direction of the axis.

A defect carriage induces wear along its complete traveling distance.

Results of FMEA - ball screw: The ball screw's assembly failures are similar to those of rotational bearings.

- Preload
  - If the preload is adjusted too low, the axial stiffness of the system will be reduced and backlash will occur. This results in a decrease of positioning accuracy.
  - If the preload is adjusted too high, friction and consequently wear of the bearing will increase. Thus the durability of the bearing is reduced.

  The effect of preload adjustment is position-independent.

- Alignment - shift
  - Increase of wear of ball screw and bearings.

- Alignment - pitch
  - Increase of wear of ball screw and bearings.

  Both alignment failures result in a position-dependent increase of friction and, thus, increase of wear next to the bearings and a reduction of durability of ball screw and bearings.

Conclusion of FMEA: In the conducted FMEA, the most sensitive parts of the power train of a ball screw-driven machine tool axis have been examined. These are the bearings and the ball screw nut because they have to transmit the complete motion force and absorb disturbance forces. Even small alignment deviations result in very high constraining forces. Furthermore, an exchange of these components is complicated and leads to a standstill of the machine tool.

5.1.2 Variations of rotational bearings and ball screws

Ball screw nuts and rotational bearings suffer identical assembly failures. Since rotational bearings are ball screws with pitch zero, they can be assumed to behave equally.

Since the rotational bearings are rotation-symmetrically constructed, only two directions, namely shift radially to rotation axes and pitch perpendicularly to rotation axes, must be considered. This is shown schematically in figure 5.1.

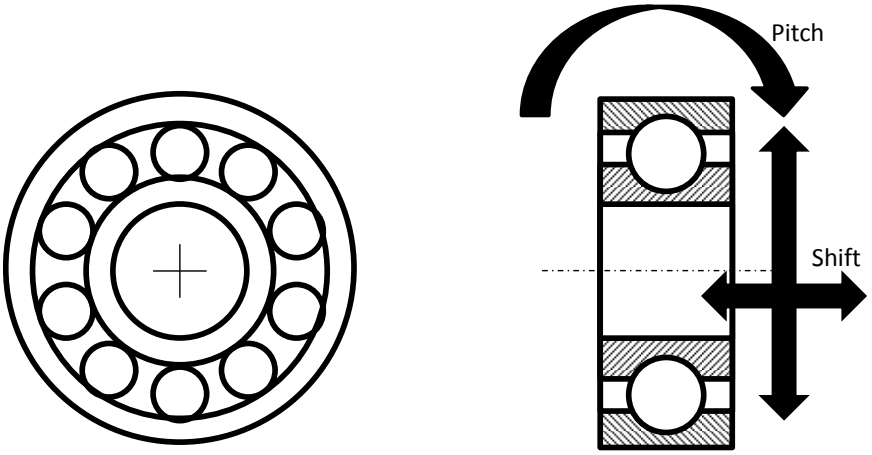

(a) Front view

(b) Side view with possible assembly failures

Figure 5.1: Assembly variations of rotational bearings like shift and pitch of the bearings are illustrated by arrows on the right.

These possible assembly failures cause a local, which means position-depending, change of friction behavior because it is correlated with the constraining force induced by the ball screw nut. This constraining force is caused by misalignment, which leads to an increase of the normal force, especially if the ball screw nut is located near a bearing. Hence, the normal force in bearing and ball screw nut increases if they are near each other, otherwise the elastic deformation of the ball screw spindle reduces the constraining forces.

These failures are affecting the coaxiality of the bearings and the ball screw nut. Since the bearings' positions are fixed, the ball screw spindle is bent. This bending depends on the position of the table and thus of the ball screw nut. Thereby, a

position-depending constraining force is induced. Positions next to the bearings lead to a maximum force and in the center of ball screw spindle to a minimum.

5.1.3 Variations of translational bearings

There are two types of failures possible in translational bearings These are firstly alignment failures of the carriages and, secondly, alignment failures of the rail, displayed in figures 5.2 and 5.3. In the following two typical failures are discussed.

Alignment failures of carriage

Since in opposite to rotational bearings there is no rotational symmetry in translational bearings, different types of assembly failures arise. In the following, the translational degree of freedom of the guide is assumed to be the z-axis. Remarkable is the direction dependency of the stiffness in vertical direction, which means the compression stiffness is higher than the tensile stiffness. This is detailed by an example in section 6.2.4. Furthermore, three rotations, namely pitch, yaw and roll, are possible. A linear bearing in front, side and top view with the possible assembly failures is illustrated in figure 5.2.

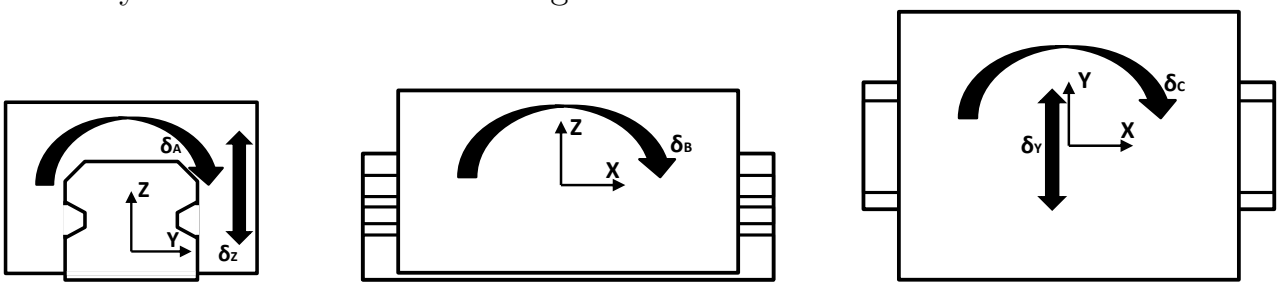

(a) Front view with rolling and shift in vertical direction

(b) Side view with pitching

(c) Top view with yawing and shift in lateral direction

Figure 5.2: Assembly failures of translational bearings.

Failures of assembling the carriage onto the table are constant along the complete traveling distance of the axis, which means the effect on friction is constant and not position-depending. This results in a constant offset of the friction torque measured by motor torque.

Alignment failures of rails

Alignment failures of guiding rails have locally the same effect as alignment failures of the carriage. However, in opposite to the carriage's alignment failures, these effects are strongly position-dependent, thus the effect is clearly correlated to the rail's assembly. Since the rail's curvature must be steady, there are no pulsation-like influences. The alignment failure of rails in axial direction Δy and the depending normal force and therewith friction ΔF_R are illustrated for a constant velocity in figure 5.3.

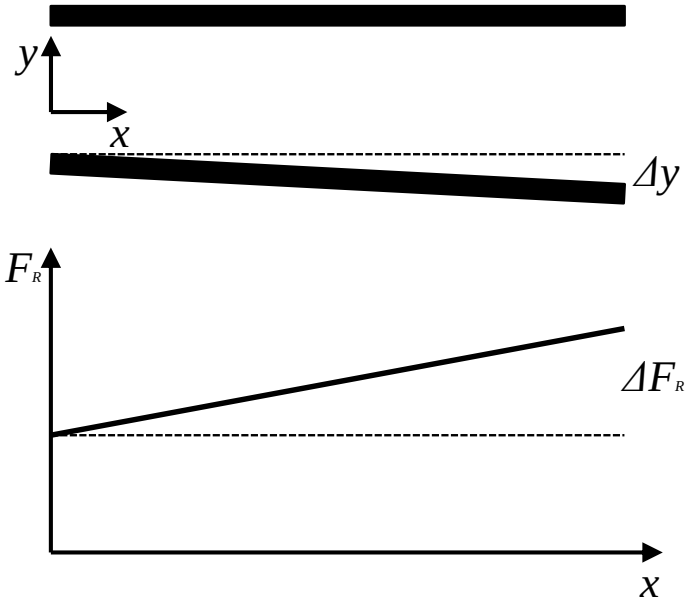

Figure 5.3: Alignment failure and effect on friction for constant velocity. The black bars in the upper part represent the guide rails with an alignment failure. On the left, these have an ideal distance and thus the friction force displayed in the lower figure is minimal. While the distance between the rails increases, the friction increases proportionally.

The displayed friction force will be valid if the rails on the left side ($x = 0$) have the nominal distance. Otherwise, a minimum of friction will occur within the traveling distance. Since there is a proportional behavior between displacement perpendicular to the traveling direction and normal force, the misalignment can be displayed easily. However, velocity-depending proportionality factors, which are not observed, yet may also exist.

5.1.4 Other variations

There are multiple sources of failures and components not mentioned, yet. These have various reasons like preload, part geometry or peripheral components.

All assembly varieties affect the guide system accuracy and by constraining force also the other bearings. Even if the deviations are within a few microns, the high stiffness of the bearings increases the load and thus reduces the durability. The rotational failures of the carriage are displayed in figure 5.4.

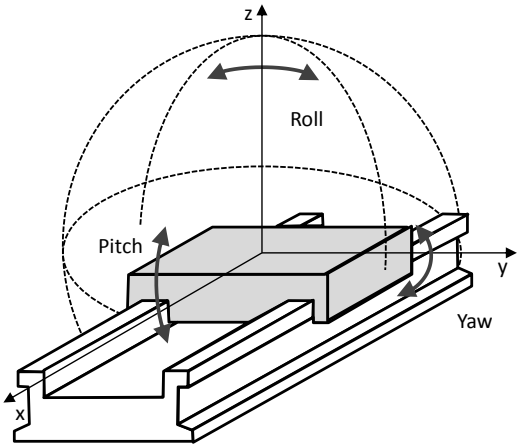

Figure 5.4: Rotational alignment failures of the guide system, which are resulting from misalignment of the rails.

Preload

The preload of bearings and ball screw nut must be adjusted to avoid backlash. There are several methods for generating preload depending on the component and the desired accuracy of the preload. In the following, components and adjusting of preload are discussed.

Spindle bearings As mentioned in section 3.2.3, the preload, which is adjusted by tightening a screw, can vary in a very wide range depending on the tensioning process, which cannot be controlled well. This results in a constant offset of friction along the complete traveling range between identical axes. Thus, the

tensing process determines the standard deviation of preload and can be assumed using the engineering guideline VDI 2230-1 (2003).

Linear bearings In linear bearings, the preload is set by the diameter of the roller bodies. These are oversized but their diameter variation is within a small range. Thus, the deviations determine the variation of preload. Since the carriages and the rails are sold as a complete system with adjusted preload, the machine tool maker cannot adjust it anymore. Thus, deviations of the preload caused by the assembly process at the machine tool manufacturing are impossible.

Ball screw There are several common methods for generating the preload in ball screw nuts. These are tensioning two nuts against each other, oversized roller bodies and a slotted nut tensioned by a screw. Thus, either the tolerances of the roller bodies or the tensioning process determine the preload variation, whereas only the latter can be influenced by the machine tool builder.

Geometrical errors

Geometrical deviations are caused by the production process of components. Even if these components are mass-produced articles, there will be a variance as described by tolerances in the engineering drawing. However, especially single pieces or small series like machine bed or carriage, which are either made by casting or welding sheet metal, lead to non-negligible geometrical deviations because the production process is prone to some inevitable uncertainties. Furthermore, the costs for machining huge parts like machine beds with certain accuracy are tremendous, thus the tolerances are kept as huge as possible.

The mentioned failures can result in both periodic fluctuations caused by rotational bearings and position-depending varieties caused by the cylindricity of the ball screw spindle or alignment of the linear bearings. However, it is nearly impossible to determine whether the effects on friction are caused by geometrical errors of parts or the assembly process of the machine tool. Since the component

supplier guarantee their products to stay within certain tolerances, which usually is an order smaller than the assembly variances, this impact can be neglected.

Peripheral components

To the peripheral components belong all parts, which are not directly responsible for the accuracy of motion. These are, for example, cable drag chain, seals, telescopic covers, bellows. Although these components have no direct influence on the geometrical accuracy, they still have an impact on the friction force. Especially for contact seals, there is a strong time- and duration-depending influence on friction. Since there is a multitude of components and assembly variations involved, it is not possible to determine single components and variations without profound technical knowledge, generated by empiric experiments. Therefore, a multitude of components must be examined at appropriate test rigs and real machine tools. It has been impossible to conduct such an empiric experimental research within this work.

5.1.5 Effect of variations

Since there is a manifold of components and assembly variations having impact on fiction behavior of machine tool axes, an itemization of their effects must be conducted. The peripheral components are not examined in detail because the tremendous multiplicity is nearly impossible to destine reason and impact clearly. This itemization is displayed in table 5.1. Here the global effect means a constant influence along the complete traveling range of the carriage and the local effect means depending on a distinct position of the axis, which is usually the carriage positioned next to the bearings.

It is obvious in any case that the preload has a global influence on the friction. Furthermore, the translational bearing is separated in carriage, which has a global impact, and rail, whose impact is correlated with the error's position. Variations of the bearings and ball screw nut have position-dependent influences.

Component	Failure	Effect
Rotational bearing	shift	local
	distortion	local
	preload	global
Ball screw	shift	local
	distortion	local
	preload	global
Translational bearing - Carriage	shift	global
	distortion	global
	preload	global
Translational bearing - Rail	shift	local
Peripheral components	various reasons	global/local

Table 5.1: Component-based illustration of sources and effects of assembly deviations on friction. Here it is distinguished between global and local effects.

Besides these mentioned impacts, there is a negative influence on the life expectancy of the components. The life expectancy of bearings under dynamic load can be calculated by the following equation:

$$L_{10} = \left(\frac{C}{P}\right)^{p} \ [10^6 \text{ rotations}] \tag{5.2}$$

Here L_{10} is the life expectancy under standard conditions, after which 10% of the bearings broke down, in million rotations. C the dynamic load rating [kN], P the equivalent dynamic load [kN], p is the life expectancy exponent depending on the roller body shape. The additional load is increasing the equivalent load. Thus, the life expectancy decreases with increasing load (FAG 1999). The components' life expectancy is not focused in this work but it is possible to use the developed method for improving the quality of duration prediction.

5.2 Measuring approach

As discussed the friction of a guiding system is a sensitive parameter and can be measured well. In order to measure machine tools or tests stand contradictory conditions must be considered. These are detailed in the following sections.

5.2.1 Conditions for measuring machine tools

Since machine tools during start-up are rather expensive producer goods, there is neither plenty of time nor personnel at the machine tool maker's shop floor to conduct laborious measurements. Thus, a simple and efficient method to measure is needed. The requirements and constraints identified together with machine tool makers are in detail:

- no external sensors
- short duration of measurement
- simple to operate (no experts needed)
- no changes in machine tool setting
- analysis to be done offline on an external device

Furthermore, it is desired by machine tool makers that this measuring method is used during service operation by maintenance staff in the future. Thus information about the development of machines during life time and effects of damages can be collected. Although it is not part of this work, the developed software will show an approach to fulfill these requirements.

Since the measuring and analysis being conducted by machine tool makers should be possible without expertise and require minimal effort, several software tools for generating NC programs and analyzing results have been developed.

- **Generation of measuring programs**: In order to generate NC programs automatically, it is necessary to examine the information for each axis. Firstly, the axis-relevant data, namely the name of the axis and its specific data, for example the minima of position and velocity and the maxima of position, velocity, acceleration and jerk must be supplied. Secondly, the measuring-specific data number of measuring points and number of velocity steps have to be provided.

- **Conversion of measurement data**: Since the data recorded by the NC controller are stored in various data formats, for example `*.xml` for data recorded with SinuCom, they must be converted into a usable format.

- **Analysis of measured data**: The analysis tool needs first a directory and a file name, secondly for each axis a motor constant, a number of measuring points and a file containing velocity data generated together with NC programs.

For this software tools, which can be used for various machine tools and are applicable without special knowledge, graphical user interfaces (GUI) are developed.

The approaches for generating a measuring NC program and an analysis of the measuring results are illustrated in detail in the following sections.

NC Program

The main objectives of machine tool makers are to keep the operability as easy as possible and the duration of the measurement as short as possible. Therefore, first an NC program based measuring approach has been chosen. Using automatically generated NC programs to produce the input signals ensures an identical procedure for every single measurement. Thus, the possibility of collision through an operating error can be avoided easily, too. Furthermore, starting an NC program needs no specific education for the start-up and maintenance personnel. The duration of the used program can be adjusted as well as the accuracy of measuring. In

a last step, the analysis tool can be attuned well to the measuring results because these are repeatable.

The used NC programs are a main program, which is responsible for positioning of the machine tool's axes, and several subprograms containing the movements of each axis, which are measured separately. Thus, the main program guarantees the avoidance of collision.

The NC program moves an axis with a distinct velocity at which a friction measurement is conducted. This measurement is repeated with several velocities wherein the resolution at small velocities is higher than at high velocities.

In order to reduce the duration, the friction is measured at distinct positions. In between these, the axis is positioned with rapid feed; the measured data of this positioning process can be filtered easily by the use of an additional parameter. This approach and the resulting time saving are schematically displayed for one particular velocity in figure 5.5. There the black line shows the standard procedure for friction measurement, which means the complete traveling range, is driven by constant velocity. The dotted line shows the approach with measurements at positions 1-3.

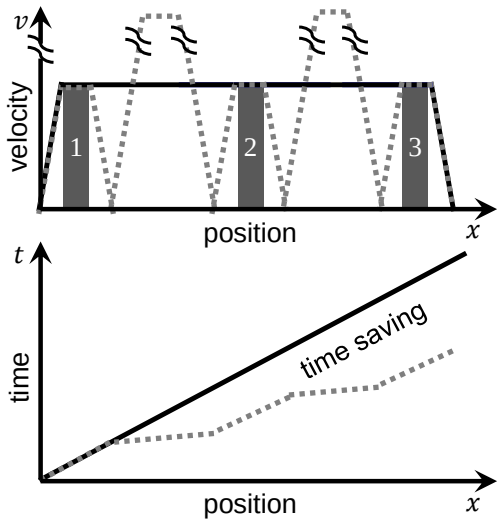

Figure 5.5: Measuring approach Reuss, Dadalau et al. (2012). The upper figure shows the velocity profile and the lower the resulting time saving. 1, 2 and 3 are the different positions. In the developed algorithm this number can be parametrized.

The first measurements have been conducted at machine tool makers' shop floors. Thus, there are no additional installations in the machines. Since there are plans to use the measuring approach by maintenance personnel at customers, where huge tools, workpieces or handling equipment might be installed, dedicated instructions must be given to avoid collisions. This means, workpiece, tool and other installations are to be removed if possible or otherwise the position limits of the NC programs must be changed.

In order to investigate this approach, the NC programs have been tested using a motor test rig. The results of this examination are described in section 5.4.1.

Analysis

In figure 5.6 raw data of friction measurement are displayed. The upper graph shows the electric current and the lower the desired and measured velocity. With regard to the current, there are peaks apparently correlated with changes of desired velocity and respective with acceleration and jerk. Obviously, these current peaks are caused by acceleration and deceleration. Thus it is necessary to cut the acceleration phase and only use a phase of constant velocity to estimate friction torque. This is reached, firstly, by writing an additional parameter out of the NC program, which is set to a distinct value, whenever there are negligible NC blocks and movements, and, secondly, by a comparison between the desired and measured velocity. If desired and measured velocity is within a certain span, the measured current is used for analysis. Furthermore, rapid feed and standstill is cut using parameters of the controller.

Since the machine tool's NC controller is not intended for laborious calculations besides path generation, the measurements are analyzed externally. Thus, during the measurement the data must be written on the hard disc of the machine tool and sent to an external device after the measurement is finished. For a first interpretation, the negligible parts for example for rapid positioning are removed and the mean value of filtered raw data is calculated. The Stribeck friction curve becomes obviously visible in the raw data as displayed in figure 5.7.

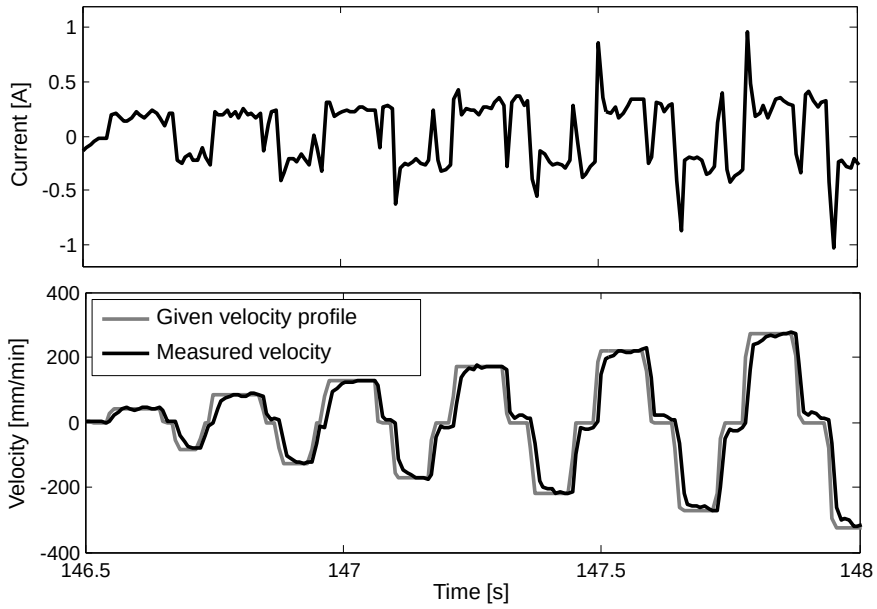

Figure 5.6: Raw data of friction measurement. The upper figure shows the electric current and the lower the desired and measured velocity.

The standard deviation of the measured friction is strongly position-dependent and has its minimum near the Stribeck velocity, which is also the minimum of friction torque. At small velocities, the increasing deviation is correlated with contacts between the surfaces caused by roughness. At higher velocities, an overshoot of motor current caused during the acceleration and deceleration phase is visible.

5.2.2 Conditions for measuring test rigs

Due to the availability of the test rig, which is not as restricted as with machine tools, measuring can be conducted with different velocities along the complete traveling distance. Here the traveling distance is driven with several constant velocities. Furthermore, there is a possibility for varying installation conditions of components.

Different measurements have been conducted under a variation of installation conditions, namely the assembly of the loose bearing and the ball screw nut. From

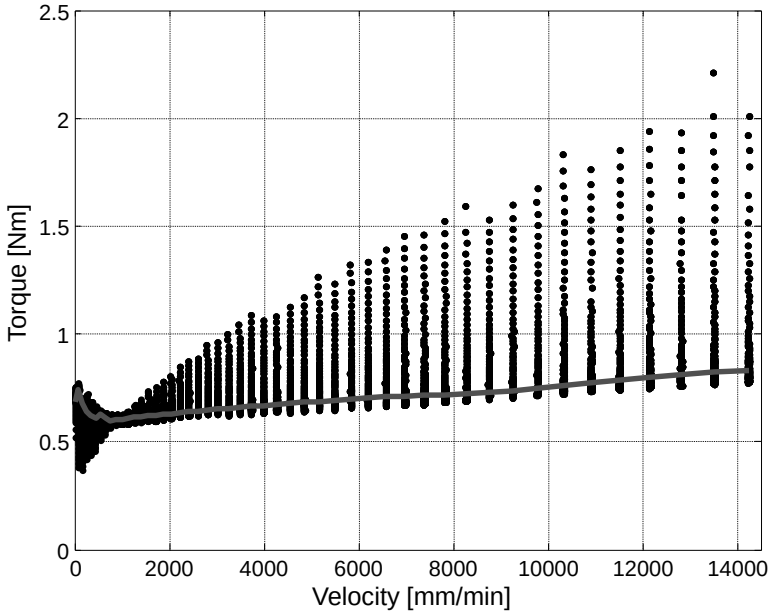

Figure 5.7: In a machine tool measured raw data and the friction estimated by calculating the mean value. Every point represents one measured sample and the gray line of the mean value shows the calculated Stribeck curve.

the measurement results the effect of variation of fixed bearing can be assumed because of the symmetrical behavior.

5.3 Measurements at machine tools in serial production

Serial examinations of two different types of machine tools are measured at production plants of two machine tool makers. In the following, miscellaneous results of measurements at Fässler AG are discussed.

5.3.1 Measured machine tool

One of the measured machine tools is the HMX 400 produced by Fässler AG, which is a gear honing machine. Honing is a fine machining operation, which means the measurements are conducted at a high precision machine tool and a lot of effort

is invested in its assembly accuracy. Therefore, the geometrical accuracy is given but still variations caused by reactive forces of assembly failures, for example of bearings or ball screw, are observable. Measuring results are discussed in section 5.3.2.

Traced data

The measured machine tool is controlled by a Sinumeric 840D sl controller with a 4ms interpolation cycle. This controller offers to trace data of the CNC in the interpolation cycle. Up to ten data sets like command and actual position and velocity can be traced. Since three axes are measured together, here for each of these three linear axes the command velocity, the actual velocity and the motor current have been recorded. 50 steps of constant velocity have been conducted. The resolution of the velocity steps has been increasing with the velocity to observe the nonlinear friction at low velocities in detail.

5.3.2 Results of machine tool measuring

In this section, several characteristic results estimated from measurements are displayed. These results show significant variances in friction behavior of identical machine tools. Since it is impossible to estimate the reasons of variations at mounted machine tools, the sources of these variances are examined with further measurements at a test rig.

Repeatability of machine tool measuring

Since it is a very important attribute, the repeatability of the measurements has to be investigated at first. For this, measurements have been conducted in similar manner three times consecutively and the results show consistent characteristics. The temperature of the fixed bearing housing has been observed with a laser

pyrometer. Since the disassembly of a machine tool is not allowed, it has been impossible to observe the temperature of other components.

This repeatability has been measured at several axes and several types of machine tools with equal results. Furthermore, a machine tool has been measured twice in three days with equal results. These results imply that, at least for short time intervals, there is a good repeatability (Reuss 2011, Reuss, Dadalau et al. 2012). In figure 5.8 measuring results of repeatability are shown. Here an identical measuring has been conducted three times with an interval of 20 minutes. Five positions have been measured, but only three representatives are displayed. The two additional positions are between 1 and 2 respectively 2 and 3 and have resulted in friction between the displayed curves. Position 1 is next to the fixed bearing, 2 in the middle of the axis and 3 next to the loose bearing. The displayed measuring has been conducted at a cantilevered axis because of the differences between each position. Remarkable is the offset of the first measuring at the first position, at which the friction is higher than at later measurements. This results from a not fully developed lubrication film at the start of the measuring procedure.

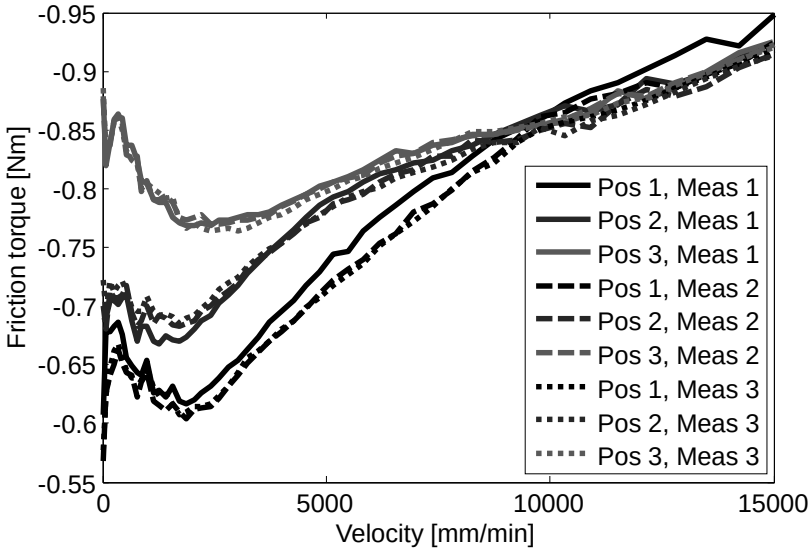

Figure 5.8: Repeatability of friction measurements illustrated with three measurements at three positions taken at intervals of 20 minutes (Reuss 2011).

Variance along axis traveling distance

Thereafter, several machine tools were measured. At one machine tool, a variation of friction torque of about 40% along the traveling distance has been observed. At a velocity of 7500 [mm/min] at position 1, a friction torque of about 7 [Nm] and, at position 5, of only about 5 [Nm] have been observed as shown in figure 5.9. These variations still have not had significant effects on the machine's accuracy, but certainly there will be an impact on the components' wear and life expectancy.

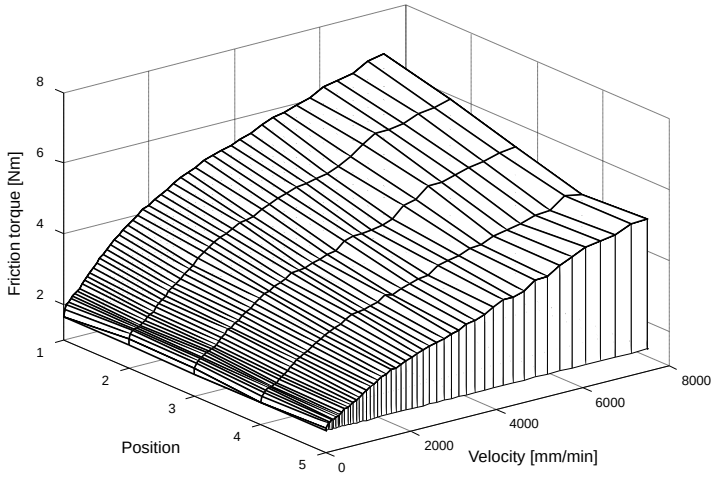

Figure 5.9: Position dependency of friction measured in a horizontal machine tool axis.

Other effects of assembly failures have been detected, too. In figure 5.10 the effect of sticking telescope covers is illustrated. This sticking has been caused by bad alignment of the telescope cover. There are two measurements of the same machine tool axis. The first measurement shows a step of about 20% in the friction curve and the second is smoother. Since the sticking had been detected during the first measurement, there was maintenance conducted, whose result is displayed in figure 5.10.

It is shown that even a simple measurement at only one machine tool axis allows detecting assembly failures and potentially identifying the involved components. However, measuring identical axes and examination of assembly failures will give both standard parameters of a well assembled axis and a better understanding of reason and impact of failures. Furthermore, with this data the identification of involved components will become more reliable and easier.

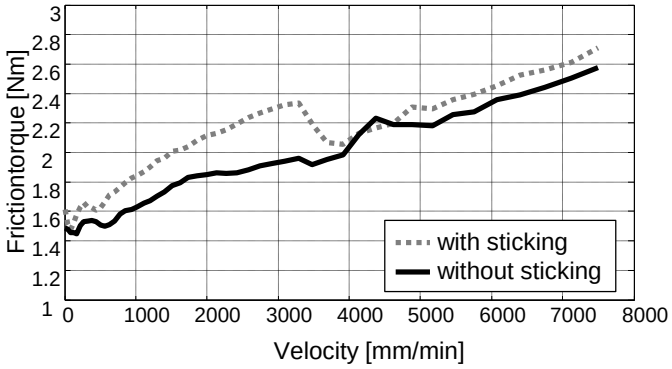

Figure 5.10: Sticking telescope cover of guiding system before and after maintenance.

Variances of identical machine tools

Beside the variances of new machine tools, the development of parameters during usage is of high interest. Therefore, both new machine tools and machine tools, which have been producing for several years, are measured and compared. The friction variance of about 50% at new machine tools has been monitored. However, during machine tool's life time, the friction curve even exceeds this area as visible in figure 5.11. A decrease of about 60% during life time of a ball screw, which is caused by preload loss, can typically be observed. However, this preload decrease has nearly no impact onto ball screws' axial stiffness unless there is no backlash, which is equal to the destruction of the bearing.

The machine tools are to be shipped after the measuring, which impedes to repeat measurements. Furthermore, it is not possible to disassemble and measure partly. This means, it is nearly impossible to determine the reason for the observed effects while measuring machine tools. Hence it is necessary to perform detailed examinations of installation conditions at appropriate test rigs.

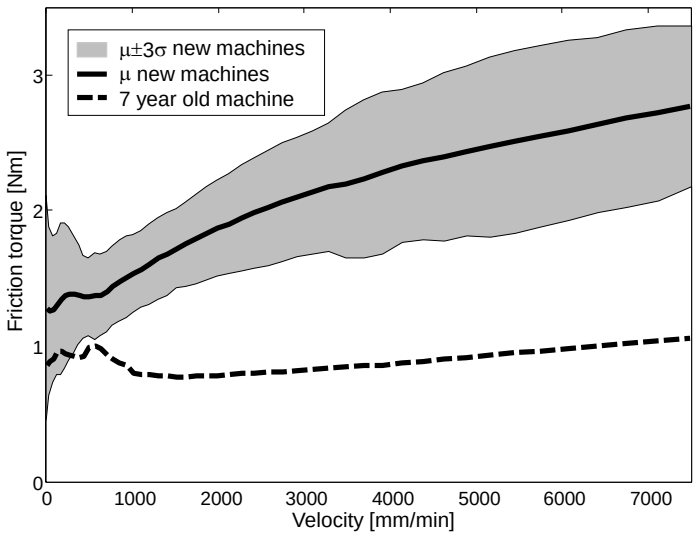

Figure 5.11: Variation of friction of identical machine tools and during life time.

5.4 Measurements at test rig

In order to reduce the mentioned lack of knowledge about the effect of varied assembly conditions of machine tool components, measurements at two test rigs are conducted. The first is a motor test rig and the second an axis test rig containing a complete ball screw-driven machine tool axis. The setting of the axis test rig has been varied, in order to estimate the effect of assembly variation. This is easily possible because there are no covers or other peripheral components. Furthermore, the measuring time is only limited by the data storage capacity of the controller, which allows conducting long term measurements.

5.4.1 Setting of motor test rig

The motor test rig uses a Beckhoff TwinCAT CNC controller connected to a Beckhoff inverter AX5103 and a synchronous servomotor AM3021 by Ethercat. This test rig is used to verify the reliability of the results of the measuring algorithm. Since this setting is from one source, the system and communication are quite stable. Furthermore, the included scope allows tracing more signals than the Sinumerik NC, which has been used at the machine tool measurements. Lastly, it has

a higher storage capacity than the Bosch NC controller used for the measurements of the axis test rig.

In figure 5.12 the result of a measurement using NC programs is displayed. Here current, velocity and position are traced. The velocities traced are the commanded and the actual velocity. Furthermore, the commanded position and the positioning lag are recorded.

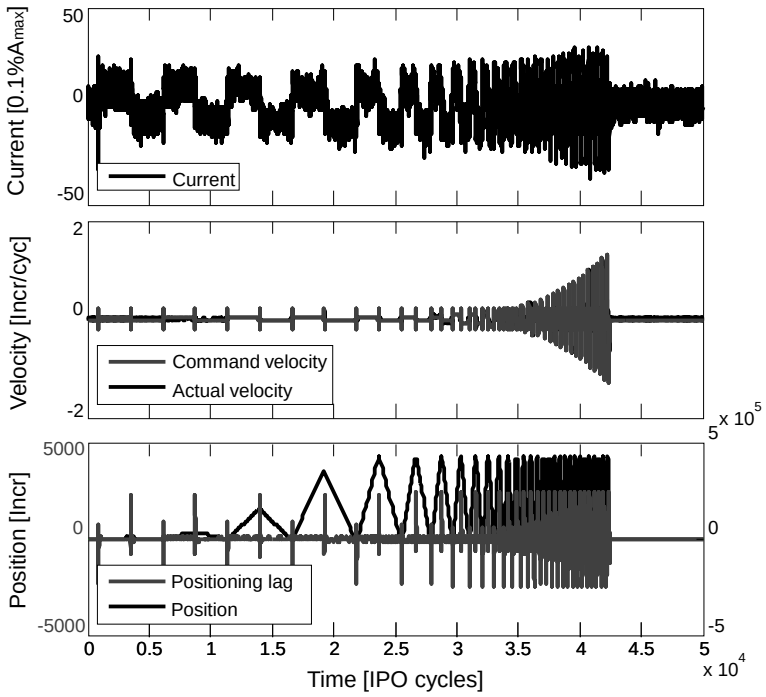

Figure 5.12: Measurement results of motor test rig using a NC program. Motor current, commanded and actual velocity and commanded position and position lag are displayed.

There the time is sampled in the interpolation cycles. The first plot shows the motor current in one tenth percent of the motor's maximal current, the second the commanded and actual velocities in increments of the measuring system per interpolation cycle and the last plot the commanded position and the position lag.

Another measurement conducted at the motor test rig is the position dependency of friction torque. Therefore, one rotation clockwise and one rotation counterclockwise with constant velocity have been measured. A low velocity has been

chosen in order to avoid acceleration influences. The measurement has been conducted several times in order to estimate the repeatability. In figure 5.13 obviously a strong position dependency is noticeable.

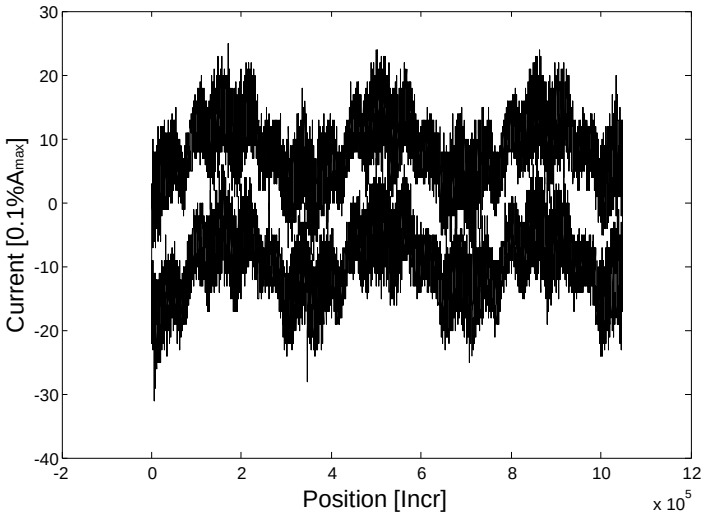

Figure 5.13: Hysteresis of motor measured during one rotation clockwise and one rotation counterclockwise.

The waviness of the measured current is obviously visible in both directions and can be measured repeatable. There are two frequencies cognizable, namely three and 18 Hertz per rotation. These result from the uncompensated cogging effect. The three Hertz represent the number of pairs of poles of the motor and the 18 Hertz are assumed to be the number of magnets.

Since this motor angle and thus the position-dependent friction torque is not time variant, it can be compensated reliably by a compensation table.

5.4.2 Mechanical setting of axis test rig

The test rig is a ball screw-driven axis assembled with components typically used in machine tools. Although it is a two axis test rig, measurements are conducted using only one of these. Its mechanical setting is detailed in figure 5.14.

A synchronous servo motor from Bosch, IndraDyn S MSK 100C-0200, is used for feed generation. Its technical data are given in following table 5.2.

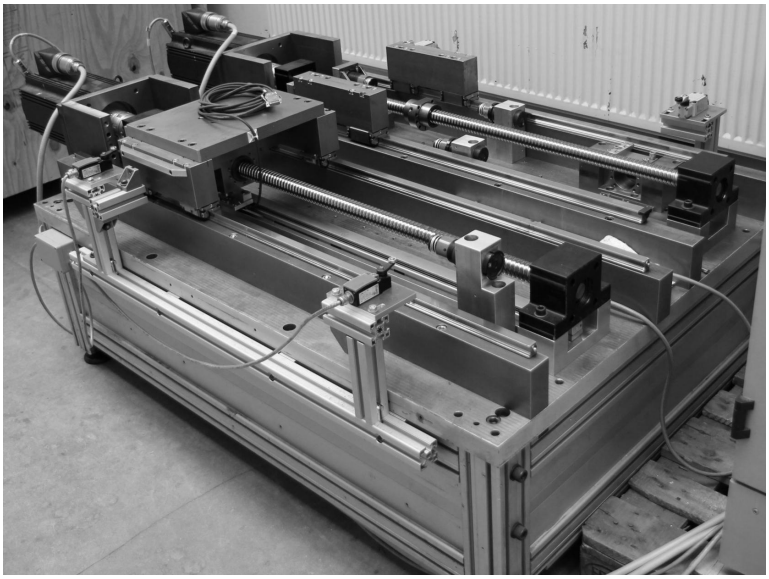

Figure 5.14: Mechanical setting of axis test rig.

Maximum speed [1/min]	Continuous torque at standstill [Nm]	Maximum torque [Nm]	Continuous current at standstill [A]	Maximum current [A]
$n_{\max} = 3500$	$M_0 = 38$	$M_{\max} = 148$	$I_0 = 17,7$	$I_{\max} = 79,7$

Table 5.2: Data of the used motor of the test rig: IndraDyn S MSK 100C-0200 (Bosch Rexroth 2010).

The coupling is a standard elastomer coupling of KTR-ROTEX GS38. The ball screw spindle is multiple threads with two threads and has a pitch of 20mm and a diameter of 40mm. The linear bearing is a 35mm ball born Rexroth R 162-2724-20.The measuring system is an absolute rotary encoder at the motor. An additional linear scale is not necessary because there are no requirements on high positioning accuracy of the carriage for measuring friction. A detailed description of the test rig's components, their mass or inertia and their stiffness is given in table 5.3. Since the damping is unknown, it is omitted.

Obviously, the masses and inertia of the rotating and translating parts of the bearings, namely roller bodies and cages, are marginally compared with the other

Component	Axial stiffness [kN/mm]	Rotational stiffness [kNmm/deg]	Mass [kg]	Inertia [kg mm^2]
Motor (Rotor)				55631
Coupling		1000	1.08	905
Ball screw and nut	200000/length		13.79	2667
Fixed bearing	200		2.41E-002	15
Loose bearing	100		2.41E-002	15
Linear bearings (Carriage)	vertical 750 horizontal 500		3.12E-002 3.12E-002	
Table			25.97	

Table 5.3: Components of the test rig and their specified mechanical parameters. Unknown or non existing parameters are omitted.

components. However, it is impossible to omit them because the chosen modeling of the bearings necessitates an intermediate part to connect joint and stiffness.

5.4.3 Measuring procedure

In order to measure the friction of the test rig, the start-up tool of Bosch Rexroth is used, (Bosch Rexroth 2008). The square wave signal shown in figure 5.15 can be used because only constant velocities are necessary for measuring friction. Since the measuring duration is limited by the data storage capacity of the controller, only one moving direction is measured. Hence, only offset, duration and sampling time must be parametrized.

In order to handle the limited storage capacity, every value of the friction is measured with a constant velocity along the complete traveling distance. Then, the opposite direction is measured with the same velocity. This procedure is conducted for several times and velocities to get a reliable friction curve.

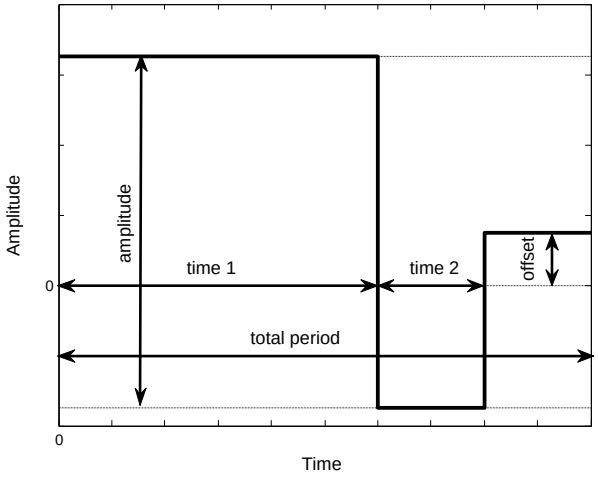

Figure 5.15: Velocity profile available at start-up software from Bosch Rexroth, (Bosch Rexroth 2008).

5.4.4 Identification of friction of feed drive components

In order to get parameters for modeling the test rig in a simulation environment, reliable estimations are necessary. Therefore, the friction of a partly disassembled test rig is measured. The observed installation conditions are, firstly, the motor itself, which means without any additional inertia. Secondly, motor with mounted ball screw, which means fixed and loose bearing but without ball screw nut and carriage, is measured. Thirdly, the friction of motor, bearings and ball screw nut, whose angular position has been fixed by a long elastic cable and, finally, the completely assembled axis are estimated. The measuring results are shown in figure 5.16(a).

Since the friction of the test rig's components can be summed up to the complete friction, the measuring results allow identifying friction of assembly groups and components. These are the motor, fixed and loose bearing together, ball screw nut and the four linear bearings as shown in figure 5.16(b). However, the motor's friction also contains the damping caused by the controller and other electrical devices, which is one major source of damping in a machine tool axis (Kunc 2007). Therefore, the dissipated energy is higher than expected by the friction of the other components.

It has to be notified that the friction of rotational bearings contains both fixed

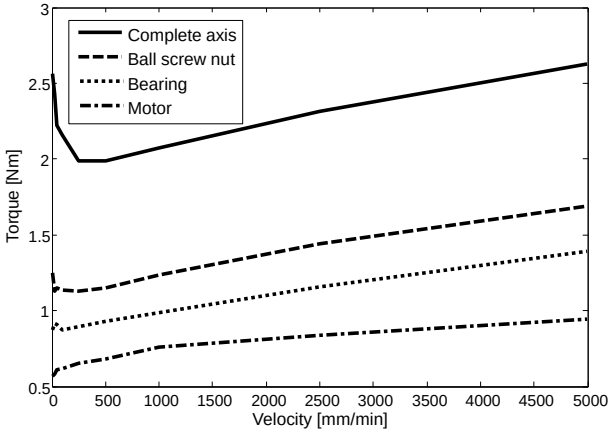

(a) Measuring results of partly disassembled test rig.

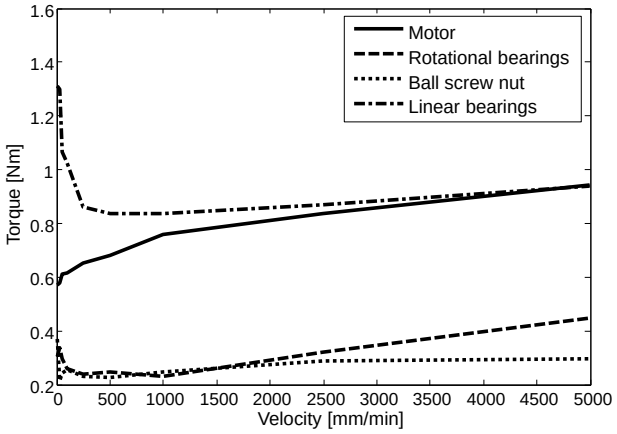

(b) Friction of components destined by measurements.

Figure 5.16: Measuring and identification results of component's friction. In (a) the measured friction of partly assembled test rig is shown and in (b) the friction of the single components is displayed.

and loose bearings and is assumed to be equal for both bearings, although in technical systems the friction of the bearings differs because of the load distribution. Furthermore, friction of linear bearings consists of friction of all four linear bearings, which is considered to be uniformly distributed on all four bearings. Thus, it becomes possible to determine the components friction and parametrize the simulation model more detailed.

Since there is no position dependency of motor and rotational bearing, these are compared by the median value of the ball screw nut's and linear bearings' friction along the complete traveling distance.

The components' friction parameters are identified using least squares method. Here, only the Coulomb and the viscous friction are determined, while other friction portions are neglected. Especially the sticktion respective the breakaway force are of minor interest because the measurements at machine tools showed an obvious influence of assembly deviations on the dynamic friction 5.9. Furthermore, these innumerous influences do not allow getting repeatable results in industrial environment because the environmental conditions are often changing. Results of the least square fit of Coulomb and viscous friction of components from measurements of the test rig are displayed in table 5.4.

To identify the Coulomb and viscous friction torques of the components, a first order linear equation is used as a simple model function, which represents one specific measuring.

$$y_1 u_k + y_2 = x_k \tag{5.3}$$

There k means the k-th measured sample, u the velocity of the measurement, y the parameter vector with the viscous parameter as first and the Coulomb friction as second element and x the measured current. This can be rewritten for all measurements as matrix equation. Thus the resulting equation is

$$Hy = x \tag{5.4}$$

As discussed in section 2.2.3 solving this equation with regard to y results in the so called pseudoinverse

$$y = \left(H^T H\right)^{-1} H^T x \tag{5.5}$$

Therein the regressor matrix H is

$$H = \begin{pmatrix} u_1 & 1 \\ u_2 & 1 \\ \vdots & \vdots \\ u_k & 1 \end{pmatrix} \tag{5.6}$$

With the resulting $y = [T_C, t_v]^{\mathrm{T}}$. Thus the friction torque results from

$$T_R = T_C + t_v v \tag{5.7}$$

Due to the unknown normal force in the contacts, the friction coefficients cannot be estimated. Hence the friction torque has been estimated by measurements and

its Coulomb and viscous parts are displayed in table 5.4. These results have been rounded.

Component	Coulomb friction [Nm]	Viscous friction [Nms/rad]
Motor	0.72	0.05
Fixed bearing	0.09	0.00048
Loose bearing	0.09	0.00048
Ball screw nut	0.25	0.00019
Linear bearing	0.205	0.000014

Table 5.4: Determined friction torque by measurements of machine tool axis without parameter variation. The linear bearing's friction has been converted into torque using the ball screw pitch.

The parameters have been given for single components and the friction force of the linear bearings has been converted into a torque with the ball screw spindle pitch h as proportional constant.

$$M_R = \frac{F_R h}{2\pi} \tag{5.8}$$

It is noticeable that compared with the other sources of viscous friction the linear bearings' viscous friction coefficient is almost independent of speed as expected and discussed in literature (Ispaylar 1996).

5.4.5 Variation of installation conditions

Since the axis of the test rig is not encapsulated by telescope covers and not used for production, it becomes possible to vary the installation conditions of components easily. The positions orthogonal to the axis direction of the loose bearing and the ball screw nut have been shifted using shimming plates, which are available in thickness steps of 0.005mm. Thus, repeatable variations can be conducted and their measuring results can be compared. In order to observe the position dependency, friction measurements are conducted at several representative sectors along

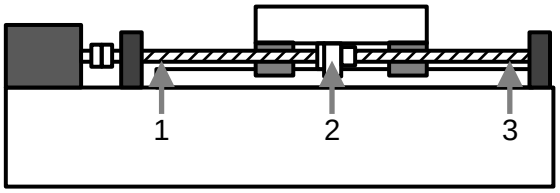

Figure 5.17: Measuring positions along axis traveling distance. The first position is near the fixed bearing, the second at the center of the axis and the third near the loose bearing.

the axis traveling distance, which are shown in figure 5.17. The first position is the carriage next to the fixed bearing, the second in the middle of the axis and the third next to the loose bearing.

Thus, in each sector around the three working points the median values of friction torque are calculated to avoid a strong impact of outliers. In opposite to the median, the mean value is more sensitive because the mean value is calculated from the measured value, while the median is the value of the middle of the list of the sorted measurement values.

$$\bar{x}_{\text{mean}} = \frac{1}{n} \sum_{i=1}^{n} x_i \tag{5.9}$$

$$\bar{x}_{\text{median}} = \begin{cases} x_{\left(\frac{n+1}{2}\right)} & n \text{ odd} \\ \frac{1}{2}\left(x_{\left(\frac{n}{2}\right)} + x_{\left(\frac{n}{2}+1\right)}\right) & n \text{ even} \end{cases} \qquad x_1 < x_2 < \ldots < x_n \tag{5.10}$$

Thus, the complete traveling range is observed and representative results are available repeatable. The development of friction along the axis can be estimated and compared with other axis.

Since the measured components have a symmetric behavior for shifting perpendicularly to rotation axis, only a shift into one direction is conducted.

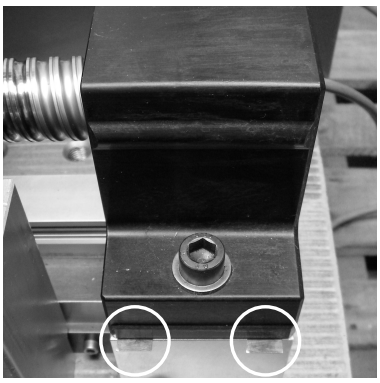

(a) Installation of metal sheets to vary assembly of loose bearing. The positions of the metal sheets are marked by white circles.

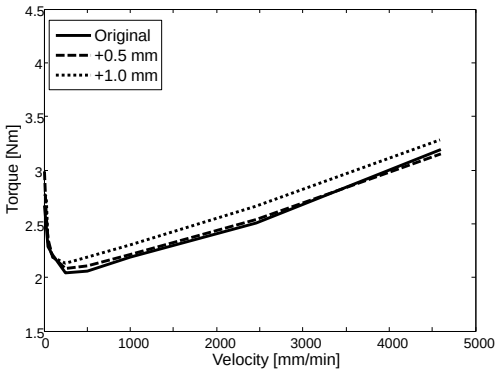

(b) Friction at position 1

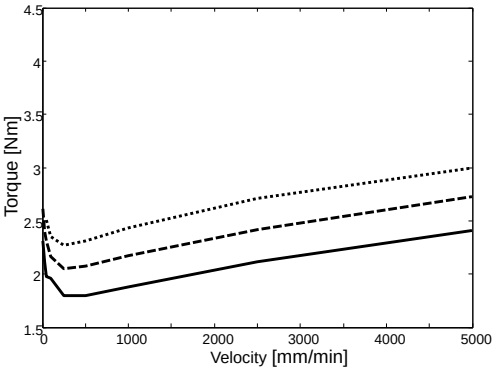

(c) Friction at position 2

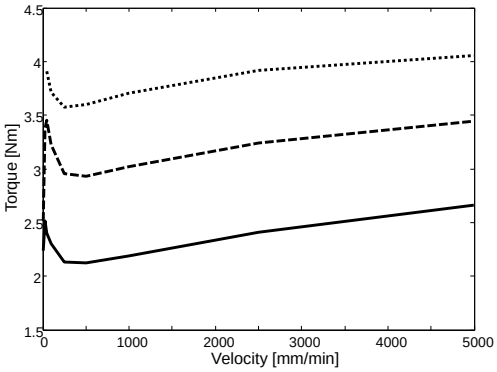

(d) Friction at position 3

Figure 5.18: Variations of loose bearing's installation condition and measuring results.

Variation of loose bearing

Assembly failures of the loose bearing will have a strong impact on the friction, in particular at positions near this bearing. This is caused by the increase of normal force in the loose bearing and the ball screw nut by constraining force. Furthermore, there will be nearly no effects at positions near the fixed bearing because the constraining force is reduced by the ball screw spindle's bending stiffness and the force flow through the ball screw nut into the machine bed. The installation conditions are varied by insertion of 0.5mm and 1mm metal sheets as shown in figure 5.18(a). The loose bearing is shifted upward perpendicularly to its rotation axis.

Obviously, the shifting of the bearing exceeds alignment failures, which usually occur during assembly of machine tools, but it shows the effects of assembly variations very clearly.

As assumed, the measuring results of the varied loose bearing displayed in figure 5.18 show a strong position dependency of variation influence. While at position 1, which is close to the fixed bearing, nearly no impact on friction is observable. There is a nearly linear increase of friction to position 3, which is next to the loose bearing. Furthermore, there is no obvious influence on the curvature of friction noticeable. At last, the increase of friction along the traveling distance seems to be proportional to the load, which is caused by the constraining force.

Variation of ball screw nut

A similar analysis is conducted to determine the effect of assembly failures of the ball screw nut. This should especially affect the friction near the bearings, whereas there is only a minor effect at the middle position of the axis traveling distance. In order to vary the alignment of the ball screw nut, the table is pushed 0.5mm upward by sheet metal, as shown in figure 5.19(a).

As displayed in figure 5.19, the measuring results confirm the assumed behavior. The variation's major impact is next to the bearings at positions 1 and 3, while there is nearly no effect at position 2. This effect is caused by constraining forces, which occur by tensing up of the ball screw spindle between bearing and ball screw nut. Mentionable is that the variation reduces the friction torque at position 1 and 3 with the same magnitude, which means the concentricity of the bearings and ball screw nut in the original assembly is worse than after shifting the ball screw nut. However, the bearings have only a small concentricity deviation.

Variation of ball screw nut and loose bearing

To detect whether the varied assembly is interdependent, both ball screw nut and loose bearing are varied at the same time. There is an obvious impact on

(a) Installation of metal sheets to vary assembly of ball screw nut by shifting of the carriage. The metal sheets are marked by white circles.

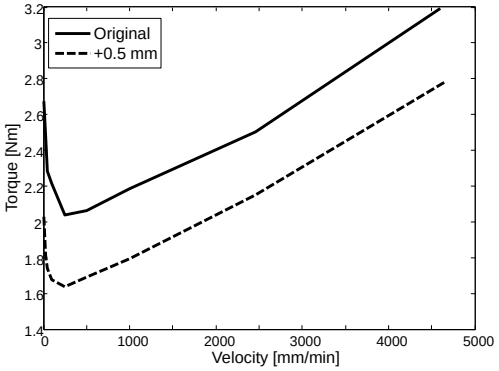

(b) Friction at position 1

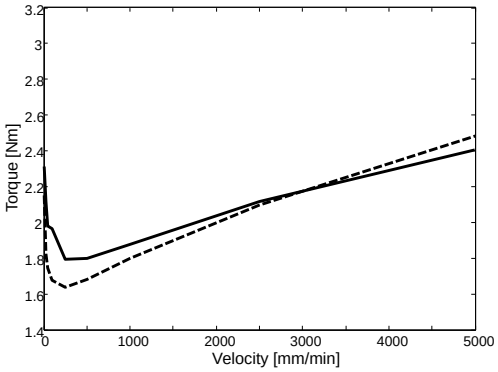

(c) Friction at position 2

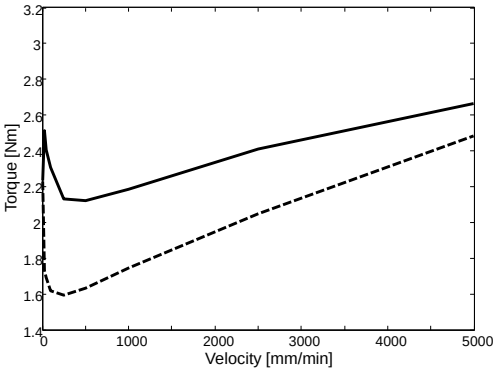

(d) Friction at position 3

Figure 5.19: Variation of ball screw nut's installation and measuring results.

friction at position 2 and 3. The absolute change of friction there is nearly equal. At position 1 nearly no effect is noticeable. The measuring results are displayed in figure 5.20. To compare several assembly variances besides the original state (solid line) and variation of bearing and nut (dotted line). The variations of each component (bearing dashed, ball screw nut dot-dashed) are displayed, too.

Opposite to an exclusive variation of the loose bearing, there is an effect on the friction at position 1 noticeable, but this impact is rather limited. At the center position 2 the shift of bearing and nut shows nearly the same behavior as the variation of the bearing. This can be explained by the shift of the two components. This has the same effect as a shift of the fixed bearing in the opposite direction. Lastly, at position 3, the friction torque results in between the friction of a shift

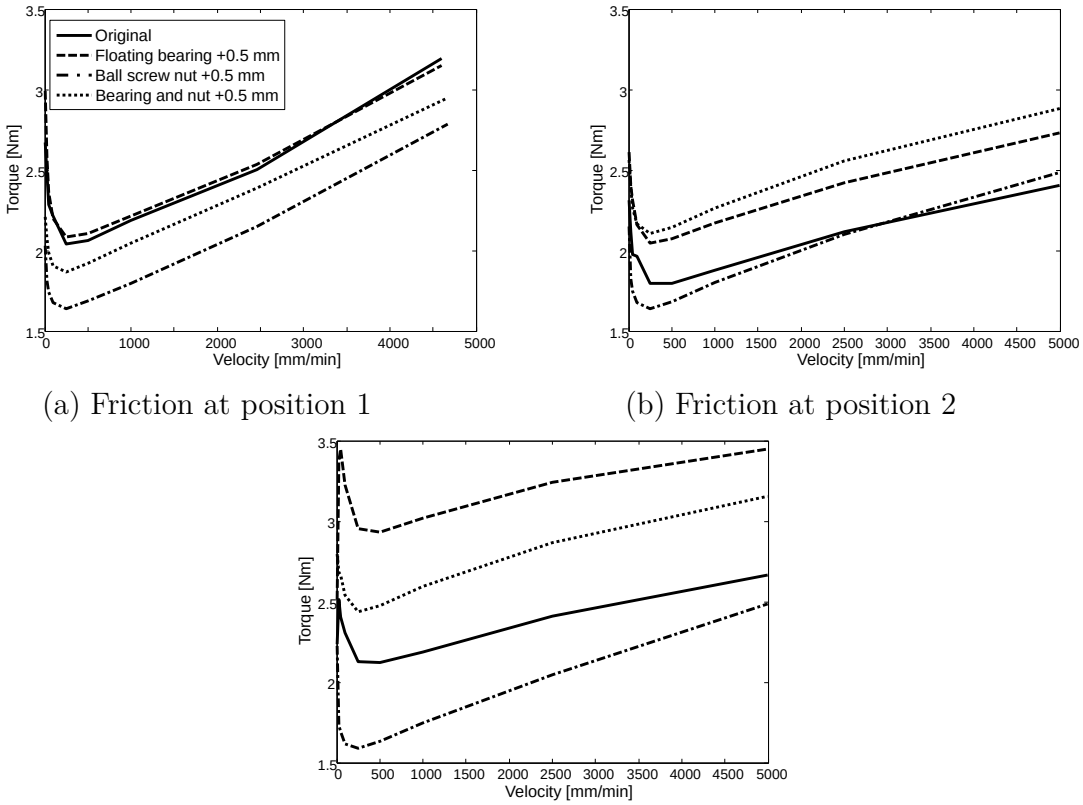

(a) Friction at position 1

(b) Friction at position 2

(c) Friction at position 3

Figure 5.20: Variation of ball screw nut's and loose bearing's installation conditions. Thereby both the bearing and the ball screw nut have been shifted.

of each single component. This results from the constellation between the varied components, which is comparable with the original state but has an effect on the fixed bearing.

5.4.6 Measuring results

The conducted measurements provide results for varied installations of ball screw nut and loose bearing. It is shown that these assembly errors have a local effect, which means there is an obvious impact near the position of the failure. In case of failures of loose bearings' mounting, the appearing constraining forces influence the friction locally. On the contrary, the mounting of the ball screw nut has an impact along the whole traveling distance but is distinct especially near the

bearings, which is caused by the constraining forces induced by bearings and ball screw. These results are compared in table 5.5.

Position	1	2	3
Loose bearing	0	+	++
Ball screw nut	+	0	+
Nut and Bearing	0	+	+

Table 5.5: Quantitative classification of assembly variations of position-depending influence on friction. 0 no influence, + significant influence, ++ strong influence

Furthermore, friction parameters of several components of the test rig have been identified. This allows a detailed and reliable parametrization of a simulation model producing reliable results.

6 Simulation of assembly variations

Simulation assists the observation of assembly errors. Thus, it becomes possible to estimate their effects for every single component, which is impossible in reality. Furthermore, assembly errors and effects, which are not measurable in reality, can be estimated by simulation. For example, this can be an error of alignment of one single guiding carriage, which is rather difficult to mount in a defined state, the axial force occurring in a bearing, which is impossible to be measured without changing the stiffness and thereby the system behavior, or the preload, which is difficult to adjust reliably.

6.1 Multibody simulation

As illustrated in the section 2.3 “Simulation of machine tools as mechatronic system”, the multibody simulation is a reliable and widespread method to describe the mechanical characteristic of a machine tool’s complete working space. Thereby it is possible to get sufficient and reliable results with limited modeling effort. Thus, a multibody model of the measured test rig is constructed. In the following sections, the modeling of the relevant parts of the ball-screw driven test rig, the modeling of friction at the components of the axis and the complete construction of the model are described in detail.

In order to model and simulate multibody systems, several software tools are available. Since a multitude of construction elements and analysis tools are in-

cluded, MSC.ADAMS, which calculates the forces by Lagrange equations, is used in the course of this work.

6.2 Modeling of axis

The components of the test rig are constructed with simple geometry elements. These elements are rigid masses and connected among each other by joints, springs' stiffness and dampers at designated points. In order to model the axis' dynamical behavior appropriately, the force transmission points, which have a major influence on the dynamical behavior, must be modeled in detail. Thus, especially the springs in direction of the flux of force are focused. These are the springs of bearings, ball screw spindle and nut and coupler. Here especially the stiffness of the ball screw spindle is position-depending. A schema of the mechanical model of the axis is shown in figure 6.1. Since the models of balls screw and bearings are complex but quite important for the dynamical behavior of the axis, their modeling is detailed in the following sections.

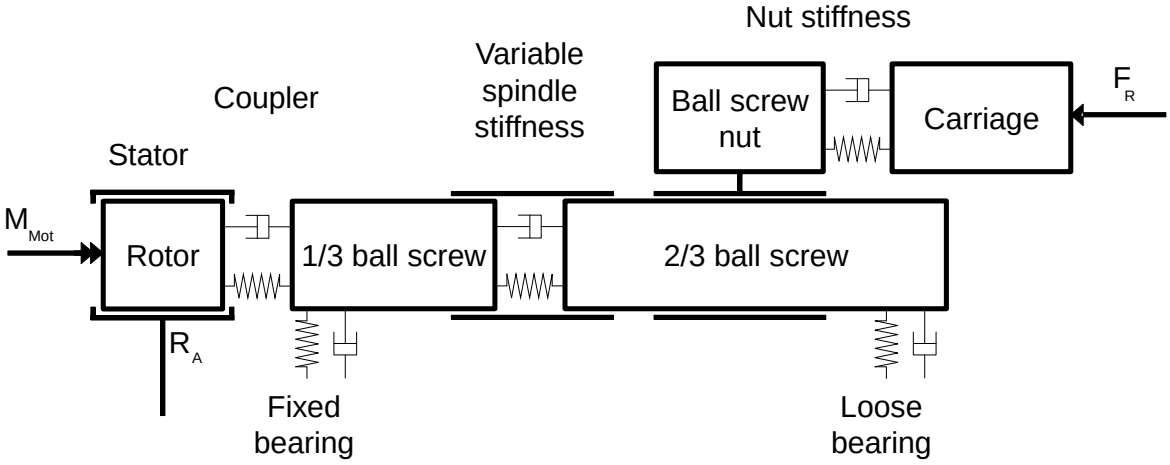

Figure 6.1: Two-dimensional schema of a mechanical model of a machine tool axis including the relevant stiffness. The four guiding wagons of the carriage and all joints besides the screw joint are omitted.

The acceleration and deceleration phase and their electric effects on damping of inverter and controller are neglected. Thus, only the phase of constant velocity is given and considered.

The model of the axis consists of the rotor, a spindle separated into two parts, one third at the fixed and two thirds at the loose bearing side, fixed and loose bearing, ball screw nut, table and four guiding wagons, which are not displayed in the figure. Thus, all in all eleven parts connected with stiffness between them and with the machine bed have been identified to be relevant for the dynamic behavior of the axis and must be modeled.

6.2.1 Modeling of variable stiffness of ball screw

Due to the influence of spindle length on axial stiffness of the ball screw, the strong influence of the carriage's position is obvious. Since rigid bodies are used to model and the springs provided by the simulation software are constant, this position dependency must be modeled using forces, in which a mathematical model can be included. Therefore, the ball screw is cut in two parts as suggested by Groß, Hamann et al. (2006) and Broos (2012) . The ball screw part connected with the fixed bearing consists of half of the coupler and one third of the ball screw, the free end consists of two thirds of the ball screw. The two parts are connected with a force, which is parametrized in all six degrees of freedom. The mathematical equations represent a spring damper model with position-depending axial stiffness. In the schema shown in figure 6.1 this force is represented by a spring damper element. The stiffness and damping parameters are estimated using the geometry of the ball screw and its material properties. In axial direction, the stiffness of the ball screw spindle c is correlated to Young's modulus E, the cross-section surface A and the length between fixed bearing and ball screw nut l. Since this length is depending on the position of the carriage x, the stiffness is also position-depending.

$$c(x) = \frac{EA}{l(x)} \tag{6.1}$$

The torsion stiffness of the ball screw c_T is calculated by the modulus of shear G, the cross-section surface A and the length between fixed bearing and loose

bearing l. In opposite to the axial stiffness, the length to calculate the torsion stiffness is not position-depending, (Frey, Dadalau et al. 2012).

$$c_T = \frac{GA}{l} \tag{6.2}$$

This modeling results in a position-depending first and a not-position-depending second eigenfrequency. These can be observed by measuring of machine tool axis. Due to the transmission ratio, usually the influence of rotational stiffness on the axial mode can be neglected, (Frey, Dadalau et al. 2012).

Since the axial stiffness of the ball screw spindle is position-dependent and the bearings' and ball screw nut's axial stiffness are not, a change of the dominant stiffness is possible. However, this behavior only occurs next to the fixed bearing, where the ball screw's axial stiffness increases tremendously. At usually used axis configurations driven by ball screw it is not possible to observe this effect because from design constraints it is impossible to position the ball screw nut close enough to the fixed bearing. The following equations explain this change of dominant stiffness and consequently eigenfrequency.

$$\frac{1}{c_{\text{ax}}} = \frac{1}{c_{\text{ax bearing}}} + \frac{1}{c_{\text{ax spindle}}} + \frac{1}{c_{\text{ax nut}}} = \frac{1}{c_{\text{ax constant}}} + \frac{1}{c_{\text{ax spindle}}} \tag{6.3}$$

$$c_{\text{ax}} = \begin{cases} c_{\text{ax constant}} & c_{\text{ax spindle}} \gg c_{\text{ax constant}} \\ c_{\text{ax spindle}} & c_{\text{ax spindle}} \ll c_{\text{ax constant}} \end{cases} \tag{6.4}$$

Obviously, there is a direct effect on the first eigenfrequency, which becomes position-depending and a change of the component with the dominant axial stiffness. However, such a change of the dominant eigenfrequency is nearly not observable in reality. A contour plot of a model of a machine tool axis with position-depending stiffness is displayed in figure 6.2.

Here only the position next to the fixed bearing is observed because the position dependency of the axial stiffness is inversely proportional and, thus, the changes

become smaller per distance to the singularity at 0, which means at the fixed bearing. The first eigenfrequency next to the fixed bearing will be higher because axial stiffness is higher next to the fixed bearing but the mass is equal.

The modeling parameters have been assumed and are given in equal units, displayed in table 6.1.

Mass	Inertia	Axial damping	Rotational damping	Axial stiffness	Rotational stiffness
500	300	10	1	$50000/x$	20000

Table 6.1: Rough assumption of parameters for estimation of a position-depending dominant eigenfrequency.

The assumed model is a coupled system of two masses showing two eigenfrequencies with the position-dependent eigenfrequency of the axial oscillation.

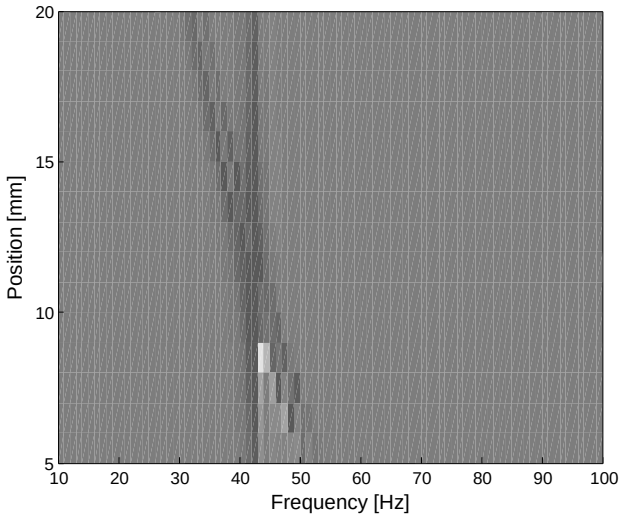

Figure 6.2: Simulation of position-dependence and change of dominant stiffness of the first eigenfrequency compared with the non-position-depending second eigenfrequency.

Obviously, one of the eigenfrequencies representing the rotary is constant, which is recognizable by the vertical peak line. The other one is position-dependent. At the intersection of both frequencies, there is an excessive peak. Thus, the eigenfrequencies excite each other and the damping is reduced near the fixed bearing.

However, the intersection is when ball screw nut and fixed bearing are very close, in the example about 10 [mm]. Certainly this position is impossible to reach in a real axis but illustrates the position-dependency of the axial eigenfrequency very clearly.

6.2.2 Modeling of joints with additional stiffness

It is possible to model joints with additional stiffness in different ways. Due to the modeling both bearings and ball screw nut are described. However, the direct connection of stiffness and constraints is unfeasible because the constraint disables any displacement besides the degree of freedom. However, this displacement is indispensable for the reaction forces of bearings. Thus, there are three different kinds of modeling of bearings. These are a single stiffness, a constraint or stiffness and constraint with an additional mass to connect the bodies. First of all, using a multi-axis spring with realization of the degrees of freedom by zero stiffness can cause severe calculation problems because the position of the spring's base should not be shifted far distances because of simulation stability. Secondly, it is not possible to emulate the stiffness by a constraint or joint. This leads to differences in mechanical behavior, for example eigenfrequencies are directly depending on stiffness. Last, the additional mass induces additional eigenfrequencies. Since this mass can be modeled very low, these frequencies are high above the frequencies interesting for machine tool simulation. The last type of modeling has been chosen and is shown schematically in figure 6.3.

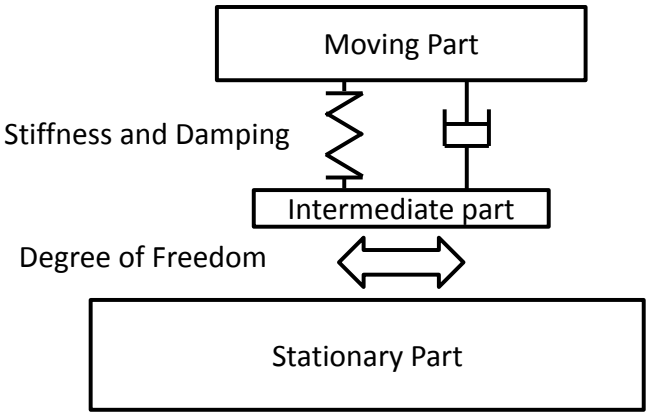

Figure 6.3: Modeling of bearings

6.2.3 Modeling of friction

Friction is modeled in detail at the components of the test rig's power train with relative velocity. For parametrization the identified friction parameters of the test rig and its components are used. Therefore, an additional force in the direction of the degree of freedom of the joints is integrated as shown in figure 6.4.

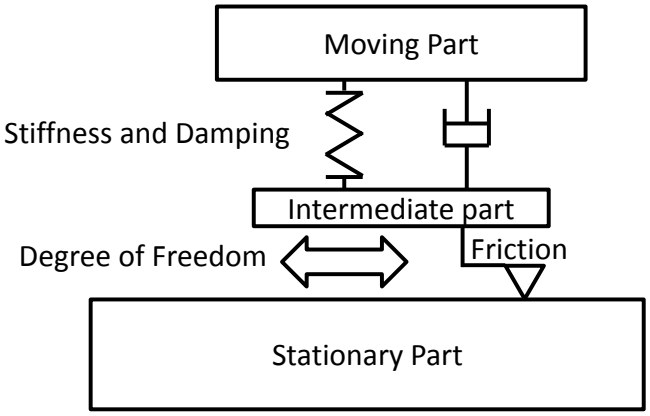

Figure 6.4: Model of joint with friction. The friction force is integrated parallel to the joint's DOF.

Since friction is not only load- but also velocity-depending, the relative velocity of the parts is also used for calculation. In order to parametrize the force dependency in the joints, the normal load in the spring-damper element is used as additional input and the velocity dependence is modeled using the viscous friction.The following equation illustrates this friction model.

$$F_R = -\text{sign}\left(v_{\text{rel}}\right)\left(F_C + f_v v_{\text{rel}}\right) \tag{6.5}$$

The part of the friction, which is not-load depending, is modeled at several components, and has been identified by measurements, as displayed in figure 5.16(b). Viscous and Coulomb friction have been estimated using a least square estimation. The identified friction values are the motor, which contains the damping of controller and electrical devices, the fixed and loose bearings, the ball screw nut and the linear bearings.

6.2.4 Modeling of direction depending-stiffness

Since the stiffness of linear bearings is dependent on the direction of shift, this behavior must be modeled. However, MSC.Adams only allows linear springs. In figure 6.5 a data sheet of Bosch Rexroth is displayed as example. There, a third order equation is used for describing the stiffness but obviously the linear term is dominant. Thus, the stiffness is linearized, which allows a rather simple modeling using spring-damper elements and force.

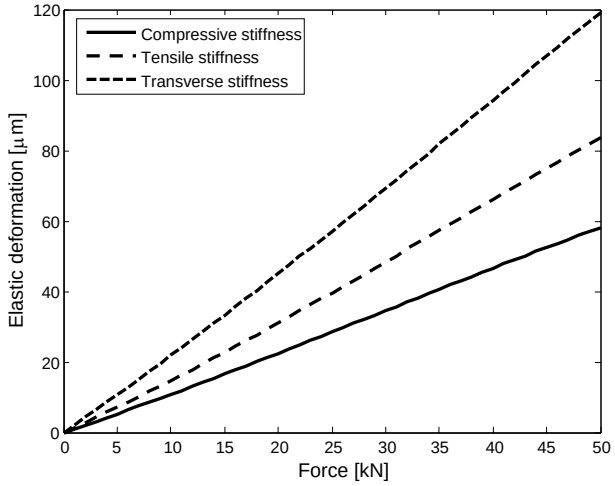

Figure 6.5: Direction-depending stiffness of linear bearing, data sheet of Bosch Rexroth RSF 1821-322-10.

Since the exact type of linear bearing and thus its parameters are unknown, the data of a bearing with the identical size have been used to model. Kipfmüller (2010) showed the validity of this assumption, which is having a parameter variation of about 14% for linear ball bearings.

In order to model the position dependency, the minimal stiffness is used to parametrize the spring. The additional stiffness is modeled as a direction-dependent spring-like force and is installed parallel to the stiffness. Usually, the tensile stiffness is smaller than the compressive stiffness, thus the force is 0 for tensile and c_{add} for comprehensive stiffness. This model is shown in the following equation. There Δz is the displacement along the vertical axis.

$$c = \begin{cases} c_{\text{tensile}} & \Delta z > 0 \\ c_{\text{compressive}} = c_{\text{tensile}} + c_{\text{add}} & \Delta z < 0 \end{cases} \tag{6.6}$$

6.3 Parameter variation

In order to model the variances of assembly conditions of components, their position is varied by shifting. A direct shift of a joint is difficult to parametrize because not only the part alone but also the root points of all appending spring-damper elements, forces and joints must be moved. Thus, an additional constraining force, which is the reaction force in reality, is used. This additional force becomes active after starting the simulation and shifts the part and all root points of its appendages. Since there is an impact force at the start of the simulation, there will be additional oscillation. However, this modeling is easier to parametrize and more stable than direct shifting and thus to be preferred.

With this additional force, the intermediate part of bearings, which is used to connect stiffness and degree of freedom, is shifted against the spring connecting it with the moving part. The shift Δx and respectively the force F can be calculated easily because the stiffness of the spring c is known.

$$\Delta x = \frac{F}{c} \tag{6.7}$$

As mentioned above, the friction force occurring between stationary and intermediate part is calculated using the force of the spring. A schema of this model is shown in figure 6.6. There Δx is the shift of the intermediate part and thus the joint's position.

The force occurring in the spring, which is the constraining force caused by the bearing, is used as normal force to calculate the force-depending part of the friction torque of ball screw nut, linear and rotational bearings as described before.

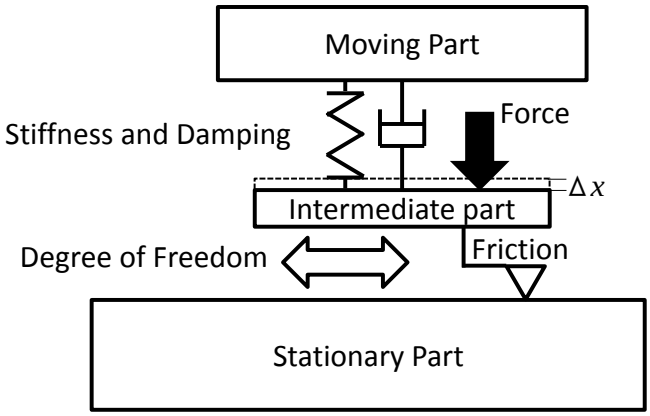

Figure 6.6: Model of joint including constraining force to vary the joints position.

As displayed, the complexity of the model of the joint increases. However, still the modeling process and parametrization are easily manageable and the results can be computed. The 3d visualization of the complete multibody model of the test rig modeled with MSC.Adams is shown in figure 6.7.

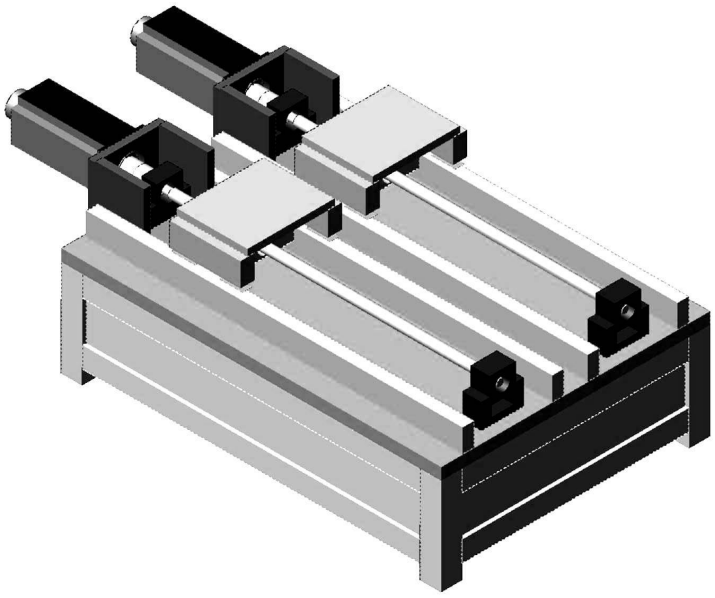

Figure 6.7: Visualization of the multibody model of test rig modeled with MSC ADAMS.

Identical with the measurements only one axis is moved during simulation to avoid influences from second axis dynamics. In the axis, which is not moving, the friction is switched off because there is a frequent change of velocity caused by transient oscillation during start of calculation. Thus the friction is switching

and increases calculation time and effort tremendously or results in abortion of simulation due to solver problems.

6.4 Simulation results

In this section, results of the simulation of the test rig model are discussed. Both the original situation and simulation under variation of mounting conditions of loose bearing and ball screw nut are examined. However, there is a significant simulation effort, especially costs of hard- and software, operating personnel, but also duration of simulation. Since the data to be stored becomes huge, there is a problem of simulating low velocities. Thus, the simulation has been performed for velocities higher than $v \geq 5$ [mm/s] = 300 [mm/min]. The maximum velocity simulated has been 4500 [mm/s] because the friction behaves nearly linearly for higher velocities and can be extrapolated. Since the Stribeck effect is not modeled, it cannot be estimated.

During the measurements, the positions of the loose bearing and the ball screw nut are varied. Thus, measurement and simulation can be compared easily. However, the simulation model also allows varying all other joints, for example fixed bearing or guiding carriage. Furthermore, the load on every connection of components and their displacement can be observed. This means, the displayed method has an excellent usability for the examination of assembly variations and their impact on all joints, respectively components.

The position dependence of friction is shown in figure 6.8(b) and compared with the original state of the model 6.8(a). Here, the position of the loose bearing is varied, which means shifted perpendicularly to its rotation axis, and the carriage moves with constant velocity along the complete traveling distance. The original state shows a nearly constant friction of fixed and loose bearing along the traveling distance. As expected, the state with the varied loose bearing shows a strongly increasing friction torque at the loose bearing, while the fixed bearing

stays constant. The maximum of friction torque is reached when the carriage is next to the loose bearing.

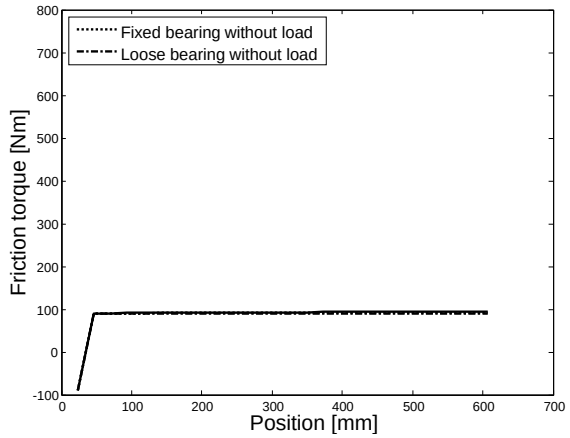

(a) Original situation of friction.

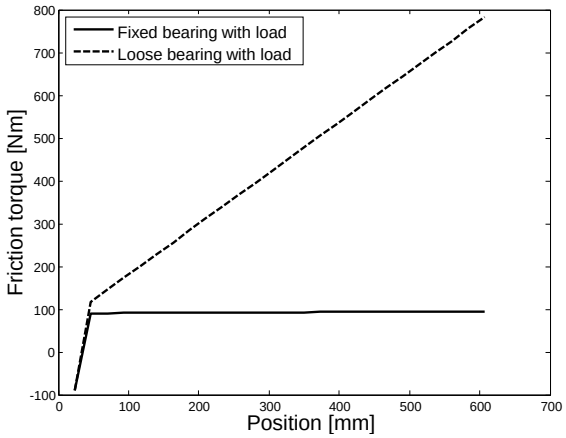

(b) Varied situation of friction with shifted loose bearing.

Figure 6.8: Position-dependence of friction torque of fixed and loose bearing at constant velocity of 5 [mm/s]. The left figure shows the original situation and the right the varied. The loose bearing shows a strong position dependency while the fixed bearing does not. The discontinuity near position zero results from singularities of the model. This is detailed in figure 6.9.

In the simulation environment it is possible to estimate the friction torque and force at every single connection of components in all directions. Furthermore, the shift and rotation of all bodies are evaluable. Thus, it is easily possible to get a very detailed idea of the distribution of friction and constraining forces on components.

In order to derive the friction curve along the complete traveling distance, the results of the individual simulations with constant velocity are combined. Thus, a surface of friction at all positions and various velocities is made by interpolation. This kind of friction contour for different combinations of varied components and other criteria permits a reliable comparison of influences on the axis behavior as shown in figures 6.9 and 6.11.

6.4.1 Friction in components

As mentioned above, one important advantage of simulation is the possibility to estimate not measurable forces. However, in order to proof the reliability of the simulation results, the behavior of the simulation model has to be compared with the behavior of the real system first. Thus, in the following, several examples of friction force or respectively torque occurring at joints and the effects of variation are displayed. In order to illustrate the functionality and reliability of this method, the same variations as during the measurements have been executed.

Loose bearing variation

As conducted during the measurements, the loose bearing has been shifted in vertical direction. The measuring results have been used for simulation.

In figure 6.9, effects of variation of loose bearing's radial position resulting from the assembly process on the friction behavior of fixed and loose bearing is illustrated. Here, the x- and y-axis are representing position and velocity of the carriage and the friction is illustrated by a contour chart of constant friction torque values in [Nmm]. While a tremendous change of friction torque at the loose bearing can be recognized, there is nearly no remarkable effect on the fixed bearing, and thus there is no change in the forces acting on the fixed bearing. As predicted, the mounting failures of the loose bearing only have a local impact, which means there are constraining forces acting on loose bearing and ball screw nut and on linear bearings but not on other components located in the force flux before the ball screw nut. Furthermore, obviously this effect is strongly position-dependent with a nearly linear increase along the traveling length of the machine tool axis.

Obviously the friction torque of the varied loose bearing 6.9(b) is linearly increasing between starting point ($x = 0$ [mm]) and terminal point ($x = 750$ [mm]), which is also observed by the measurements described before. This linear behavior has been modeled with respect to the measuring results discussed in section

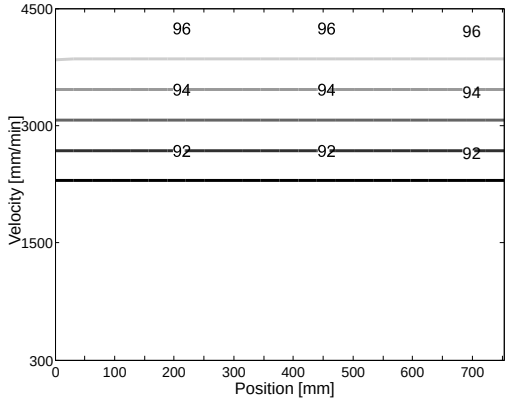

(a) Original situation of friction of loose bearing.

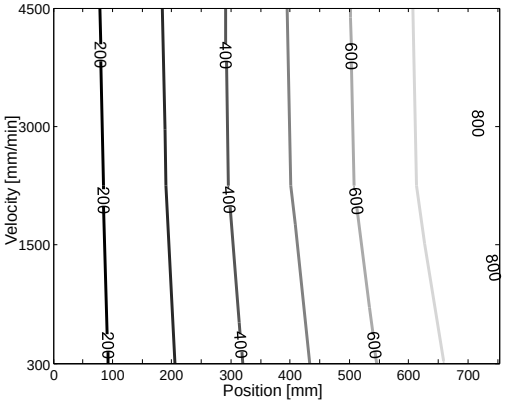

(b) Varied situation of friction of loose bearing.

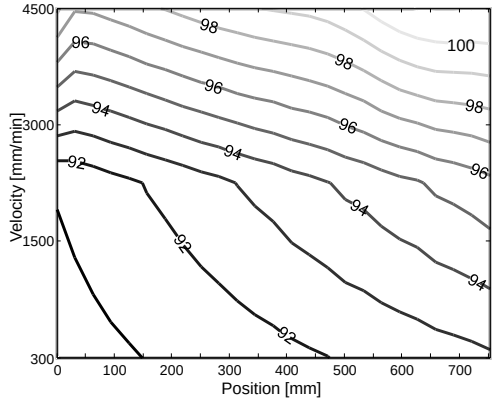

(c) Original situation of friction of fixed bearing.

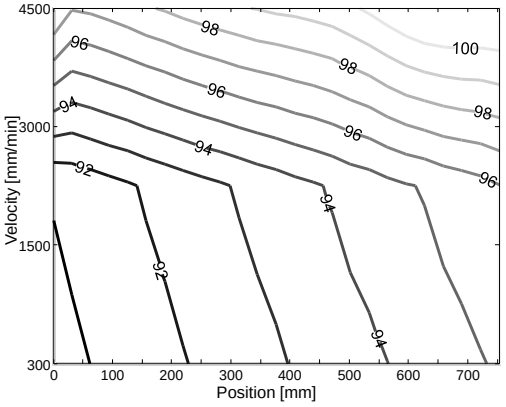

(d) Varied situation of friction of fixed bearing.

Figure 6.9: Effect of variation of loose bearing on fixed and loose bearings' friction behavior.

5.4.5. A strong velocity-dependence of loose bearing's friction torque is nearly not recognizable.

There is no significant impact on fixed bearing's behavior detectable, this means there is no change in the fixed bearing's radial position and also no constraining force is induced. Thus, neither the alignment of the coupling nor the alignment of rotor and thereby the friction torque of the motor will be effected by the assembly condition of the loose bearing. Hence detailed observations of these components and their friction behavior have been omitted.

This position-dependency of the friction of loose bearing and ball screw nut, which

is not displayed, can also be observed in the total friction, which is measured using the motor current and calculated using the motor's torque constant. The total friction is the summation of all frictions of the components, which means the sum of the complete dissipating energy. In figure 6.10 the total friction torque of rotating components in original and varied state are displayed. In the simulation model the sources of friction are motor, fixed and loose bearing and ball screw. There is an obvious position dependency, which is caused by the friction of the shifted loose bearing and the reacting forces of ball screw nut. Thus, the friction has a maximum with the carriage next to the loose bearing.

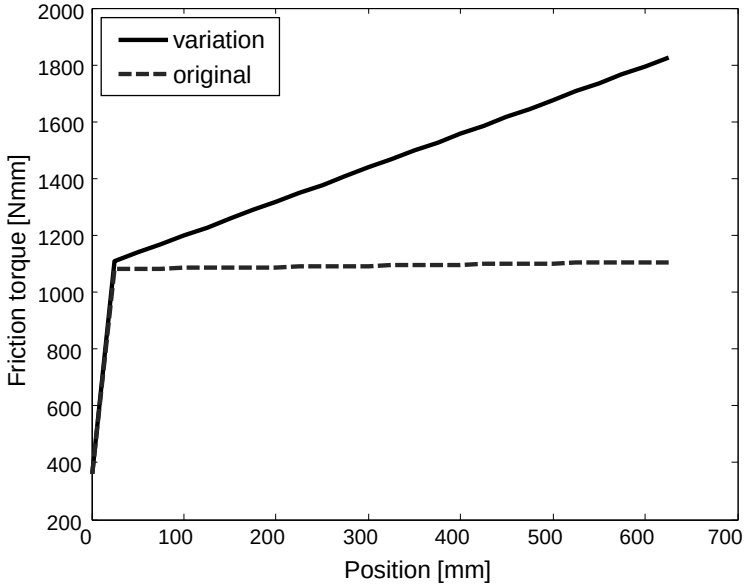

Figure 6.10: Comparison of total friction of all rotating components in original and varied state of the loose bearing along traveling distance. The discontinuity near position zero results from singularities in the model.

The simulated friction and the measured friction's dimension are well matched. There are differences, which are caused by simplifications made in the modeling process.

Ball screw variation

The ball screw nut's coaxial alignment has been varied during measurements. Thus, this variation also is modeled and simulated in the multibody simulation.

The position of the nut and therewith the screw joint is moved like the loose bearing described in section 6.3 by using an external force.

The complete calculated friction is shown in figure 6.11. Both position and velocity dependency of friction caused by variation are displayed in contour plot and illustrated in detail for three positions, near fixed bearing, near loose bearing and in the middle of the traveling distance. As observed during the measurements and discussed in section 5.4.5, there is, as expected, an evident minimum of friction torque in the center of the traveling distance and there are two maxima of friction when the carriage is next to the bearings. Furthermore, the friction distribution is nearly symmetrical, which results from the assumption of identical mechanical behavior and ideal alignment of both fixed and loose bearing.

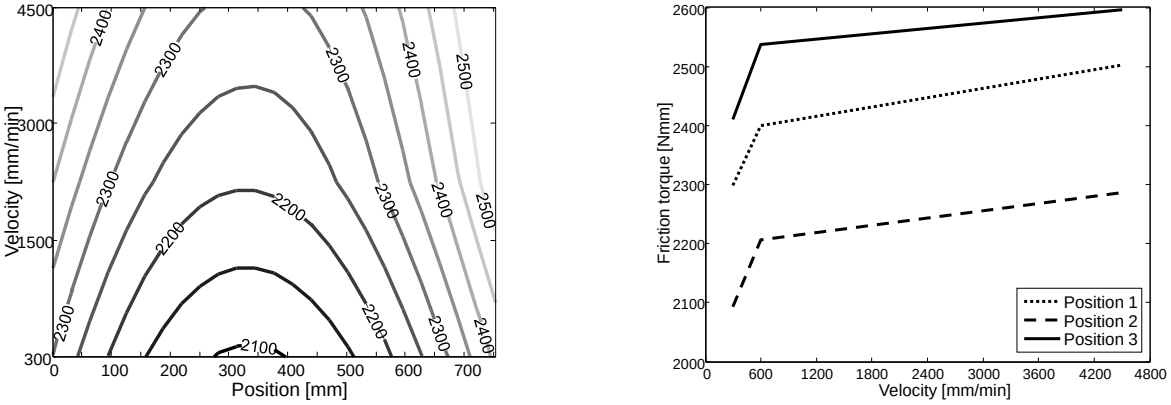

(a) Contour of friction torque's dependence on position and velocity.

(b) Position dependency of friction torque.

Figure 6.11: Effect on friction torque by variation of ball screw nut's mounting. In the center of the traveling range a minimum of force occurs.

This displayed distribution of friction torque results from the constraining force having a minimum in the center of the traveling range. Thus the normal force, which is proportional to the friction, and acting on the spindle nut and the bearings has a minimum, too. Hence, the bending resistance of the ball screw spindle and thus the alignment error of the ball screw nut directly influence the normal force and friction torque of the axis.

6.4.2 Recapitulation of simulation results

It has been illustrated, with a comparatively simple multibody model and a rough friction model, that a reliable simulation of the test rig and different variations of assembly conditions of components are possible. The simulation results are comprehensible and comparable with the measurements.

However, because no standard software is used for simulation, the modeling and parametrization of the machine tool model still needs expert knowledge and well-educated personnel. Furthermore, the interpretation of the simulation results requires a similar detailed knowledge of the mechanical and electrical behavior and the sources of friction and damping of machine tools as the interpretation of measurement results.

7 Experimental results and relevance for machine tool assembly

Since both measurements and simulation have been conducted, their results must be compared and resulting conclusions derived. Thus, assembly processes sensible to variances can be determined and machine tool producing companies are able to improve their assembly processes as well as to focus the construction and production on these sensible processes. In this chapter, firstly, the experimental results of measurement and simulation are displayed and compared. Secondly, the relevance of these results for the assembly process is presented.

7.1 Comparison of simulation and measurement

Since the reasons for variation of friction of machine tools are unclear and only individual machines like the test rig, which contains all interesting components, are identified in detail, this is modeled as multibody model. Here the variations, which are conducted during the measurements, namely the position of the loose bearing and the spindle nut perpendicular to the axis, are examined. Since these are representative and further variations are connected with high mounting effort, further experiments are not conducted. Furthermore, there is a multitude of possible failure combinations and influences, which result in a very high experimental

complexity. Therefore, a comprehensive experimental examination of assembly failures at a test rig is very difficult and at a machine tool even impossible.

However, as discussed in chapter 6, in simulation models it is also possible to vary other joints easily, for example fixed bearing or guiding carriage. Even complex variations, for example alignment of the guiding rail, can be modeled by position-depending functions. Furthermore, a simulation model allows parameter studies with limited effort because there is no need for a completely new setup of the model.

The comparability of the measurements and simulation results is restricted because the assembly of the test rig is not ideal, which means certainly there are assembly deviations, which are not considered by the simulation model. Thus, an exact modeling of reality and variations is not possible. However, the developed simulation method shows a reliable match and reproducible results of complex machines' mechanical behavior under variation of assembly conditions. Furthermore, this allows modeling the margin of deviation caused by the maximum tolerances.

7.1.1 Measurement results

As expected, measurements of identical machine tools are different and reveal a different behavior, which is caused by assembly deviations. Since it is expected identical machine tools producing identical machining results and also having the same life expectancy, this variation of their behavior is undesired. In order to determine the reasons for the observed differences, measurements at a test rig with different assembly failures are conducted. These are variations of the position of loose bearing and ball screw nut causing severe changes of normal forces within these and their neighboring components. Since the friction is proportional to the normal force, the friction of these components is strongly affected as well.

The reliability of the developed measuring algorithm using an NC program has been tested with two different NC controllers, namely Sinumerik and TwinCAT. Since DIN ISO code has been used, it will certainly work for machine tool axes

driven by other controllers, if these allow recording of motor current and command and actual velocity. Hence, it is possible to provide similar measuring algorithms for these.

It has been shown that the results at identical conditions, for example machine tool after warming-up, are repeatable. Even by measuring one single axis, assembly failures can be detected and their reason can be estimated. Last but not least, identical axes show a qualitatively similar characteristic, which means the measured friction force has a Stribeck behavior. However, certain deviations, caused by assembly deviations and tolerances, are remarkable.

At an axis test rig for ball screw driven machine tool axes a multitude of measurements under variation of assembly conditions has been conducted. Here the ball screw nut and the loose bearing have been varied. The effects of variations can be explained reliably and become quantitatively predictable.

Thus dependable results for reason and effect of assembly failures are determined for various core components. These have been used for a realistic and reliable parametrization of the simulation models.

7.1.2 Simulation results

The simulation of assembly deviations is possible and can be used to predict the impact of these deviations on components. Thus, it becomes possible to estimate the severity with regard to other components and the machines life expectancy.

There are several challenges getting reliable results by using simulation models. However, still experts are needed for modeling and parametrization of the simulation. The interpretation of results needs experienced personnel, too. Otherwise, severe misinterpretations are possible. In figure 7.1 the measurement and simulation results are compared at a position near the fixed bearing without variation. Here a coincidence of friction behavior is obvious.

Furthermore, there is a significant simulation effort needed especially regarding hard and software but also duration of the simulation, which means high expenses

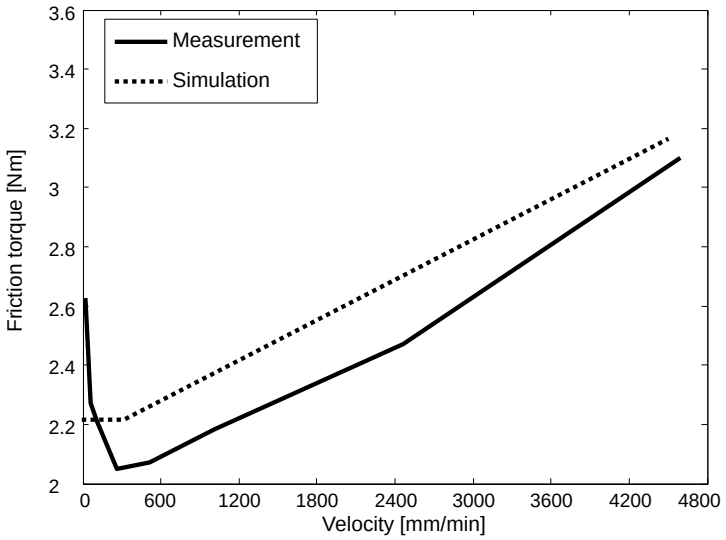

Figure 7.1: Comparison of measurement and simulation result at position near the fixed bearing without variation.

for licenses and hardware. Since the data volume to be stored becomes huge, there is a problem to simulate low velocities. Therefore, as mentioned in chapter 6, the simulation only has been performed for velocities between $v \geq 5$ [mm/s] = 300 [mm/min] and 4500[mm/min]. Since the friction shows a nearly linear increase, higher velocities can be extrapolated. Although the lowest velocity is below the Stribeck velocity, this effect cannot be observed because the Stribeck effect has not been modeled; due to this, there is no further negative influence on the accuracy of the model.

Thus, it must be estimated, whether the expected simulation results justify this personnel and computational effort. However, the possibility of observing forces in all joints and the flexibility of parametrization, justifies additional effort.

Simulation and measurement have a significant accordance. This is exemplarily illustrated by a comparison of the position dependency of the loose bearing's variation in figure 7.2, in which the complete friction torque of all components at the same positions is displayed as described in section 5.4.5. In order to improve the comparability, the measured friction curves at the three working points are plotted below the simulation results.

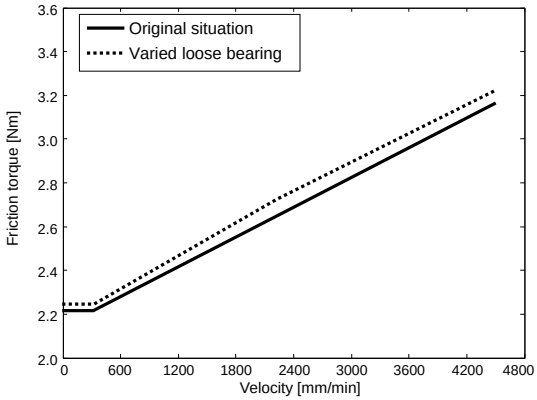

(a) Friction at position 1 - simulation.

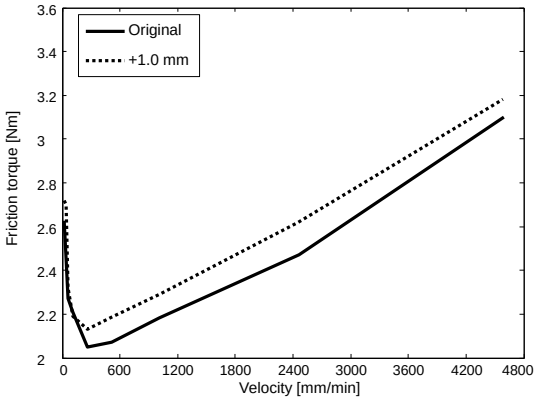

(b) Friction at position 1 - measurement.

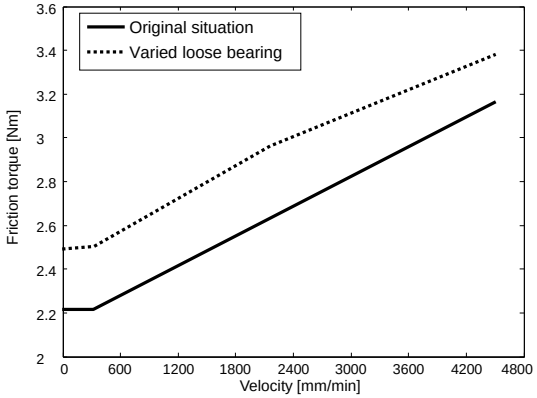

(c) Friction at position 2 - simulation.

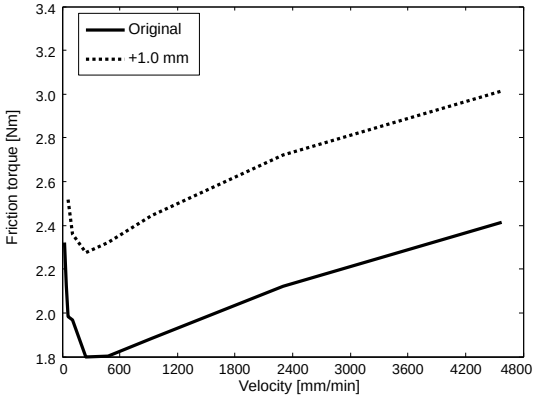

(d) Friction at position 2 - measurement.

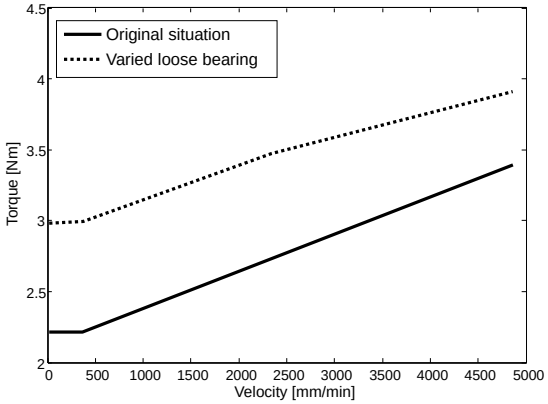

(e) Friction at position 3 - simulation.

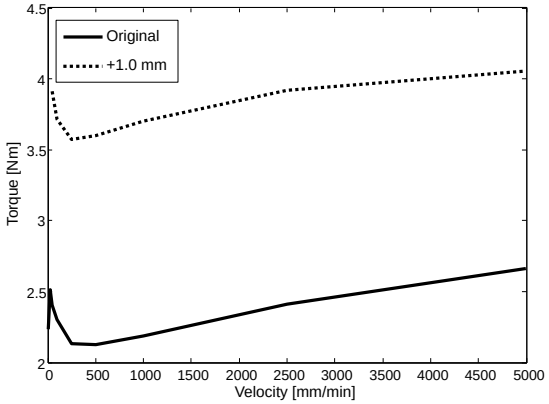

(f) Friction at position 3 - measurement.

Figure 7.2: Comparison of simulation and measurement of friction during loose bearing variation. On the right side the measurements and on the left the simulation results are displayed.

The displayed and compared curves in figure 7.2 show that, even with a comparatively simple multibody model, the simulation results are fitting the measurements

of the test rig discussed in chapter 5 very well. The obvious deviations are caused by parameter, which have not been modeled. These are the especially the Stribeck behavior, which mainly causes the deviation at low velocities, and the rolling friction in the contacts, which effects the slope of the friction curve. Furthermore, local effects have not been modeled and the modeling of the shift by an additional force does not represent the reality correctly. However, the simplification of the model mainly affects the friction at low velocities and thus it is possible to use the evolved method to estimate the impact of possible assembly failures in early stages of the product development process and consequently determine tolerances of assembly interfaces. Furthermore, forces in the bearings can be estimated and used for an enhanced calculation of the life expectancy.

Since the amount of data increases, its handling becomes more complicated and the required duration of the simulation and result estimation is extended tremendously. Thus, it becomes difficult to execute the simulation along the complete traveling distance for small velocities. In order to avoid this difficulty, the simulation should be conducted at specified working points along the axis. For ball screw driven axes the positions next to the bearings and in the middle of the traveling distance are sufficient. However, in order to receive more detailed results, more working points are necessary.

7.2 Relevance for machine tool assembly

As shown by FMEA in section 5.1, the ball screw and the fixed bearing are the components that usually fail by damage, which means these are the most sensitive to assembly failures. Thus, especially the assembly process of these and the components directly affecting them must be conducted carefully. Here, an exact and reproducible process for adjusting the preload is recommended. Furthermore, the alignment of bearings and ball screw nut along the complete traveling range must be guaranteed.

The motor has a strong angular-dependent current characteristic, the so-called cogging effect. Since it is time-invariant, it can be compensated easily. It needs not to be considered with respect to the influence on components' duration after compensation because there is no further impact.

It is shown that the fixed and loose bearings have a local impact because the constraining forces can bend the ball screw spindle. The bending of the spindle depends on the cross-section area of the spindle and the position of the ball screw nut. If the nut is near the bearing, a very high constraining force occurs. Thus, if there is a misalignment between bearing and spindle and the working point is near the misaligned bearing, this constraining force will reduce the duration of both ball screw nut and bearing.

Often the working point of a machine tool is next to the fixed bearing and constraining forces are caused by alignment failures between bearing and ball screw nut. Since the feed and the machining direction are alternating, the friction forces, whose absolute value is depending on normal force and moving direction, are alternating as well. Thus, the duration of components is tremendously reduced, which explains the earliest damages at fixed bearing and ball screw nut.

The linear bearings have influence on friction, locally as well as along the whole distance. The local failure is related to the alignment failure of the guide rails and the global to the exactness of the mounting of the wagons.

Since a constant offset of friction torque is easier to handle with regard to calculation of components' duration and compensation algorithms than a position-depending one, effort should be spend on ensuring the alignment of spindle and fixed and loose bearing as well as linear bearings' guideways. Furthermore, the guideways have a strong impact on the positioning accuracy.

8 Conclusion

8.1 Recapitulation

Firstly, by measuring static friction it is shown that there are severe differences of friction and mechanical behavior between identical machine tools recognizable. These are caused by components' and assembly variances. These differences are mainly caused by assembly deviations of the bearing system. Since the bearings are rigid, even a small deviation leads to tremendous constraining force. These constraining forces can result in a reduced life expectancy of the involved components. In order to determine the reasons of the observed variances and effects, a test rig of a machine tool axis is built.

Secondly, selected assembly parameters are varied at a test rig to determine their impact on friction behavior. Here, a local impact of assembly variances of rotational bearings and ball screw nut is identified. Furthermore, in order to parametrize the simulation model, the friction of components - bearings, ball screw and motor - is estimated.

Thirdly, a multibody model is developed, which allows varying assembly parameters. There, the impact of assembly variations on various components, which is partly impossible to measure, can be estimated by simulation. Furthermore, the simulation allows distinct variation and their combination.

However, a detailed knowledge of machine tools and their properties are necessary. Only if a reliable model of the machine tool is given, the simulation results under variation of the components' behavior are reliable.

Still, it is nearly impossible to determine the reasons of variation because it is a complex combination of variances of components' properties, deviations of assembly process and external sources like temperature or lubrication conditions. Therefore, in the simulation model these are combined in variance of external forces acting on a component, which is shifting its position. This means there is one variation parameter for each component. Thus, it becomes easily possible to simulate assembly variations. The maximal variation of these parameters can be distinguished by the assembly deviation and deviation of components. Both can be determined by tolerances.

Although simulation is a proper approach for examination effects of parameter variation, still there is expert knowledge necessary for modeling and parametrization. Furthermore, the effort to get reliable results by simulation is as difficult as conducting experiments at a test rig and the interpretation of simulation results is usually complicated and requires experience. Hence it is not possible to use the discussed simulation approach in the construction process of machine tools, yet.

8.2 Perspective

Since the presented method allows a detailed knowledge about the load acting in the machine tools components with regard to assembly failures, the calculation of duration can be improved. Thus, the planning of preventive maintenance can be done for individual machine tools.

Early defect detection reduces costs tremendously. Thus, a detailed knowledge of possible failures and their effects is of great importance. Therefore, both components' parameter variation and assembly process have to be examined in detail. Especially in the machine tool industry, there still is a lack of knowledge about the exactness of assembly processes because the production lot is small and the number of customer oriented varieties is huge.

In future, the friction measurement can be included into the warm-up cycles of machine tools, which are conducted after a longer standstill, for example after a weekend. This allows comparing the newly estimated friction parameters with the parameters already available from other measurements conducted regularly from the start-up. Thus, it becomes possible to monitor trends and detect severe changes of behavior at an early stage without causing additional effort and costs.

Further effort must be spent, in order to reduce the modeling effort, to increase the manageability of simulation tools and to improve the interpretability of simulation results.

Bibliography

Abler, Felten et al. 2004 — Abler, J., Felten, K., Kobialka, C., Lierse, T., Mundt, A., Pomp, J., and Sulzer, G., 2004. *Verzahntechnik - Informationen für die Praxis*, Liebherr Verzahntechnik GmbH, Kempten, 2nd edn.

Al-Bender, Lampaert et al. 2005 — Al-Bender, F., Lampaert, V., and Swevers, J., 2005. The Generalized Maxwell-Slip Model: A Novel Model for Friction Simulation and Compensation, *IEEE Transactions on Automatic Control* **vol. 50**(11) pp. 1883–1887

Albrecht 2009 — Albrecht, A., 2009. *Wärmedehnungskompensierte Rekonstruktion von Prozesskräften an Vorschubantrieben*, Ph.D. thesis, Universität Braunschweig

Armstrong-Hélouvry, DuPont et al. 1994 — Armstrong-Hélouvry, B., DuPont, P., and Canudas De Wit, C., 1994. A survey of Models, Analysis Tools and Compensation Methods for the Controls of Machines with Friction, *Automatica* **vol. 30**(7) pp. 1083–1134

Baly 2005 — Baly, H., 2005. *Reibung fettgeschmierter Wälzlager*, Ph.D. thesis, Universität Hannover

Baudisch 2003 — Baudisch, T., 2003. *Simulationsumgebung zur Auslegung der Bewegungsdynamik des mechatronischen Systems Werkzeugmaschine*, Ph.D. thesis, Technische Universität München

Beckhoff Automation 2014 — Beckhoff Automation, June 2014. *TS3300 | TwinCAT Scope 2 Tutorial - Scope View 2*, Beckhoff Automation GmbH

Beitz and Grote 2001 — Beitz, W. and Grote, K.-H. (eds.), 2001. *Dubbel*, Springer Verlag, 20th edn.

Bosch Rexroth 2006 — Bosch Rexroth, 2006. *Handbuch Lineartechnik*, Bosch Rexroth AG, Schweinfurt

Bosch Rexroth 2008 — Bosch Rexroth, 2008. *IndraWorks 09V02.0085*, Bosch Rexroth AG

Bosch Rexroth 2010 — Bosch Rexroth, 2010. *Synchronous servo motors - IndraDyn S - MSK - to meet all requirements*, Bosch Rexroth AG - Electric Drives and Controls, P.O. Box 13 57 97803 Lohr Germany

Botz 1992 — Botz, M., 1992. *Zur Dynamik von Mehrkörpersystemen mit elastischen Balken*, Ph.D. thesis, Universität Darmstadt

Brecher, Fey et al. 2012 — Brecher, C., Fey, M., and Bäumler, S., 2012. Identification method for damping parameters of roller linear guides, *Production Engineering Research and Development* **vol. 6**(4-5) pp. 505–512, doi:10.1007/s11740-012-0400-z

Broos 2012 — Broos, A., 2012. *Simulationsgestützte Ermittlung der Komponentenbelastung für die Lebensdauerprognose an Werkzeugmaschinen*,

Ph.D. thesis, Karlsruhe Institute of Technology (KIT)

Canudas de Wit, Olsson et al. 1995

Canudas de Wit, C., Olsson, H., Åström, K. J., and Lischinsky, P., 1995. A New Model for Control of Systems with Friction, *IEEE Transactions on Automatic Control* **vol. 40**(3) pp. 419–425

Craig and Bampton 1968

Craig, R. R. Jr. and Bampton, M. C.C., July 1968. Coupling of Substructures for Dynamic Analysis, *AIAA Journal* **vol. 6**(7) pp. 1313–1319

Croon and Pruschek 2005

Croon, N. and Pruschek, P., 2005. Gekoppelte Simulation; in Simulationstechnik in der Produktion, In Brecher, C., Pritschow, G., Krüger, J., Uhlmann, E., and Verl, A. (eds.), *Simulationstechnik in der Produktion*, Düsseldorf: VDI-Verlag, no. No. 658 In Fortschritt-Berichte VDI, chap. 7, pp. 81–99, reihe 2 edn.

Dahl 1968

Dahl, P. R., May 1968. *A solid friction model*, report Aerospace Report No. TOR-0158(3107-18)-1, The Aerospace Corporation, El Secundo, CA

DGQ 2012

DGQ, 2012. *FMEA - Fehlermöglichkeits- und Einflussanalyse*, Tech. Rep., DGQ Deutsche Gesellschaft für Qualität e.V., Frankfurt

DIN 69051-6 1989

DIN 69051-6, April 1989. *DIN 69051 Teil 6: Kugelgewindetriebe - Berechnung der statistischen Steifigkeit*, industrial standard, DIN Deutsches Institut für Normung e.V.

DIN EN 60812 2006 — DIN EN 60812, November 2006. *DIN EN 60812: Analysetechniken für die Funktionsfähigkeit von Systemen - Verfahren für die Fehlerzustandsart- und -auswirkungsanalyse (FMEA)*, industrial standard, DIN Deutsches Institut für Normung e.V.

DIN EN ISO 13849-1 2008 — DIN EN ISO 13849-1, December 2008. *DIN EN ISO 13849-1: Sicherheit von Maschinen - Sicherheitsbezogene Teile von Steuerungen - Teil 1: Allgemeine Gestaltungsleitsätze*, industrial standard, DIN Deutsches Institut für Normung e.V.

DIN EN ISO 9000 2005 — DIN EN ISO 9000, December 2005. *DIN EN ISO 9000: Qualitätsmanagementsysteme - Grundlagen und Begriffe*, industrial standard, DIN Deutsches Institut für Normung e.V.

DIN ISO 10791-1 2001 — DIN ISO 10791-1, January 2001. *DIN ISO 10791 Teil 1: Prüfbedingungen für Bearbeitungszentren - Teil 1: Geometrische Prüfungen für Maschinen mit waagerechter Spindel und mit zusätzlichen Fräsköpfen (waagerechte Z-Achse)*, industrial standard, DIN Deutsches Institut für Normung e.V.

DIN ISO 10791-4 2001 — DIN ISO 10791-4, January 2001. *DIN ISO 10791 Teil 4: Prüfbedingungen für Bearbeitungszentren - Teil 4: Genauigkeit und Wiederholpräzision der Positionierung linearer und rotierender Achsen*, industrial standard, DIN Deutsches Institut für Normung e.V.

DIN ISO 230-1 1999 — DIN ISO 230-1, July 1999. *DIN ISO 230 Teil 1: Prüfregeln für Werkzeugmaschinen - Teil 1: Geometrische Genauigkeit von Maschinen, die ohne Last oder unter Schlichtbedingungen arbeiten*, industrial standard, DIN Deutsches Institut für Normung e.V.

DIN ISO 230-2 2011 — DIN ISO 230-2, January 2011. *DIN ISO 230 Teil 2: Prüfregeln für Werkzeugmaschinen - Teil 2: Bestimmung der Positioniergenauigkeit und der Wiederholpräzision der Positionierung von numerisch gesteuerten Achsen (Entwurf)*, industrial standard, DIN Deutsches Institut für Normung e.V.

DIN ISO 230-4 2001 — DIN ISO 230-4, May 2001. *DIN ISO 230 Teil 4: Prüfregeln für Werkzeugmaschinen - Teil 4: Kreisformprüfungen für numerisch gesteuerte Werkzeugmaschinen*, industrial standard, DIN Deutsches Institut für Normung e.V.

Drinčić 2012 — Drinčić, B., 2012. *Mechanical Models of Friction That Exhibit Hysteresis, Stick-Slip, and the Stribeck Effect*, Ph.D. thesis, University of Michigan

Ewins 2000 — Ewins, D. J., 2000. *Modal testing: theory, practice and application*, Baldock, Hertfordshire: Research Studies Press Ltd., 2nd edn.

FAG 1999 — FAG, 1999. *FAG Wälzlager - Kugellager, Rollenlager, Gehäuse, Zubehör*, FAG Kugelfischer Georg Schäfer AG, Schweinfurt, katalog wl 41 520/3 db edn.

Fey 2013 — Fey, M., July 2013. Dämpfung in Maschinenelementen

Fleischer, Schopp et al. 2007 — Fleischer, J., Schopp, M., Broos, A., and Wieser, J., 2007. Datenbasis für lastabhängige Prozesseingriffe - Modularisierung und Analyse von Ausfallursachen zur Erhöhung der Verfügbarkeit von Werkzeugmaschinen, *wt Werkstattstechnik online* **vol. 7/8** pp. 491–497

Frey, Walther et al. 2010 — Frey, S., Walther, M., and Verl, A., 2010. Periodic variation of preloading in ball screws, *Production Engineering Research and Development* doi:10.1007/s11740-010-0207-8

Frey, Dadalau et al. 2012 — Frey, S., Dadalau, A., and Verl, A., 2012. Expedient modeling of ball screw feed drives, *Production Engineering Research and Development*

Fujita, Matsubara et al. 2011 — Fujita, T., Matsubara, A., and Yamada, S., 2011. Analysis of Friction in Linear Motion Rolling Bearing with Locomotive Multi-Bristle Model - Influence of Slipping Velocity Distribution on Friction Characteristics, *Journal of the Japan Society of Mechanical Engineers (JSME)* **vol. 77**(778) pp. 318–327

Gauss 1825 — Gauss, C. F., 1825. *Theoria Combinationis Observationum Erroribus Minimis Obnoxiae*, Göttingen

Groß, Hamann et al. 2006 — Groß, H., Hamann, J., and Wiegärtner, G., 2006. *Elektrische Vorschubantriebe in der Automatisierungstechnik: Grundlagen, Berechnung, Bemessung*, Erlangen: Publicis Corporate Publishing, 2nd edn.

Haessig and Friedland 1990 — Haessig, D. A. and Friedland, B., May 1990. On the Modelling and Simulation of Friction, In *Proceedings of the 1990 American Control Conference*, pp. 1256–1261

Hauger, Schnell et al. 2002 — Hauger, W., Schnell, W., and Gross, D., 2002. *Technische Mechanik 3 - Kinetik*, Springer, 7th edn.

Heidenhain 2013 — Heidenhain, September 2013. *Dynamic Precision - dynamisch mit hoher Genauigkeit bearbeiten*, Dr. Johannes Heidenhain GmbH

Heimann, Gerth et al. 2007 — Heimann, B., Gerth, W., and Popp, K., 2007. *Mechatronik: Komponenten, Methoden, Beispiele*, München: Fachbuchverlag Leipzig im Carl-Hanser-Verlag, 3rd edn.

Hertz 1881 — Hertz, H., 1881. Ueber die Berührung fester elastischer Körper, *Journal für die reine und angewandte Mathematik* **vol. 92**(2) pp. 156–171

Hielscher 2008 — Hielscher, T., 2008. *Qualitätsmanagement in fertigungstechnischen Prozessketten: Vorgehensweise zur fehlerbasierten Optimierung der gefertigten Bauteilqualität*, Ph.D. thesis, Technische Universität Kaiserslautern

Hofmann 2012 — Hofmann, S., 2012. *Identifikation parametrischer Modelle für geregelte elektromechanische Achsen mit modifizierter sukzessiver Polkompensation*, Ph.D. thesis, Technical University Chemnitz

INA 1968 — INA, 1968. *Maßkatalog D302*, INA-Nadellager - Industriewerke Schaeffler, Herzogenaurach

Isermann 2008 — Isermann, R., 2008. *Mechatronische Systeme: Grundlagen*, Berlin: Springer Verlag, 2nd edn.

Ispaylar 1996 — Ispaylar, M. H., 1996. *Betriebseigenschaften von Profilschienen-Wälzführungen*, Ph.D. thesis, Rheinisch-Westfälische Technische Hochschule Aachen (RWTH Aachen)

Ito 1957 — Ito, S., 1957. Analysis of rolling friction between steel ball and race track, *Bearing Engineer* **vol. 6**(1) pp. 784–792, (in Japanese)

Jamaludin, Brussel et al. 2008 — Jamaludin, Z., Brussel, H. v., and Swevers, J., March 2008. Quadrant Glitch Compensation using Friction Model-Based Feedforward and an Inverse-Model-Based Disturbance Observer, In *IEEE International Workshop on Advanced Motion Control 2008 (AMC'08)*, pp. 212–217

Karnopp 1985 — Karnopp, D., 1985. Computer simulation of stick-slip friction in mechanical dynamic systems, *ASME Journal of Dynamic Systems, Measurment and Control* **vol. 107**(1) pp. 100–103

Kato 2000 — Kato, K., 2000. Wear in relation to friction — a review, *Wear* **vol. 241** pp. 151–157

Kimura, Sekizawa et al. 2002 — Kimura, Y., Sekizawa, M., and Nitanai, A., 2002. Wear and fatigue in rolling contact, *Wear* **vol. 253** pp. 9–16

Kipfmüller 2010 — Kipfmüller, M., 2010. *Aufwandsoptimierte Simulation von Werkzeugmaschinen*, Ph.D. thesis, Karlsruhe Institute of Technology (KIT)

Klein 2011 — Klein, W. H., 2011. *Zustandsüberwachung von Rollen-Profilschienenführungen und Kugelgewindetrieben*, Ph.D. thesis, Rheinisch-Westfälische Technische Hochschule Aachen (RWTH Aachen)

Kunc 2007 — Kunc, M., 2007. *Analyse relevanter Dämpfungseinflüsse in Werkzeugmaschinen*, Researchreport FWF 0179, Forschungsvereinigung Werkzeugmaschinen und Fertigungstechnik e.V. (FWF), Frankfurt am Main

Kunc 2013 — Kunc, M., 2013. *Identifikation und Modellierung von nichtlinearen Dämpfungseffekten in Vorschubachsen für Werkzeugmaschinen*, Ph.D. thesis, Rheinisch-Westfälische Technische Hochschule Aachen (RWTH Aachen)

Löwenfeld 1955 — Löwenfeld, K., 1955. Die Dämpfung bei Werkzeugmaschinen, In *2. FOKOMA, Maschinenmarkt*

Matsubara, Sayama et al. 2014 — Matsubara, A., Sayama, A., Sakai, T., and Reuss, M., 2014. Analysis of Measured Friction of Rolling Balls in Raceway Grooves, *International Journal of Automation Technology* **vol. 8**(6) pp. 811–819, doi:10.20965/ijat.2014.p0811

Molinari 2007 — Molinari, B., 2007. *Robust Design - Werkzeuge und Strategien*, Student research project

Montalvão e Silva and Mendes Maia 1997 — Montalvão e Silva, J. M. and Mendes Maia, N. M., 1997. *Theoretical and Experimental Modal analysis*, Research Studies Press Ltd.

MTS 2017 — MTS, 2017. *Grundsätzliches zur Messung von Kräften*, Messtechnik Schaffhausen GmbH, Schaffhausen

Muhs, Wittel et al. 2003 — Muhs, D., Wittel, H., Becker, M., Jannasch, D., and Voßiek, J., 2003. *Roloff/Matek Maschinenelemente*, Vieweg

Neithardt 2004 — Neithardt, W., 2004. *Methodik zur Simulation und Optimierung von Werkzeugmaschinen in der Konzept- und Entwurfsphase auf Basis der Mehrkörpersimulation*, Ph.D. thesis, Karlsruhe Institute of Technology (KIT)

Niehues, Schwarz et al. 2012 — Niehues, K., Schwarz, S., and Zaeh, M. F., 2012. Reliable material damping ratio determination in machine tool structures, *Production Engineering Reserch and Development* **vol. 6**(4-5) pp. 475–484, doi:10.1007/s11740-012-0393-7

Olsson, Åström et al. 1998 — Olsson, H., Åström, K. J., Canudas de Wit, C., Gäfvert, M., and Lischinsky, P., 1998. Friction Models and Friction Compensation, *European Journal of Control* **vol. 4**(3) pp. 176–195, doi: 10.1016/S0947-3580(98)70113-X

Petersen and Pedersen 2008 — Petersen, K. B. and Pedersen, M. S., 2008. *The Matrix Cookbook*

Petuelli 1983 — Petuelli, G., 1983. *Theoretische und experimentelle Bestimmung der Steifigkeits- und Dämpfungseigenschaften normalbelasteter Fügestellen*, Ph.D. thesis, Rheinisch-Westfälische Technische Hochschule Aachen (RWTH Aachen)

Popov 2009 — Popov, V. L., 2009. *Kontaktmechanik und Reibung: ein Lehr- und Anwendungsbuch der Nanotribologie bis zur numerischen Simulation*, Berlin: Springer, 1st edn.

Pruschek 2009 — Pruschek, P., 2009. *Verfahren zur anwendungsgerechten Parametrierung der Steuerung und Regelung von Vorschubachsen*, Ph.D. thesis, University of Stuttgart

Queins 2005 — Queins, M., 2005. *Simulation des dynamischen Verhaltens von Werkzeugmaschinen mit Hilfe flexibler Mehrkörpermodelle*, Ph.D. thesis, Rheinisch-Westfälische Technische Hochschule Aachen (RWTH Aachen)

Reinhart 1996 — Reinhart, G., 1996. *Qualitätsmanagement: ein Kurs für Studium und Praxis*, Berlin: Springer

Reuss 2011 — Reuss, M., July 2011. Statistische Auswertung des Reibverhaltens baugleicher Werkzeugmaschinen, In *Innovationstage - Lageregelseminar*, Stuttgart

Reuss 2016 — Reuss, M., 2016. Reasons and impact of assembly variations on machine tools, *Journal of Advanced Mechanical Design, Systems, and Manufacturing* **vol. 10**(5), doi:10.1299/jamdsm.2016jamdsm0077

Reuss, Dadalau et al. 2012 — Reuss, M., Dadalau, A., and Verl, A., 29.-30.10. 2012. Friction Variances of Linear Machine Tool Axes, In *Proceedings of the 3rd CIRP Conference on Process Machine Interactions (3rd PMI)*, pp. 115–119, doi:10.1016/j.procir.2012.10.021

Reuss, Sakai et al. 2016 — Reuss, M., Sakai, T., and Matsubara, A., 14.-16.11. 2016. Contact and friction behavior of rolling element in linear bearing, In *Proceedings of the The 16th International Conference on Precision Engineering*, Hamamatsu

Rinne and Mittag 1995 — Rinne, H. and Mittag, H.-J., 1995. *Statistische Methoden der Qualitätssicherung*, Hanser

Roenpage, Staudter et al. 2006 — Roenpage, O., Staudter, C., Meran, R., John, A., and Beernaert, C., 2006. *Six Sigma+Lean Toolset: Verbesserungsprojekte erfolgreich durchführen*, Springer, 2nd edn.

Ruderman and Bertram 2011 — Ruderman, M. and Bertram, T., 2011. Modified Maxwell-slip Model of Presliding Friction, In *Preprints of the 18th IFAC World Congress*, pp. 10764–10769

Ruths and Israelachvili 2011 — Ruths, M. and Israelachvili, J. N., 2011. *Nanotribology and Nanomechanics II*, Springer

Schmidt 2005 — Schmidt, J., 2005. *Ausgewählte Kapitel der Fertigungstechnik*, Lecture notes, Institut für Produktionstechnik (wbk), Karlsruher Institut für Technology

Schopp and Munzinger 2009 — Schopp, M. and Munzinger, C., 2009. Analyse des Ausfallverhaltens von Werkzeugmaschinen, In *Steigerung der Verfügbarkeit durch Überlastbegrenzung und prozessparallele Last- und Verschleißüberwachung (OPTILAST)*, Apprimus Verlag

Seemann 2006 — Seemann, W., 2006. *Mehrkörperdynamik*, Lecture notes, Institut für Technische Mechnik, Karlsruher Institut für Technology

Shabana 2005 — Shabana, A. A., 2005. *Dynamics of multibody systems*, Cambridge: Cambridge University Press, 3rd edn.

Siemens 2008 — Siemens, 2008. *SinuCom Inbetriebnahme-/ Servicetools - Bedienhandbuch*, Siemens AG, München, 7th edn.

Soda, Kimura et al. 1970 — Soda, N., Kimura, Y., and Sekizawa, M., 1970. Wear occurring in rolling-sliding contact, *Proceedings of the Japan Society of Machine Tool Engineers* **vol. 37** p. 2204 ff., (in Japanese)

Spur 1996 — Spur, G., 1996. *Die Genauigkeit von Maschinen: eine Konstruktionslehre*, München: Hanser

Steinert 1996 — Steinert, T., 1996. *Das Reibmoment von Kugellagern mit bordgeführtem Käfig*, Ph.D. thesis, Rheinisch-Westfälische Technische Hochschule Aachen (RWTH Aachen)

Stiller 2006 — Stiller, C., 2006. *Grundlagen der Mess- und Regelungstechnik*, Berichte aus der Steuerungs- und Regelungstechnik, Aachen: Shaker

Taguchi and Asian Productivity Organization 1986 — Taguchi, G. and Asian Productivity Organization, 1986. *Introduction to quality engineering: designing quality into products and processes*, Asian Productivity Organization

Taguchi, Chowdhury et al. 2000 — Taguchi, G., Chowdhury, S., and Taguchi, S., 2000. *Robust Engineering*, McGraw-Hill

Teutsch 2005 — Teutsch, R., 2005. *Kontaktmodelle und Strategien zur Simulation von Wälzlagern*

und Wälzführungen, Ph.D. thesis, Technical University Kaiserslautern

Tietjen and Müller 2003 — Tietjen, T. and Müller, D.H., 2003. *FMEA-Praxis: das Komplettpaket für Training und Anwendung*, Hanser, ISBN 9783446223226

VDI 2206 2004 — VDI 2206, June 2004. *VDI-Richtlinie 2206: Entwicklungsmethodik für mechatronische Systeme*, industrial standard, VDI Verein Deutscher Ingenieure e.V.

VDI 2230-1 2003 — VDI 2230-1, February 2003. *VDI-Richtlinie 2230, Blatt 1: Systematische Berechnung hochbeanspruchter Schraubenverbindungen*, industrial standard, VDI Verein Deutscher Ingenieure e.V.

VDW 2012 — VDW, 2012. Die deutsche Werkzeugmaschinenindustrie im Jahr 2011 (The German Machine Tool Industry in 2011), Frankfurt

VDW 2014 — VDW, 2014. Die deutsche Werkzeugmaschinenindustrie im Jahr 2013 (The German Machine Tool Industry in 2013), Frankfurt

Walther 2011 — Walther, M., 2011. *Antriebsbasierte Zustandsdiagnose von Vorschubantrieben*, Ph.D. thesis, University of Stuttgart

Weck and Brecher 2006a — Weck, M. and Brecher, C., 2006. *Werkzeugmaschinen - Konstruktion und Berechnung*, vol. 2, Springer Verlag, 8th edn.

Weck and Brecher 2006b — Weck, M. and Brecher, C., 2006. *Werkzeugmaschinen - Messtechnische Untersuchung und Beurteilung*, vol. 5, Springer Verlag, 7th edn.

Wittenburg 1977 — Wittenburg, J., 1977. *Dynamics of systems of rigid bodies: with 42 problems*, Stuttgart: Teubner Verlag, 1st edn.

Zäh, Niehues et al. 2011 — Zäh, M. F., Niehues, K., and Schwarz, S., November 2011. Struktur- und Fügestellendämpfung in Werkzeugmaschinenstrukturen - Material and Joint Damping in Machine Tool Structures, In *2. VDI Fachtagung Schwingungsdämpfung*, VDI-Verlag GmbH, no. 2164 In VDI-Berichte, pp. 21–34

Exchangeability of machine tools requires identical results of identical machining operation. For estimating the behavior of machine tools, the interaction of electromechanic system and controller must be observed together. This allows to measure friction at start-up in serial production of machine tools and at the production plants of machine tool consumers without any additional measuring equipment. By measuring friction severe variances of the feed axes have been detected, which are mainly caused by assembly variances. Especially the alignments and preloads of bearings and ball screw have a severe influence. A test rig is used to identify components' friction behavior and to induce definite variations of assembly conditions. In order to improve the significance and to estimate the effect of assembly variances in detail, a modeling method based on multibody simulation has been developed and verified.

ISBN 978-3-8396-1256-9

9 783839 612569

FRAUNHOFER VERLAG